

# DISSERTATION

submitted to the  
Combined Faculties for the Natural Sciences and for Mathematics  
of the Ruperto-Carola University of Heidelberg, Germany

For the degree of  
Doctor of Natural Sciences

presented by  
Valeska Reichel, Pharmacist  
born in Bremen, Germany

Oral examination: 13.02.2006



# **Molecular and Functional Analyses of Transport Proteins for Organic Anions**

Referees: Prof. Dr. Gert Fricker  
Prof. Dr. Ulrich Hilgenfeld



# Acknowledgements

Special thanks go to **Prof. Dr. G. Fricker** for the interesting research subject, the support and the interesting discussions.

I would like to thank **Prof. Dr. U. Hilgenfeld** for the second opinion and **Prof. Dr. J. Reichling** and **Prof. Dr. U. Massing** for being members of my defense committee.

My gratitude goes to **Dr. D.S. Miller** for an interesting research period at the Mount Desert Island Biological Laboratory, the active discussion and his helpful suggestions concerning my manuscripts.

I also would like to thank **Dr. R. Masereeuw** for the internship at the Nijmegen Centre for Molecular Life Sciences and the excellent support concerning experiments, discussion of results and manuscripts.

Special thanks go to **Johannes Bartsch** who always gave me support and affection and helped me with all computer problems.

I would like to thank all the **colleagues** at the department of Pharmaceutical Technology of the University of Heidelberg, the MDIBL and the NCMLS for the good working climate and their support, special thanks go to **Melanie Ott** for the helpful discussions and the cordial friendship.

Thanks to **Boehringer Ingelheim Fonds** and **Erwin Riesch Stiftung** for the scholarships.

Last but not least my thanks go to my **parents** who always believed in me.



## **Parts of this thesis were presented in:**

Reichel V., Masereeuw R., Van den Heuvel J.J.M.W., Miller D.S., Fricker G.: Transport of a fluorescent cAMP analog by Multidrug Resistance-associated Proteins MRP2 (ABCC2) and MRP4 (ABCC4). American Journal of Physiology: Comparative Physiology: Submitted

Reichel V., DiPasquale K.D., Miller D.S., Fricker G.: Texas Red Transport in Rat and Shark Choroid Plexus: A Comparison. American Journal of Physiology: Comparative Physiology: Submitted

Reichel V., Baehr C.H., Fricker G.: Expression, Localization and Functional Analyses of P-Glycoprotein at the Choroid Plexus. Naunyn-Schmiedeberg's Archives of Pharmacology: 2004; 369: Supplement 1

Reichel V., Miller D.S., Masereeuw R., Fricker G.: Functional Analyses of Multidrug Resistance Protein 4 (Mrp4) in renal proximal tubules. Naunyn-Schmiedeberg's Archives of Pharmacology: 2005; 371: Supplement 1

Reichel V., DiPasquale K.D., Miller D.S., Fricker G.: Transport of a fluorescent cAMP analog in killifish, *Fundulus heteroclitus*, renal proximal tubules. The Bulletin, MDI Biological Laboratory: 2005, V. 44, 114-115

## **Posters**

Reichel V., Baehr C.H., Fricker G.: Expression, Localization and Functional Analyses of P-Glycoprotein at the Choroid Plexus. 45. DGPT Spring Meeting, Mainz: 2004

Reichel V., Miller D.S., Masereeuw R., Fricker G.: Functional Analyses of Multidrug Resistance Protein 4 (Mrp4) in renal proximal tubules. 46. DGPT Spring Meeting, Mainz: 2005

Reichel V., DiPasquale K.D., Miller D.S., Fricker G.: Texas Red Transport in Intact Rat Choroid Plexus. VIth Conference on Cerebral Vascular Biology, Münster: 2005

## **Invited Lectures**

Reichel V.: Texas Red Transport across Choroid Plexus Epithelium. IIIth Transporter meeting of the pharmaceutical industry, Ingelheim: 2005



## Zusammenfassung

Reichel, Valeska, Apothekerin, Tag der mündlichen Prüfung: 13.02.06

### Molekulare und funktionelle Charakterisierung von Transportproteinen für Organische Anionen

Referent: Prof. Dr. Gert Fricker, Koreferent : Prof. Dr. Ulrich Hilgenfeldt

Die Blut-Cerebrospinalflüssigkeit (CSF)-Schranke (BCSFS), wird von den Choroid Plexüs (CP) gebildet und stellt zusammen mit der Blut-Hirn-Schranke eine wichtige Barriere zwischen Blut und Gehirn dar. Da die BCSFS nur für kleine, lipidlösliche und ungeladene Moleküle durchlässig ist, ist es von besonderem Interesse, aktive Transportprozesse für geladene Substanzen in diesem Gewebe zu untersuchen, da viele ZNS-Wirkstoffe und Wirkstoffkandidaten Substrate aktiver Transportproteine sind. Transportprozesse im CP ähneln denen im proximalen Tubulus der Niere. Deshalb wurden vergleichende Experimente mit verschiedenen Modell-Anionen mit isoliertem proximalen Nierentubulus des Killifisch und mit CP von Ratte und Dornhai durchgeführt.

- Zunächst wurde der Transport des fluoreszierenden cAMP-Analogons fluo-cAMP untersucht: Inhibitorstudien legen den Transport von fluo-cAMP durch die Exportproteine Mrp2 und Mrp4 nahe. Im Gegensatz zum Transport des Mrp2-Substrates Fluorescein-Methotrexat (FL-MTX) wird der Transport in der Niere nicht durch die Proteinkinasen A (PK) A und C (PKC) reguliert. Zur besseren Charakterisierung der kinetischen Parameter wurde der Transport von fluo-cAMP in Membranvesikeln aus MRP2 bzw. MRP4 überexprimierenden Zellen untersucht. Beide MRPs transportieren fluo-cAMP mit gleich hoher Affinität. Anders als in der Niere scheint Mrp4 im CP nicht am Transport von fluo-cAMP beteiligt zu sein, allerdings geben Inhibitionsexperimente mit konkurrierenden selektiven Substraten Hinweise für eine Beteiligung von Mrp1. Die Regulation des Transportes von fluo-cAMP im Ratten-CP erfolgt nicht über PKA, PKC oder die Mitogen-aktivierte PK (MAPK).
- Der Transport von Texas Red (TR) und FL-MTX wurde im CP der Ratte und des Dornhais untersucht. TR wird durch Ratten-CPs in einem zweistufigen Prozess transportiert, der Metabolismus-getrieben, Na<sup>+</sup>-abhängig, potentialunabhängig und auch unabhängig von Mrp1, Mrp2 und Mrp4 ist. Im Hai ist der Transport von TR Na<sup>+</sup>-unabhängig, wobei die Aufnahme über ein Oat-Protein zu erfolgen scheint, während der basolaterale Efflux mutmasslich über das Oatp2-Protein und Mrp1 erfolgt.
- Die apikale Aufnahme von FL-MTX im Ratten-CP ist ebenfalls Na<sup>+</sup>-abhängig, der basolaterale Efflux ist potentialunabhängig und erfolgt wahrscheinlich auch über Mrp1 und Oatp2. PKA-Aktivierung führt zu einer Aktivierung des FL-MTX Effluxes. Im Dornhai wird FL-MTX durch die gleichen Transportproteine transportiert. Im Gegensatz zur Ratte führt eine PKA-Aktivierung zu einem reduzierten Efflux von FL-MTX, während PKC-Aktivierung zu einer Herabregulierung des Transports von FL-MTX führte.



## Abstract

Reichel, Valeska, Pharmacist, Oral Examination: 13.02.06

### Molecular and Functional Analyses of Transport Proteins for Organic Anions

Supervisor: Prof. Dr. Gert Fricker, Co-Supervisor: Prof. Dr. Ulrich Hilgenfeldt

The blood-cerebrospinal fluid (CSF)-barrier (CSFB) is formed by the Choroid Plexūs (CP). Together with the blood brain barrier it represents an important barrier between brain and circulating blood. Since it can only be passed by small, lipid-soluble and uncharged molecules it is of particular interest to study active transport processes for charged substances across this tissue, especially because many drugs are substrates for these transport proteins. Transporters in the CP are similar to those in the kidney. Therefore, I performed comparative experiments with model organic anions in isolated proximal kidney tubules of killfish and CP of rat and spiny dogfish shark.

- First, I studied transport of the fluorescent cAMP analog fluo-cAMP. Inhibition studies indicate transport mediated by the export proteins Mrp2 and Mrp4. In contrast to transport of the Mrp2-substrate fluorescein-methotrexate (FL-MTX), transport is not regulated by protein kinase (PK) A, and PKC. For better characterization of kinetic parameters I studied transport of fluo-cAMP in membrane vesicles of MRP2 and MRP4 overexpressing cells. Both MRPs transported fluo-cAMP with similar affinities. Different from results obtained from experiments using renal proximal tubules, fluo-cAMP transport in CP seems not to be mediated by Mrp4, whereas a participation of Mrp1 is likely. Regulation of fluo-cAMP transport in rat CP is not mediated by PKA, PKC or mitogen activated PK (MAPK).
- Transport of Texas Red (TR) and FL-MTX was studied in CP of rat and spiny dogfish shark. Transport of TR across rat CP is a two-step mechanism, which is metabolism-driven, Na<sup>+</sup>-dependent, potential independent and also independent from Mrp1, Mrp2 and Mrp4. In dogfish shark CP TR transport is Na<sup>+</sup>-independent, with apical uptake apparently mediated by an Oat-protein, whereas basolateral efflux seems to be mediated by Oatp2 and Mrp1.
- Apical uptake of FL-MTX in rat CP is also Na<sup>+</sup>-independent with a potential independent basolateral efflux, which is presumably mediated via Mrp1 and Oatp2. Activation of PKA results in an activation of FL-MTX efflux. In dogfish shark FL-MTX is transported via the same transport proteins. But in contrast to rat CP, activation of PKA results in a reduced efflux of FL-MTX, whereas activation of PKC leads to a downregulation of FL-MTX transport.



---

|           |   |           |
|-----------|---|-----------|
| <b>1</b>  | <b>Introduction</b>   | <b>1</b>  |
| 1.1       | Barriers to the Brain   | 1         |
| 1.2       | Choroid Plexus Anatomy  | 2         |
| 1.3       | Morphology of Choroid Plexus Epithelial Cells                     | 4         |
| 1.4       | Choroid Plexus Function   | 5         |
| 1.5       | Transport Mechanisms at the Choroid Plexus                        | 9         |
| 1.6       | Transporters for Organic Anions                                   | 10        |
| 1.6.1     | Solute Carrier (SLC) Family                                       | 12        |
| 1.6.1.1   | The Organic Anion Transporting Polypeptide Family ( <i>Slco</i> ) | 13        |
| 1.6.1.2   | The Proton Oligopeptide Cotransporter Family ( <i>Slc15</i> )     | 14        |
| 1.6.1.3   | The Organic Ion Transporter Family ( <i>Slc22a</i> )              | 15        |
| 1.6.1.3.1 | Organic Anion Transporter ( <i>Oat</i> )                          | 15        |
| 1.6.1.3.2 | Organic Cation Transporter ( <i>Oct</i> )                         | 16        |
| 1.6.1.3.3 | Carnitine/Organic Cation Transporter ( <i>Octn</i> )              | 17        |
| 1.6.2     | ATP Binding Cassette Superfamily                                  | 17        |
| 1.6.2.1   | Multidrug Resistance-Associated Proteins ( <i>Mrp/Abcc</i> )      | 18        |
| 1.6.2.2   | P-Glycoprotein ( <i>P-gp/ABCB1</i> )                              | 19        |
| 1.7       | Localization of Organic Anion Transporters                        | 20        |
| <b>2</b>  | <b>Purpose of the study</b>                                       | <b>22</b> |
| 2.1       | Fluo-cAMP Transport in Killifish Proximal Tubulus                 | 22        |
| 2.2       | Fluo-cAMP Transport in Membrane Vesicles                          | 22        |
| 2.3       | Fluo-cAMP Transport in Rat Choroid Plexus                         | 23        |
| 2.4       | Texas Red Transport in Rat and Shark CP                           | 23        |
| 2.5       | Regulation of Fluorescein-Methotrexate Transport                  | 23        |
| <b>3</b>  | <b>Materials and Methods</b>                                      | <b>24</b> |
| 3.1       | Materials   | 24        |
| 3.2       | MDCKII and Sf9-Cells  | 25        |
| 3.2.1     | Cell Culture  | 25        |

|            |  |           |
|------------|--|-----------|
| 3.2.2      | Isolation of Crude Membrane Vesicles                                   | 25        |
| <b>3.3</b> | <b>Tissues <i>Ex Vivo</i></b>  | <b>26</b> |
| 3.3.1      | Killifish Proximal Tubulus <i>Ex Vivo</i>                              | 26        |
| 3.3.2      | Rat Choroid Plexus <i>Ex Vivo</i>                                      | 27        |
| 3.3.3      | Dogfish Shark Choroid Plexus <i>Ex Vivo</i>                            | 27        |
| <b>3.4</b> | <b>Gene Expression</b>   | <b>27</b> |
| 3.4.1      | Total RNA Isolation  | 27        |
| 3.4.2      | Reverse Transcription  | 28        |
| 3.4.3      | Polymerase Chain Reaction  | 28        |
| 3.4.4      | Semiquantitative RT-PCR  | 29        |
| 3.4.5      | Immunocytological Staining   | 29        |
| <b>3.5</b> | <b>Functional Analyses</b>   | <b>30</b> |
| 3.5.1      | Uptake Studies in Membrane Vesicles                                    | 30        |
| 3.5.2      | Transport Studies in Killifish Proximal Tubulus                        | 31        |
| 3.5.3      | Transport Studies in Rat and Dogfish Shark Choroid Plexus              | 31        |
| <b>3.6</b> | <b>Statistics</b>  | <b>32</b> |
| <b>4</b>   | <b>Results</b>   | <b>33</b> |
| <b>4.1</b> | <b>Molecular Analyses</b>  | <b>33</b> |
| 4.1.1      | Mrp4 Gene Expression in Rat Choroid Plexus                             | 33        |
| 4.1.2      | Immunostaining in Choroid Plexus and Proximal Tubulus                  | 34        |
| <b>4.2</b> | <b>Functional Analyses</b>   | <b>36</b> |
| 4.2.1      | Transport Studies in Killifish Proximal Tubulus                        | 37        |
| 4.2.2      | Uptake Studies in Membrane Vesicles                                    | 50        |
| 4.2.3      | Transport Studies in Rat and Shark Choroid Plexus                      | 55        |
| 4.2.3.1    | Fluo-cAMP Transport in Rat Choroid Plexus                              | 55        |
| 4.2.3.2    | [ <sup>3</sup> H]-cGMP transport in rat CP                             | 69        |
| 4.2.3.3    | Texas Red Transport in Rat and Dogfish Shark Choroid Plexus            | 70        |
| 4.2.3.4    | Regulation of Fluorescein-Methotrexate Transport in Rat Choroid Plexus | 85        |
| <b>5</b>   | <b>Discussion</b>  | <b>90</b> |
| <b>5.1</b> | <b>Fluo-cAMP Transport in Killifish Proximal Tubules</b>               | <b>92</b> |
| <b>5.2</b> | <b>Fluo-cAMP Transport in Membrane Vesicles</b>                        | <b>93</b> |

|             |  |            |
|-------------|--|------------|
| <b>5.3</b>  | <b>Regulation of Fluo-cAMP Transport in Killifish Kidney</b> | <b>94</b>  |
| <b>5.4</b>  | <b>Fluo-cAMP Transport in Rat Choroid Plexus</b>             | <b>94</b>  |
| <b>5.5</b>  | <b>Comparison of Fluo-cAMP and Fluorescein Transport</b>     | <b>96</b>  |
| <b>5.6</b>  | <b>Comparison of Fluo-cAMP and FL-MTX Transport</b>          | <b>97</b>  |
| <b>5.7</b>  | <b>Regulation of Fluo-cAMP and FL-MTX Transport</b>          | <b>97</b>  |
| <b>5.8</b>  | <b>FL and FL-MTX Transport in Shark Choroid Plexus</b>       | <b>98</b>  |
| <b>5.9</b>  | <b>Texas Red Transport in Rat and Shark CP</b>               | <b>99</b>  |
| <b>5.10</b> | <b>Comparison of TR, FL and FL-MTX Transport</b>             | <b>101</b> |
| <b>6</b>    | <b>Summary</b>   | <b>102</b> |
| <b>7</b>    | <b>Outlook</b>   | <b>105</b> |
| <b>8</b>    | <b>References</b>  | <b>107</b> |

## Abbreviations

---

|                  |  |
|------------------|--|
| 5-ALA            | 5-Aminolevulinic Acid                                  |
| 2,4-D            | 2,4-Dichlorophenoxyacetic Acid                         |
| ABC              | ATP-Binding Cassette                                   |
| AMP              | Adenosine Monophosphate                                |
| AMV-RT           | Avian Myeloblastosis Virus Reverse Transcriptase       |
| ATP              | Adenosine Triphosphate                                 |
| AZT              | Azidothymidine   |
| aCSF             | Artificial Cerebrospinal Fluid                         |
| BBB              | Blood-Brain-Barrier                                    |
| BBM              | Brush Border Membrane                                  |
| BCSFB            | Blood-Cerebrospinal Fluid-Barrier                      |
| BIM              | Bisindolylmaleimide                                    |
| BLM              | Basolateral Membrane                                   |
| BP               | Base Pair  |
| BSP              | Bromosulphophthalein                                   |
| cAMP             | Cyclic Adenosine Monophosphate                         |
| cGMP             | Cyclic Guanosine Monophosphate                         |
| CNS              | Central Nervous System                                 |
| CP               | Choroid Plexus   |
| CSF              | Cerebrospinal Fluid                                    |
| Da               | Dalton   |
| DHEAS            | Dehydroepiandrosterone Sulfate                         |
| DMSO             | Dimethylsulfoxide                                      |
| DNA              | Deoxyribonucleic Acid                                  |
| DNP-SG           | S-(Dinitrophenyl)-Glutathione                          |
| E217 $\beta$ G   | Estradiol-17 $\beta$ -D-Glucuronide                    |
| ECF              | Extracellular Fluid                                    |
| ER               | Elasmobranch Ringer                                    |
| ES               | Estrone Sulfate  |
| FDA              | Fluorescein-Diacetate                                  |
| FL               | Fluorescein  |
| FL-MTX           | Fluorescein-Methotrexate                               |
| Fluo-cAMP        | 8-[[2-[(fluoresceinylthioureido)amino]ethyl]thio]-cAMP |
| Fors             | Forskolin  |
| GFP              | Green Fluorescent Protein                              |
| GlySar           | Glycylsarcosine  |
| GST              | Glutathione-S-Transferases                             |
| ICF              | Intracellular Fluid                                    |
| kDa              | Kilodalton   |
| LTC <sub>4</sub> | Leukotriene C <sub>4</sub>                             |
| LY               | Lucifer Yellow   |
| MAPK             | Mitogen-activated protein kinase                       |
| MDCK             | Madin-Darby Canine Kidney                              |
| MDR              | Multidrug Resistance                                   |
| Mrp              | Multidrug Resistance-Associated Protein                |
| MTX              | Methotrexate   |
| NaCN             | Sodium Cyanide   |
| NMN              | N-Methylnicotinamide                                   |
| Oat              | Organic Anion Transporter                              |
| Oatp             | Organic Anion Transporting Polypeptide                 |

## Abbreviations

---

|        |   |
|--------|---|
| Oct    | Organic Cation Transporter                      |
| PAH    | <i>p</i> -Aminohippuric Acid                    |
| PBGD   | Porphobilinogen Deaminase                       |
| PCR    | Polymerase Chain Reaction                       |
| PG     | Prostaglandine                                  |
| P-gp   | P-Glycoprotein                                  |
| PK     | Proteinkinase                                   |
| PMA    | Phorbol-12-Myristate-13-Acetate                 |
| PMEA   | 9-(2-Phosphonylmethoxyethyl)adenine             |
| PMT    | Photomultiplier                                 |
| RNA    | Ribonucleic Acid                                |
| RT-PCR | Reverse Transcription-Polymerase Chain Reaction |
| SEM    | Standard Error of Mean                          |
| Sf9    | Spodoptera Frugiperda                           |
| SLC    | Solute Carrier                                  |
| T3     | Triiodothyronine                                |
| T4     | Thyroxine                                       |
| Tauro  | Taurocholate                                    |
| TEA    | Tetraethylammonium                              |



# 1 Introduction

## 1.1 Barriers to the Brain

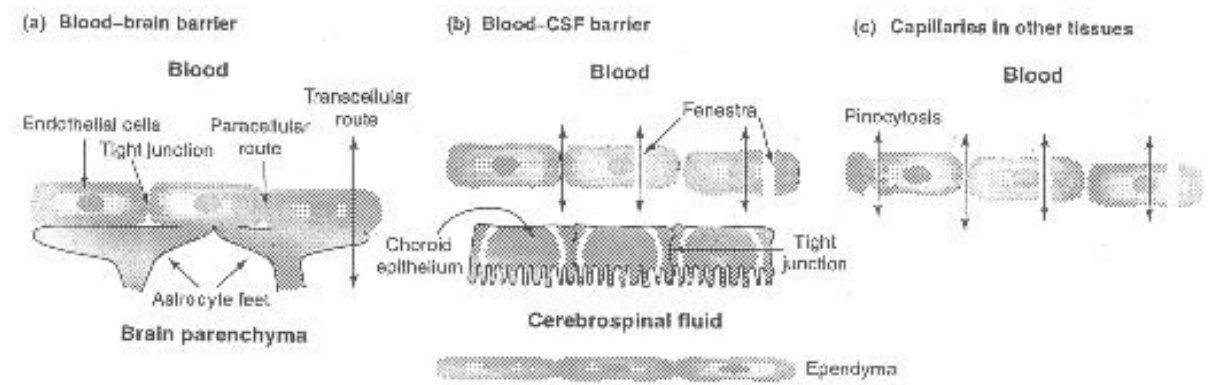
The homeostasis in the brain is a crucial factor for correct neurone function because the brain is very sensitive to changes in the surrounding environment and the extracellular milieu. Substance exchange is a critical factor for brain homeostasis and most water soluble substances can hardly enter the brain by passive diffusion, or be removed, to ensure stability in the composition of brain fluids. Removing metabolites or xenobiotics actively from the brain is an important protective mechanism (Johanson, 1998; Haselbach et al., 2001; Spector/Johanson, 1991).

Due to these active mechanisms, pharmacotherapy of brain diseases including brain cancer, HIV, schizophrenia, meningitis, depression or epilepsy is difficult, because most of the drugs cannot advent their targets in the central nervous system (CNS) (Bachmayer et al., 2005; Ghersi-Egea/Strazielle, 2001; Löscher/Potschka, 2005; Miller, 2004).

To provide environmental stability, the barriers in the brain work together to maintain homeostasis of extracellular fluid (ECF). Two barrier systems are present in the brain to regulate substance distribution between blood stream and CNS: the blood-brain-barrier (BBB) and the blood-cerebrospinal fluid (CSF)-barrier (BCSFB). The BBB is formed by the brain capillaries, which form a network all-over the brain and almost reach the neurons. Brain capillary endothelial cells act as direct barrier between blood and brain tissue. Barrier function of the blood-brain barrier is composed of tight junctions between endothelial cells, low endocytosis rate and specific transport and carrier molecules. Astrocytes, pericytes and the extracellular matrix components control the integrity of this barrier (Gloor et al., 2001; Haselbach et al., 2001; Löscher/Potschka, 2005; Nilsson et al., 1992; Spector/Johanson, 1991).

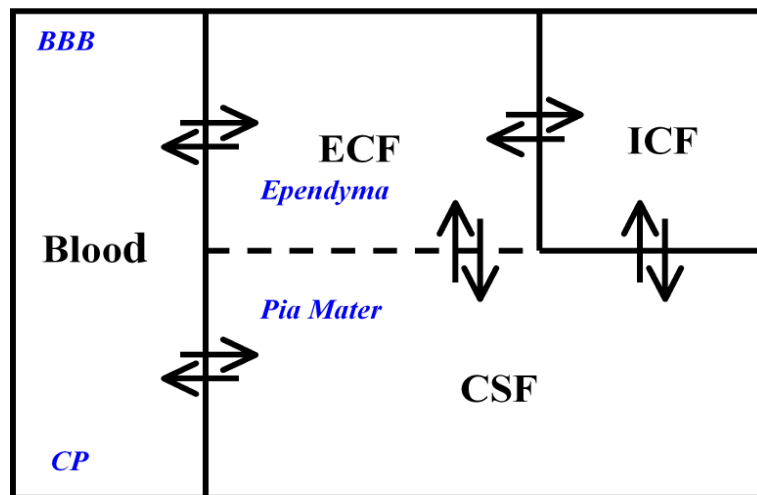
The second important barrier in the brain is the BCSFB comprised of the choroid plexuses (CPs) and the arachnoid membrane which coats the brain. Barrier function is formed by choroid plexus epithelial cells. The arachnoidea is only a passive barrier, which is impermeable for water-soluble substances. (Haselbach et al., 2001; Johanson, 1998; Nilsson et al., 1992; Spector/Johanson, 1991). Figure 1 shows the different barrier compositions of BBB and BCSFB.

**Figure 1:** Capillaries at the BBB (a), BCSFB (b) and other tissues (c). At the BBB brain capillary endothelial cells are connected to each other by tight junctions, which prevent substance exchange through the paracellular route. At the BCSFB capillaries are fenestrated, tight junctions between CP epithelial cells form the barrier. In other capillaries free substance exchange between capillary facing solutes is possible. Figure is modified from Kusahara/Sugiyama, 2001.



Between brain fluids, CSF and ECF, substances can pass unhampered by simple diffusion. But also to and from the compartment of intracellular fluid (ICF) a permanent fluid flow takes place. Substance exchange between ECF and ICF or CSF and ICF is driven by selective transport mechanisms as in the barriers between blood and brain, because the ICF compartment is separated from ECF and CSF through the plasma membrane (Nilsson et al., 1992). In Figure 2 the different compartments and possibilities for substance exchange are shown.

**Figure 2:** The different fluid compartments in the brain. Substance exchange is unhampered between ECF and CSF and driven by selective mechanisms between CSF and ICF, ECF and ICF, CSF and blood and ECF and blood. ECF: extracellular fluid, ICF: intracellular fluid, CSF: cerebrospinal fluid. Figure is modified from Nilsson et al., 1992.

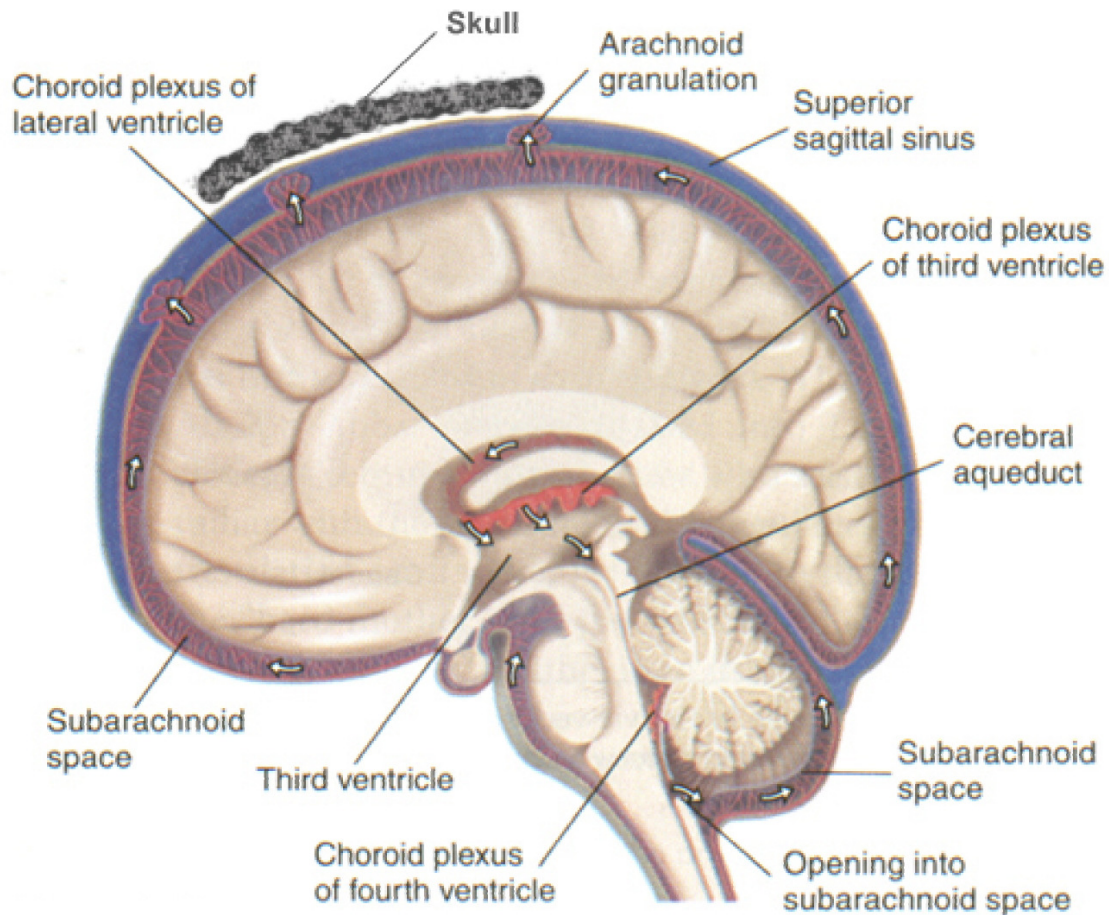


## 1.2 Choroid Plexus Anatomy

In all mammals, except for *Amphioxus*, the CPs are present and localized to the third and fourth ventricles of the brain and to the lateral ventricles of each hemisphere (Alebouyeh et

al., 2003; Nilsson et al., 1992). 90% of CP mass are located to equal parts in the lateral and third ventricles, only 10% are in the fourth ventricle (Johanson, 1999). Localization of CPs in mammalian brains is shown in Figure 3.

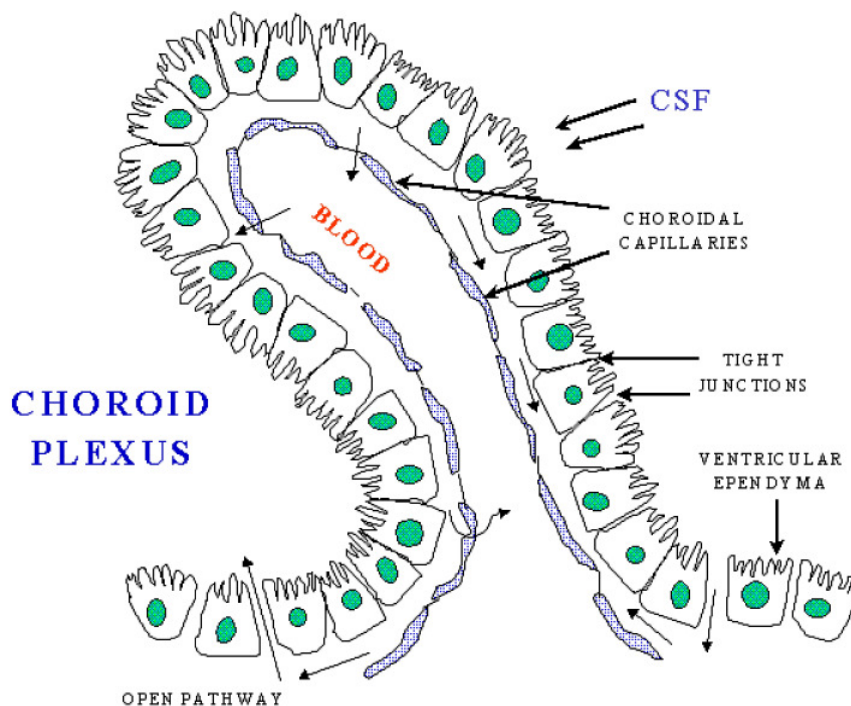
**Figure 3:** Localization of CPs in the brain. The CPs are located to the ventricles as shown below. Figure from: Nervous System Form and Function (colorado/edu).



CP tissue is a leaf-like, highly vascularized tissue. The CPs are composed of fine blood capillaries surrounded by a monolayer of CP epithelial cells (Spector/Johanson, 1991). The epithelial cells are connected to each other by tight junctions which are very leak-proof. Different to those of the BBB, capillaries of the CPs are fenestrated and thus admit the passage of macromolecules into surrounding tissue. The surface area of the CP is increased by numerous villi. Each villus is composed of a single epithelium underlying the highly vascularized supporting tissue (Nilsson et al., 1992). The adjacent ependymal cells coat the ventricles and are more permeable than CP epithelial cells, they separate CSF and nerve tissue, the ependymal cells form a monolayer as well. At the outside of the brain, the pia-glial membrane forms the interface between CSF and neighbouring cortical tissue. Together with the arachnoidea, the pia-glial membrane constitutes the meningeal, composed of dura mater

and pia mater. Different to CP epithelial cells, ependymal and pia-gial cells are connected to each other by gap junctions. Gap junctions form a partial belt around cells and are more permeable than tight junctions. Unhampered diffusion from CSF across the ependymal and pia-gial cells is possible, thereby substances can reach their targets in the CNS, e.g. neurons or glia cells (Johanson, 1995; Nilsson et al., 1992; Spector/Johanson, 1991). Figure 4 shows a villus with surrounding CP epithelium and vicinal ependyma.

**Figure 4:** A single CP villus consisting of a blood capillary surrounded by a single layer of CP epithelial cells. CP epithelial cells are connected to each other by tight junctions which prevent free molecule exchange. Next to CP epithelial cells the ependyma is shown. Ependymal cells form a monolayer as well but are connected to each other by gap junctions, an unhampered substance exchange is assured. Figure from Anatomy and Physiologie of Blood CSF barrier, arizona/edu.



### 1.3 Morphology of Choroid Plexus Epithelial Cells

CP epithelial cells are polarized, at the basolateral membrane they have contact to the blood, the apical membrane faces the CSF (Johanson, 1995). In its ultrastructure CP epithelial cell membrane shows basal infoldings and apical microvilli. These membrane modifications are characteristic for transporting epithelia (Cserr, 1971). Ultrastructurally CP epithelial cells are similar to the kidney epithelium (Johanson, 1995). Due to the well-developed microvilli at the apical membrane, surface of CP epithelium is strongly magnified. Previous assumptions compare surface of the BBB and BCSFB with a ratio of 5000:1, but by the increase of CP epithelial membrane due to microvilli, the ratio was corrected to 2:1. CP epithelial cells are

characterized by large, round nuclei, plenteous mitochondria and rough endoplasmatic reticulum (Nilsson et al., 1992).

## 1.4 Choroid Plexus Function

Several functions are described for CP tissue, which depend primarily on the epithelium. As described above an important function of CP epithelium is the barrier function which is a physical function. Only lipophilic substances can pass through the barrier, while hydrophilic substances and macromolecules are excluded from the brain. Water-soluble substances or macromolecules can overcome the barrier only by active and specific transport systems. A small leak of the described substances can occur in the brain, this leak is somewhat larger for CP epithelial cells than for the endothelial cells of the BBB. CP epithelium has vital functions as well. Many substances that are necessary for maintenance of the brain are transported actively through CP epithelium. CP epithelium supplies brain with vitamins (e.g. thiamine, vitamin B1), glucose, ribonucleosides, desoxyribonucleosides and amino acids (Nilsson et al., 1992; Spector/Johanson, 1991).

CSF secretion is one of the most important functions of the CP. The secretory morphology of the epithelium, the localization of  $\text{Na}^+/\text{K}^+$ -ATPase to the apical membrane and analyses of freshly secreted fluid from the CP gave evidence that CP secretes CSF (Cserr, 1971; Nilsson et al., 1992). Now it is generally agreed, that the CP is the major site of CSF production. 90% of CSF are produced by the CPs, only 10% are secreted by extrachoroidal sources (Cserr, 1971). The main extrachoroidal source are probably the endothelial cells of brain capillaries which form the BBB. In mammals the turnover rate of CSF is high, about 0.5 % of the total volume per minute or 4-5 times the total volume per day (Nilsson et al., 1992). The way of CSF flow was described by Fishman, 1992: CSF is produced by CP epithelial cells and circulates from the telencephalon to the rombencephalon into subarachnoidal spaces and then to the forth ventricle, the sisterna magna and basal cisterns. The circulation is followed by absorption into the venous blood via arachnoid villi. The CSF is a clear, colourless solution with a constant pH of 7.35. It is composed of 99% water and 1% micronutrients and proteins, these ingredients are taken from the blood. For absorption of these substances a strong blood flow is required, needed are four to five millimeters per minute per gramm tissue. Water is secreted by CP epithelium by constitution of an ionic concentration gradient at the membranes between epithelial cells. The liquor composition is permanent almost identical, independently from concentrations in the flowing blood (Spector/Johanson, 1991). The main

constituents of the CSF are  $\text{Na}^+$ ,  $\text{Cl}^-$  and  $\text{HCO}_3^-$ . The typical CSF composition is shown in Table 1. Since CP epithelial cells are the major site of CSF production, these epithelial cells play a central role in regulation of brain homeostasis, protection of the brain and excretion of metabolites (Haselbach et al., 2001; Nilsson et al., 1992). CP tissue is not only a source for the CSF and with it nutrients and proteins, it also clears the CSF from proteins and metabolites (Johanson, 1999).

**Table 1:** Typical composition of CSF produced by CP epithelium. Major ingredients are  $\text{Na}^+$ ,  $\text{Cl}^-$  and  $\text{HCO}_3^-$ . The table is modified from Fishman, 1992.

| <b>Elektrolytes (mEq/l)</b> |      | <b>Amino Acids (<math>\mu\text{M}</math>)</b> |      |
|-----------------------------|------|---|------|
| $\text{Na}^+$               | 138  | Alanine                                       | 26.0 |
| $\text{K}^+$                | 2.8  | Arginine                                      | 22.4 |
| $\text{Cl}^-$               | 119  | Aspartic Acid                                 | 0.2  |
| $\text{HCO}_3^-$            | 22   | Aparagine                                     | 13.5 |
| $\text{Ca}^{2+}$            | 2.1  | Glutamic Acid                                 | 26.1 |
| $\text{Mg}^{2+}$            | 2.3  | Glutamine                                     | 552  |
| $\text{PO}_4^-$             | 0.5  | Glycine                                       | 5.9  |
| <b>Metabolites (mM)</b>     |      | Histidine                                     | 12.3 |
| Glucose                     | 3.3  | Isoleucin                                     | 6.2  |
| Lactate                     | 1.6  | Leucine                                       | 14.8 |
| Pyruvate                    | 0.08 | Lysine  | 20.8 |
| Urea                        | 4.7  | Methionine                                    | 2.5  |
| Creatinine                  | 0.09 | Ornithine                                     | 3.8  |
| <b>Proteins (mg/l)</b>      |      | Phenylalanine                                 | 9.9  |
| Albumin                     | 155  | Phosphoserine                                 | 4.2  |
| IgA                         | 1.3  | Serine  | 29.5 |
| IgG                         | 12.3 | Taurine                                       | 7.6  |
| IgM                         | 0.6  | Threonine                                     | 35.5 |
| Transferrin                 | 14.4 | Tyrosine                                      | 9.5  |
| Total protein               | 350  | Valine  | 19.9 |

CP epithelium is also a site for synthesis and secretion of plasma proteins as transferrin, ceruloplasmin, cystatin C and  $\beta_2$ -microglobulin. These polypeptides are known to be synthesized in CP and brain parenchyma. Several proteins are synthesized exclusively in CP epithelium, including transthyretin (TTR, prealbumin), IGF-II (Nilsson et al., 1992),

cytokines, growth factors and neuropeptides (Chodobski/Szmydynger-Chodobska, 2001).

Table 2 shows a list of polypeptides previously found in CP epithelium.

**Table 2:** Polypeptides previously found in CSF. Several of these polypeptides are actively secreted by CP epithelium. Table modified from Chodobski/Szmydynger-Chodobska, 2001.

| <b>Polypeptide</b>   | <b>Secretion by CP</b> |
|--|------------------------|
| Adrenomedullin   | Yes                    |
| Apolipoprotein J/clusterin   |                        |
| $\beta$ -Amyloid precursor protein   |                        |
| Basic fibroblast growth factor/fibroblast growth factor-2                      |                        |
| Brain-derived neurotrophic factor  |                        |
| $\beta$ -Trace protein/prostaglandin D synthase                                | Yes                    |
| Cystatin C   |                        |
| Endothelin 1   | Yes                    |
| Hepatocyte growth factor   |                        |
| Insulin-like growth factor-II  | Yes                    |
| Insulin-like growth factor binding protein 2-6                                 | Yes                    |
| Interleukin-1 $\beta$  |                        |
| Nerve growth factor  |                        |
| Neurothrophin-3 and 4  |                        |
| Transferrin  | Yes                    |
| Transforming growth factor- $\beta$ (isoforms $\beta$ 1, $\beta$ 2, $\beta$ 3) |                        |
| Transthyretin/prealbumin   | Yes                    |
| Tumor necrosis factor- $\alpha$  |                        |
| Vascular endothelial growth factor   |                        |
| Vasopressin  | Yes                    |

The CP is a target for exogenous and endogenous polypeptides as well. Various polypeptide receptors are expressed in CP epithelium (Table 3). The substrates to these polypeptide receptors seem to have a function in controlling the secretory function of CP epithelium. Some of the blood-born or centrally released peptides are potent regulators of CSF formation, whereas the importance of this physiological role is not fully understood. A role of these polypeptides in CP hemodynamics and endocrine regulation is suggested, too (Chodobski/Szmydynger-Chodobska, 2001, Nilsson et al., 1992).

**Table 3:** Polypeptide receptors located to CP epithelium and their ligands. Some ligands are supposed to be modulators of CSF formation and secretion by CP epithelium, but the physiological role is not fully understood. Table modified from Chodobski/Szmydynger-Chodobska, 2001; Nilsson et al., 1992.

| <b>Ligand</b>   | <b>Receptor</b>                     |
|---|-------------------------------------|
| Acetylcholine   | Muscarinic receptor                 |
| Angiotensin II  | AT <sub>1A</sub> , AT <sub>1B</sub> |
| Apolipoprotein E                                      | apoER2                              |
| Apolipoprotein J/clusterin                            | gp330/megalin                       |
| Atrial natriuretic peptide, Brain natriuretic peptide | NPR-A, NPR-C                        |
| Bradykinin  | B <sub>2</sub>                      |
| Brain-derived neurotrophic factor                     | TrkB, p <sup>75NTR</sup>            |
| Corticotropin-releasing factor                        | CRF-R2                              |
| Dopamine  | D <sub>1</sub>                      |
| Endothelin  | ET <sub>A</sub> , ET <sub>B</sub>   |
| Fibroblast growth factor                              | FGFR1, FGFR2                        |
| Gamma-aminobutyric acid                               | GABA A                              |
| Growth hormone  | GHR                                 |
| Histamine   | H <sub>2</sub>                      |
| 5-Hydroxytryptamine                                   | 5-HT <sub>1C</sub>                  |
| Insulin   | Insulin receptor                    |
| Insulin-like growth factor I and II                   | IGF-1R, IGF-2R, Man 6-P             |
| Interleukin-1   | IL-1R1                              |
| Leptin  | OB-Rb, OB-Rc, OB-Rf                 |
| Melatonin   | Melatonin receptor                  |
| Nerve growth factor                                   | p <sup>75NTR</sup>                  |
| Noradrenaline   | β <sub>1</sub> , β <sub>2</sub>     |
| Prolactin   | PRL-R                               |
| Transforming growth factor-β                          | TβRII                               |
| Tryptamine  | T-2                                 |
| Vascular endothelial growth factor                    | VEGFR-1, VEGFR-2                    |
| Vasoactive intestinal polypeptide                     | VIP1, VIP2-                         |
| Vasopressin   | V <sub>1a</sub> , V <sub>1b</sub>   |

Many xenobiotics underly metabolic processes that reduce their toxicology or pharmacological activity or rather increase their water solubility and subsequently allow their

renal or hepatic elimination. This biotransformation consists of two phases: phase-I and phase-II metabolism. Phase-I reactions are biotransformations that alter xenobiotic molecules by oxidation, reduction or hydrolysis. One of the most important phase-I reactions is oxidative biotransformation by monooxygenases that contain hemoproteins of cytochrome P-450 type. Several isoenzymes of cytochrome P-450 are known, which are structured in different subfamilies and families. Phase-II is a conjugation reaction: xenobiotic molecules or phase-I metabolites are coupled to endogenous substances. Enzymes concerned with phase-II biotransformations are specific transferases. Most phase-II conjugates are acids that can be eliminated easily (Mutschler, 1997). Drug metabolism takes place especially in kidney, liver and gut, but also in CP drug metabolizing enzymes were found. Thus, CP epithelium represents not only a physical, but also an enzymatic barrier. In CP epithelium the isoforms CYP 2B1,2 and CYP 1A1 of the phase-I enzyme cytochrome P-450 were detected. Other phase-I metabolizing enzymes found in CP are monoamine oxidase and the membrane-bound form of epoxide hydrolase. Phase-II metabolizing enzymes in CP epithelium include the cerebral form of UDP-glucuronosyltransferase, glutathione-S-transferases (GST) isoforms  $\alpha$ ,  $\mu$ ,  $\pi$  and glutathione peroxidase. Therefore, CP epithelium is an important site for detoxification of xenobiotics (Gherssi-Egea/Strazielle, 2001).

### **1.5 Transport Mechanisms at the Choroid Plexus**

Substance permeation through lipid membranes can follow different mechanisms. These different mechanisms are important for substance transport through CP epithelium, on one hand for supplying the brain with substances from blood, on the other hand for elimination of eventually toxic metabolites out of the CNS.

Passive diffusion is energy-independent, substance transport takes place along a concentration gradient. Passive diffusion depends on concentration gradient, membrane area, membrane diameter, partition coefficient and diffusion coefficient of the substance. For diffusion through lipid membranes lipid solubility, charge and molecular size of a substance are the crucial factors. Diffusion processes cannot be inhibited competitively or by metabolic inhibitors. Facilitated diffusion is mediated by carriers, driving force is the concentration gradient between two compartments. Substances with low membrane permeability correlate with carrier molecules and the complex can diffuse through the membrane. This process is selective and saturable, carrier mediated diffusion can be inhibited competitively, but not by

metabolic inhibitors. Further transport mechanisms are pinocytosis, phagocytosis and persorption.

Different to passive diffusion, active transport processes are against a concentration gradient and energy dependent with, e.g. ATP as source of potential energy. Because of the energy dependency active transport processes can be inhibited competitive and by metabolic inhibitors (Mutschler, 1997).

In CP tissue the brush border membrane (BBM) faces the CSF and the basolateral membrane (BLM) faces the blood. Tight junctions between the cells prevent free exchange of compounds between blood and CSF (Kusuhara et al., 2004). Only small-sized, uncharged and lipid-soluble substances can diffuse through CP epithelial cells. Other compounds have to be transported actively through the polarized epithelial cells. These transport processes are composed of three steps: uptake into the cell at the apical membrane of CP epithelial cells, crossing the cytoplasm and efflux at the basolateral membrane of the cell or the other way round. The molecular basis for transport are multiple groups of transport proteins expressed in CP epithelium. For most water soluble substances, that cannot pass the epithelium through passive diffusion, both transmembrane steps are mediated by transporters, different transport proteins are involved in uptake and efflux step. Table 4 shows transport proteins expressed in CP epithelium in rat. Transport processes can be visualized by confocal laserscanning microscopy. The distribution of different fluorescent molecules can be chased and quantified using this tool. Formerly radiolabeled substances were used to analyze transport processes in CP epithelium, but only accumulation in the whole tissue can be measured, seeing that only apical transport processes can be assessed. With confocal laserscanning microscopy the whole three-step mechanism composed of apical uptake, intracellular crossing through the cytoplasm and basolateral efflux can be traced (Miller, 2004).

### **1.6 Transporters for Organic Anions**

As shown in Table 4 several transport proteins are localized to CP epithelium. Time and again new organic anion transporters are cloned, characterized and shown to be expressed in CP epithelial cells. A part of the transporters is already localized to either the apical or basolateral membrane of CP epithelium. All these transporters, localized asymmetrically to the polarized epithelium, drive concentrative, energy dependent, vectorial transport (Kusuhara et al, 2004; Miller, 2004).

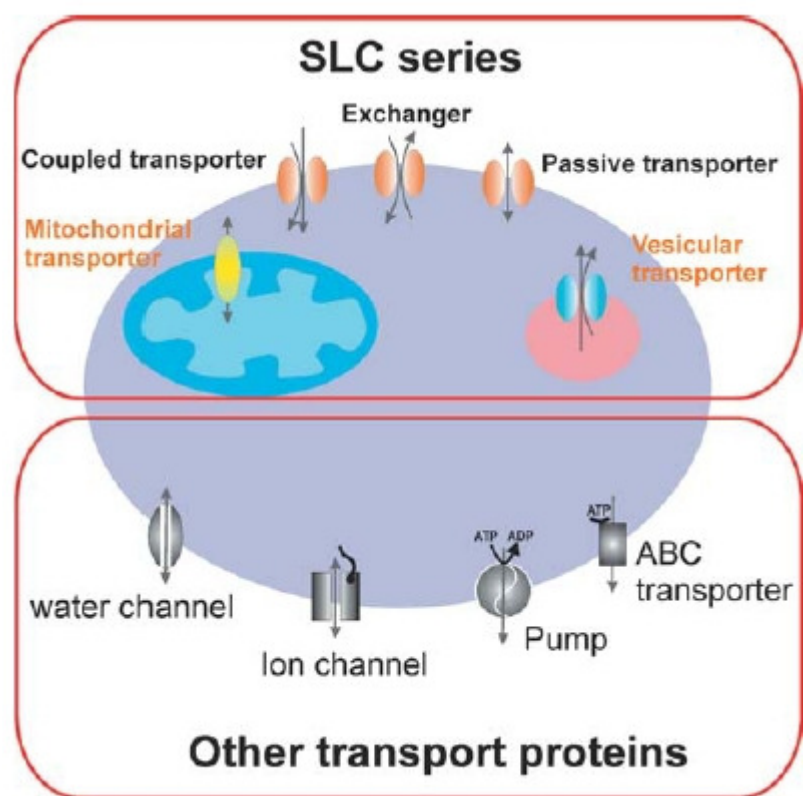
**Table 4:** Major active transport proteins that are located to the CP of rats. Localization is identified for a few transporters, for most of them localization remains to be analyzed. BLM: basolateral membrane; BBM: brush border membrane, ND: not detected. Table modified from Choudhuri et al., 2003; Kusuhara et al., 2004; Leggas et al., 2004, Rao et al., 1999.

| <b>Name</b>   | <b>Gene symbol</b>     | <b>Localisation</b>     |
|---|------------------------|-------------------------|
| <u>Organic anion transporting polypeptide (Oatp) family</u> |                        |                         |
| Oatp2   | <i>Slco1a4/Oatp1a4</i> | BLM                     |
| Oatp3   | <i>Slco1a5/Oatp1a5</i> | BBM                     |
| Oatp9/moat1   | <i>Slco2b1/Oatp2b1</i> | ND                      |
| Oatp12  | <i>Slco4a1/Oatp4a1</i> | ND                      |
| Oatp14/BSAT1  | <i>Slco1c1/Oatp1c1</i> | ND                      |
| <u>Organic anion transporter (Oat) family</u>               |                        |                         |
| Oat1  | <i>Slc22a6</i>         | ND                      |
| Oat2/NLT  | <i>Slc22a7</i>         | ND                      |
| Oat3  | <i>Slc22a8</i>         | BBM                     |
| <u>Organic cation transporter (Oct) family</u>              |                        |                         |
| Oct 1 <sup>a)</sup>   | <i>Slc22a1</i>         | ND                      |
| Oct 2 <sup>a)</sup>   | <i>Slc22a2</i>         | BBM <sup>b)</sup>       |
| Oct3  | <i>Slc22a3</i>         | ND                      |
| <u>Octn family</u>  |                        |                         |
| Octn1   | <i>Slc22a4</i>         | ND                      |
| Octn2/CT1   | <i>Slc22a5</i>         | ND                      |
| <u>Peptide transporter</u>                                  |                        |                         |
| Pept2   | <i>Slc15a2</i>         | ND                      |
| <u>ABC transporter: P-glycoprotein</u>                      |                        |                         |
| Mdr1a   | <i>Abcb1a</i>          | Subapical <sup>a)</sup> |
| Mdr1b   | <i>Abcb1b</i>          | Subapical <sup>a)</sup> |
| Mdr2  | <i>Abcb2</i>           | ND                      |
| <u>Multidrug resistance protein (Mrp) family</u>            |                        |                         |
| Mrp1  | <i>Abcc1</i>           | BLM                     |
| Mrp2  | <i>Abcc2</i>           | ND                      |
| Mrp3  | <i>Abcc3</i>           | ND                      |
| Mrp4  | <i>Abcc4</i>           | BLM                     |
| Mrp5  | <i>Abcc5</i>           | ND                      |
| Mrp6  | <i>Abcc6</i>           | ND                      |

<sup>a)</sup>controversial <sup>b)</sup>localization of the chimeric protein (rOct2-GFP)

Often these transporters exhibit overlapping substrate specificities. For this reason it is difficult to identify transport proteins involved in transport of specific anionic xenobiotics or metabolites. In Figure 5 transport proteins and their different mechanisms of transport mediation are shown. Active and passive transport mechanisms are pictured, passive transport is energy-independent and follows a concentration gradient as described above. Active transport proteins can be classified in ion coupled transporters, influx or efflux transporters or exchangers (Hediger et al., 2004; Kusuhara et al., 2004; Miller, 2004).

**Figure 5:** Transport proteins of the SLC family and different transporters. SLC transporters are membrane-bound, either located to the plasma membrane or in intracellular compartment membranes. Passive transporters, ion coupled transporters and exchanger belong to the SLC transporter family. The non-SLC transport proteins as ABC transporters, ATP-dependent efflux pumps, ion channels and water channels can also be expressed in intracellular compartments. Figure from Hediger et al., 2004.



### 1.6.1 Solute Carrier (SLC) Family

Currently, the gene superfamily of solute carriers (SLC) consists of 43 families and 298 transporter genes, but constantly new transporters of the SLC family are identified. The SLC family include genes encoding passive transporters, ion coupled transporters and exchangers, transport proteins are membrane-bound. Transport proteins belong to the SLC family when 20-25% of amino acid sequence is identical to those of other proteins of the SLC family. Gene defects in numerous members of the SLC family are shown to play a role in different diseases. A number of transporters are important for pharmaceutical perspectives.

Transporters belonging to the SLC family can mediate uptake into the cell, efflux out of the cell or act as exchangers. Glucose transporters, neurotransmitter transporters, intestinal bile acid transporters and cation-Cl<sup>-</sup> cotransporters are used as drug targets (Hediger et al., 2004). In CP epithelium several members of the SLC family are expressed. Most of these transporters are detected at mRNA level, localization to the basolateral or apical membrane of CP epithelial cells remains to be analyzed (Choudhuri et al., 2003). As shown in Table 4, SLC transporters of the families *Slco*, *Slc15*, and *Slc22* are expressed in CP.

### 1.6.1.1 The Organic Anion Transporting Polypeptide Family (*Slco*)

Fourteen members of the organic anion transporting polypeptide (Oatp) family have been identified in rodents (Hagenbuch et al., 2003). In rat CP epithelium rOatp3 (*Slco1a5*, Oatp1a5) is the most abundant isoform which is located to the BBM (Kusuhara et al., 2003). Expression of other isoforms in rat CP was analyzed: rOatp2 (*Slco1a4*, Oatp1a4), rOatp9 (*Slco2b1*, Oatp2b1), rOatp12 (*Slco4a1*, Oatp4a1) and rOatp14 (*Slco1c1*, Oatp1c1) were detected, mRNA expression of rOatp4 (*Slco1b2*, Oatp1b2), rOatp5 (*Slco1a6*, Oatp1a6) and rOat-K1/Oat-K2 (*Slco1a3*, *Slco1a3*) was below detection limit. According to expression on mRNA level, expression of rOatp9, rOatp12 and rOatp2 in rat CP is much lower than expression of rOatp3 (Choudhuri et al., 2003).

rOatp3 cDNA encodes a 670-amino acid protein of approximately 80 kDa with 12 putative transmembrane domains. The tissue distribution of rOatp3 is still under discussion, northern blot analyses using the 3' non-coding region as probe detected rOatp3 expression in the kidney (Abe et al., 1998), analyses using the RNase protection assay revealed rOatp3 expression in the brain, small intestine, lung and retina, but no expression in kidney or liver (Walters et al., 2000). Quantification of Oatp3 mRNA expression using the branched DNA signal amplification method revealed abundant expression in the lung, cerebellum and female cerebral cortex and expression to a lesser extent in the intestine (Li et al., 2002). rOatp3 has a broad substrate specificity including amphipatic organic anions as bile acids, estradiol-17 $\beta$ -D-glucuronide (E217 $\beta$ G), estrone sulfate (ES), dehydroepiandrosterone sulfate (DHEAS) and thyroid hormones (Abe et al., 1998; Cattori et al., 2001; Kusuhara et al., 2003; Ohtsuki et al., 2003).

The cDNA for Oatp2 encodes a 661-amino acid protein with a molecular mass of 92 kDa (Reichel et al., 1999). Substrate specificity of rOatp2 is similar to that of rOatp1 and rOatp3 with a higher affinity to cardiac glykosides such as ouabain and digoxin (Cattori et al., 2001).

Further substrates of rOatp2 are bulky organic cations as N-(4,4-azo-n-pentyl)-21-deoxyajmalinium, N-methyl-quinidine, N-methyl-quinine, rocuronium and anionic peptides as BQ-123, [D-Pen2,D-Pen5]enkephalin and deltorphin II (Gao et al., 2000). rOatp2 is a bidirectional transport protein (Li et al., 2000) that is expressed to the BLM of CP epithelium. In CP epithelium rOatp2 seems to be involved in the excretion of its substrates out of the CNS into blood, but also in uptake from the blood into epithelial cells (Kusuhara et al., 2004).

rOatp9 is ubiquitously expressed in the body. In rat brain rOatp9 is expressed in the neuronal cells of the CNS, especially in hippocampus and cerebellum, but expression was below detection limit in rat CP using northern blots and in situ hybridization (Nishio et al., 2000). However, Choudhuri et al. (2003) detected mRNA of rOatp9 in CP tissue. Substrates of rOatp9 include prostaglandins (PGE<sub>2</sub>, PGD<sub>2</sub> and PGE<sub>1</sub>), leukotriene C<sub>4</sub> (LTC<sub>4</sub>) and thromboxan B<sub>2</sub> (Kobayashi et al., 2003).

rOatp12 is the rodent analog of hOATP-E, the only known substrate of rOatp12 is triiodothyronine (T<sub>3</sub>), whereas the human analog transports T<sub>3</sub>, thyroxine (T<sub>4</sub>), reverse T<sub>3</sub> and E217βG (Sato et al., 2003).

rOatp14 was primarily identified as BBB-specific anion transporter 1 (BSAT1) (Li et al., 2001), its cDNA consists of 2148 base pairs (bp) that encode a 716 amino acid protein with 12 putative membrane-spanning domains. Substrates of rOatp14 are organic anions as E217βG, cerivastatin and troglitazone, as well as T<sub>4</sub> and reverse T<sub>3</sub>. T<sub>4</sub> is the substrate which shows highest affinity to rOatp14 among its mentioned substrates. Sugiyama et al. could detect protein expression of rOatp14 in CP using western blot analyses (Sugiyama et al., 2003).

### **1.6.1.2 The Proton Oligopeptide Cotransporter Family (*Slc15*)**

The Slc15 gene family encodes for peptide transporters. In rat CP Pept2 (*Slc15a2*) has been located to the apical membrane of CP epithelial cells. Different to Pept1 (*Slc15a1*), which is expressed to highest rates in small intestine, gonads and kidney in rat, Pept2 expression is highest in kidney, brain and lung (Lu/Klaassen, 2005). In kidney proximal tubules epithelium Pept2 is located to the brush border membrane as well as Pept1, but Pept1 is located to the S1 and S2 segment of kidney proximal tubules whereas Pept2 is located to the S3 segment (Russel et al., 2002). Pept2 is an electrogenic H<sup>+</sup>-dependent cotransporter which mediates transport of its substrates in a Na<sup>+</sup>-dependent manner. Pept2 accepts di- and tripeptides as well

as peptide-mimetic drugs, such as  $\beta$ -lactam antibiotics containing an  $\alpha$ -amino-group as several penicilline and cephalosporine as substrates. Further substances transported by Pept2 include angiotensin-converting enzyme inhibitors (Kusuhara et al., 2004) and valacyclovir. Pept2 mediated transport processes can be inhibited by ampicillin, amoxicillin, cyclacillin, cephalixin, cefadroxil, cephradine, cefdinir, ceftibuten, cefixime and bestatin. The transporter Pept1 has a similar substrate spectrum including glycylysarcosin (GlySar), 5-aminolevulinic acid (5-ALA), cefixime, L-Dopa-L-Phe and Val-azidothymidine. In the intestine Pept1 may contribute to the intestinal absorption of orally administered xenobiotics, whereas Pept1 and Pept2 in the kidney may play a role in accumulation of glomerular-filtered xenobiotics (Russel et al., 2002). The functional role of Pept2 in CP epithelium was analyzed by Ocheltree et al. (2004). In gene knockout mice they had the possibility to analyze function of one transport protein that belongs to multiple gene families. The results of transport studies in Pept2 null animals in comparison to wild-type mice indicate that active uptake of GlySar was reduced about 95 % in Pept2 null mice. Similar results were found for active uptake of the peptidomimetic compound 5-ALA, 5-ALA uptake was reduced about 92 % in Pept2 null mice compared to wild-type animals. Taken together the results give evidence that Pept2 is the sole transporter for transport of 5-ALA and GlySar in CP. Pept2 seems to play an important role in the trafficking of endogenous and exogenous peptidomimetics and polypeptides between CSF and blood (Ocheltree et al., 2004).

### **1.6.1.3 The Organic Ion Transporter Family (*Slc22a*)**

The organic ion transporter family is a superfamily composed of organic anion transporter (Oat, *Slc22a*), organic cation transporter (Oct, *Slc22a*), carnitine/organic cation transporter (Octn, *Slc22a*), CT2 and URAT1. CT2 is a transporter for carnitine whereas URAT1 transports urate. The transporters of the Oat, Oct and Octn family are of particularly interest for transport processes in the CP and will be detailed in the following chapters.

#### **1.6.1.3.1 Organic Anion Transporter (Oat)**

Four Oat genes have been identified, in rodents the organic anion transporters Oat1-3 and Oat5 are described. Choudhuri et al. (2003) detected mRNA of three Oats in rat CP: rOat1 (*Slc22a6*), rOat2 (*Slc22a7*) and rOat3 (*Slc22a8*). rOat3 is the most abundant isoform in rat CP, followed by rOat1 and rOat2 (Choudhuri et al., 2003). Protein expression of rOat3 could be demonstrated using western blot analyses, but rOat1 could not be detected (Nagata et al.,

2002). Immunolocalization showed localization of rOat3 to the BBM of the CP (Nagata et al., 2002) and BLM of kidney proximal tubules (Russel et al., 2002). Oat3 has a broad substrate specificity including amphipathic organic anions as E217 $\beta$ G, ES and DHEAS, hydrophilic organic anions as *p*-aminohippurate (PAH) and benzylpenicillin and the organic cation cimetidine (Kusuhara et al., 2004; Nagata et al., 2002; Russel et al., 2002). Oat3 mediated transport processes can be inhibited by i.a. probenecid, bromosulphophthalein (BSP), indocyanine green and furosemide (Russel et al., 2002). It is likely that rOat3 acts as an exchanger and an outward concentration gradient of dicarboxylates (e.g.  $\alpha$ -ketoglutarate), formed by the sodium-dependent dicarboxylate co-transporter and the tricarboxylic acid or citric acid (TCA) cycle, drives rOat3-mediated transport (Kusuhara et al., 2004). Experiments with mOat3 knockout mice showed that Oat3 plays a role in transport function in CP. Fluorescein (FL) transport in CP was markedly reduced in CP of Oat3 knockout mice compared to wildtype mice (Sweet et al., 2002).

rOat1 was described as a classical organic anion transporter in the kidney (Sweet et al., 1997). It is located to the BLM of kidney proximal tubules and shows a broad substrate specificity as well as rOat3. rOat1 substrates include organic anions as PAH, acyclovir and  $\beta$ -lactam antibiotics as cephaloridine and benzylpenicilline, nucleoside analogs as azidothymidine (AZT) or 9-(2-phosphonylmethoxyethyl)adenine (PMEA) and nonsteroidal anti-inflammatory drugs as salicylate and acetylsalicylate (Kusuhara et al., 2004; Russel et al., 2002; Sweet et al., 1997). rOat1 mediates transport processes as an exchanger (Sweet et al., 1997).

rOat2 was registered as a novel-liver specific transporter (NLT) (Sekine et al., 1998; Simonson et al., 1994) with a relatively broad substrate specificity. NLT or Oat2 transports  $\alpha$ -ketoglutarate, prostaglandine E<sub>2</sub> (PGE<sub>2</sub>), PAH, methotrexate (MTX) and acetylsalicylate (Russel et al., 2002).

### 1.6.1.3.2 Organic Cation Transporter (Oct)

Organic cation transporter (Oct) are multispecific facilitative transporters for hydrophilic and small organic cations. In rodents three isoforms have been isolated: Oct1-Oct3 (Van Montfoort et al., 2003). The Oct isoform expression in rat CP is controversial, Sweet et al. (2001) used cDNA from rat CP as a template and revealed expression of rOct2 (*Slc22a2*) and rOct3 (*Slc22a3*), but not rOct1 (*Slc22a1*) in rat CP using PCR analyses. Contrary to these findings, Choudhuri et al. (2003) quantified mRNA expression in rat CP and found low expression rates for rOct1 and rOct3 in rat CP, rOct2 expression level was below detection

limit. rOct1 is expressed abundantly in the kidney, liver and intestine (to a less extent) in rat (Grundemann et al., 1994). rOct1 is an uptake transporter and transport processes mediated by rOct1 are membrane voltage dependent. The Oct isoforms have a similar substrate specificity including small and hydrophilic organic cations as tetraethylammonium (TEA) and N-methylnicotinamide (NMN). rOct2 exhibits a relatively lower affinity to TEA compared to affinities of rOct1 and rOct3 (Jonker/Schinkel, 2004). The localization of rOct1, rOct2 and rOct3 in CP epithelium remains to be identified. A chimeric protein of rOct2-green fluorescent protein fusion construct (GFP) was produced and transfected to isolated rat CP. The fluorescence associated with rOct2-GFP was localized to the BBM of CP epithelium, suggesting an apical localization of rOct2, if expressed in rat CP (Sweet et al., 2001). Different knockout mice have been developed recently. Mouse strains of Oct1, Oct2, Oct3 knockouts and Oct1/Oct2 double knockout mice have been established (Jonker et al., 2001; Jonker et al., 2003; Zwart et al., 2001), but transport experiments in isolated CPs were not done by now (Kusuhara et al., 2004).

### 1.6.1.3.3 Carnitine/Organic Cation Transporter (Octn)

Three isoforms of the Octn family have been isolated in rodents: Octn1-Octn3 (Koepsell/Endou, 2004). Abundant expression of rOctn2 (*Slc22a5*) has been demonstrated in rat CP, rOctn1 (*Slc22a4*) was detected to a lesser extent, whereas rOctn3 (*Slc22a6*) expression remains to be analyzed (Choudhuri et al., 2003). Octn2 is a sodium-dependent carnitine transporter (Sekine et al., 1998) which also transports TEA (Tamai et al., 2000). hOCTN1 is regarded to be a H<sup>+</sup>/organic cation exchanger that is multispecific and pH-dependent. Substrates for hOCTN1 include organic cations as pyrilamine, quinidine and verapamil as well as carnitine. Interestingly cation uptake mediated by hOCTN1 is sodium independent whereas carnitine uptake mediated by hOCTN1 shows sodium dependency (Yabuuchi et al., 1999).

## 1.6.2 ATP Binding Cassette Superfamily

The ATP binding cassette (ABC) superfamily is characterized by the cytoplasmic localization of the ABC and the unidirectional efflux transport of its substrates. The ABC acts as a catalysator for ATP hydrolysis which is essential for transport processes mediated by ABC transporters (Kusuhara et al., 2004). The following sections attend to the multidrug

resistance-associated proteins (Mrp/Abcc) and P-glycoprotein (P-gp), because expression of these transport proteins was previously analyzed in CP epithelium.

### 1.6.2.1 Multidrug Resistance-Associated Proteins (Mrp/Abcc)

Nine structurally and functionally related multidrug resistance-associated protein (MRP) family members have been identified (MRP1-9). The isoforms are different concerning their localization, expression levels, and substrate specificity (Van de Water et al., 2005). mRNA expression of Mrp1-Mrp6 in rat CP was investigated by Choudhuri et al., 2003. An abundant expression rate of Mrp1 (*Abcc1*), Mrp4 (*Abcc4*) and Mrp5 (*Abcc5*) was found, whereas Mrp6 (*Abcc6*) showed a moderate expression. Mrp2 (*Abcc2*) and Mrp3 (*Abcc3*) expression rates in rat CP were very low (Choudhuri et al., 2003). Expression levels of Mrp7-Mrp9 are not analyzed by now.

Mrp1 expression and localization in rat CP is well investigated. As described above, mRNA expression of Mrp1 is high in CP (Choudhuri et al., 2003), protein expression experiments using western blot analyses have localized Mrp1 to the basolateral membrane of CP epithelium (Nishino et al., 1999; Ohtsuki et al., 2003). The mRNA of MRP1 encodes for a 1531 amino acid protein with an apparent molecular weight of 190 kDa and 17 transmembrane domains with two cytoplasmically located ABCs (Cole et al., 1992). Mrp1 is a basolateral efflux transporter in rat CP, it has a wide substrate specificity including amphipathic organic anions as LTC<sub>4</sub>, E217βG, etoposide-glucuronide and reduced glutathione. Mrp1 mediated transport processes can be inhibited by addition of e.g. probenecid, MK571, cyclosporin A, PSC833 and indomethacine (Russel et al., 2002).

MRP4 mRNA encodes for a 1325 amino acid protein with a molecular weight of 170 kDa and 12 putative transmembrane domains (Van Aubele et al., 2002). In CP epithelium Mrp4 seems to be located to the BLM (Leggas et al., 2004; present study), this colocalization to Mrp1 indicates involvement of Mrp4 in basolateral efflux of its substrates into blood. Substrates of Mrp4 are the second messengers cAMP and cGMP (Chen et al., 2001; Van Aubele et al., 2002), it also transports acyclic nucleoside phosphonates, for example PMEA (adefovir) and monophosphorylated nucleoside analogs such as azidothymidine-monophosphate (AZT-MP, zidovudine-monophosphate) (Lee et al., 2000). In addition, Mrp4 substrates include PAH and methotrexate (Lee et al., 2000; Smeets et al., 2004). Mrp4 mediated transport can be reduced by probenecid, dipyrindamole, S-(dinitrophenyl)-glutathione (DNP-SG) and other substances (Russel et al., 2002). Leggas et al. developed Mrp4 knockout mice and showed that topotecan

accumulated in brains of the knockout animals due to the absence of Mrp4 which actively eliminates topotecan into blood (Leggas et al., 2004).

MRP5 gene encodes for a protein with a molecular weight of approximately 185 kDa (Jedlitschky et al., 2000), 1437 amino acids and 12 putative transmembrane domains (Van Aubele et al., 2002). Within the Mrp family Mrp5 is most closely related to Mrp4, both transport proteins lack the first five membrane-spanning regions and share a similar substrate specificity (Wijnholds et al., 2000). Substrates of Mrp5 include i.a. DNP-SG, PMEA, cAMP, cGMP and fluorescein-diacetate (FDA) (Russel et al., 2002). Localization of Mrp5 protein in rat CP remains to be established.

Mrp6 protein consists of 1503 amino acids with three membrane spanning domains (MSD1-3). In mice Mrp6 gene is expressed predominantly in liver and kidney, low level expression in other tissues was detected as well. Mrp6 substrates include glutathione conjugated to LTC<sub>4</sub>, N-ethylmaleimide (Matsuzaki et al., 2005) and BQ123 (Russel et al., 2002). Moderate mRNA expression of Mrp6 was detected in rat CP (Choudhuri et al., 2003), but protein expression or localization remains to be analyzed.

### **1.6.2.2 P-Glycoprotein (P-gp/*ABCB1*)**

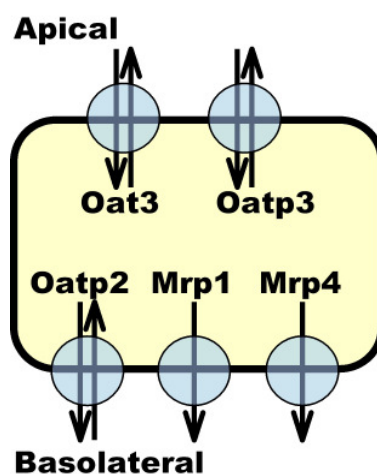
P-gp gene encodes for a 1289 amino acid protein with a molecular weight of approximately 140-170 kDa and 12 transmembrane domains with two cytoplasmically located ATP-binding cassettes. In rodents two isoforms, Mdr1a (*Abcb4*) and Mdr1b (*Abcb1*), are commensurate to the human ortholog MDR1. Mdr1 is an important efflux transport protein involved in multidrug resistance in brain capillary endothelial cells forming the BBB and in the small intestine (Schinkel et al., 1994). Substrate specificity of P-gp is broad and includes hydrophobic neutral or cationic substances, i.a. fexofenadine, E217βG, cancer drugs as doxorubicine, vincristine, immunosuppressive drugs as cyclosporin A, HIV protease inhibitors such as ritonavir and saquinavir and cardiac drugs like quidine. P-gp activity can be reduced by addition of several inhibitors as verapamil, cyclosporine A, mifepristone and quinidine (Sun et al., 2003). At the BBB P-gp is an efflux transporter of particular interest, because it plays a major role in the phenomenon of multidrug resistance, many pharmaceutical drugs cannot overcome the BBB because they are transported out of the brain capillary endothelial cells back into blood by P-gp (Löscher/Potschka, 2005).

In CP epithelium P-gp seems to be located subapical, Rao et al.(1999) detected this localization in primary cell cultures of rat CP epithelial cells grown on filters. In a previous study we approved this localization in isolated rat CPs, no functionality could be verified using porcine CP cell culture (Reichel et al., 2004).

## 1.7 Localization of Organic Anion Transporters

Due to the number of different transport proteins and varieties in substrate specificities, it is important to localize these transporters to the different membranes of polarized cells. In CP epithelium the basolateral membrane faces the blood, whereas the apical membrane faces the CSF. Not much is known about localization of transport proteins in the CP, transporters with known localizations are shown in Figure 6.

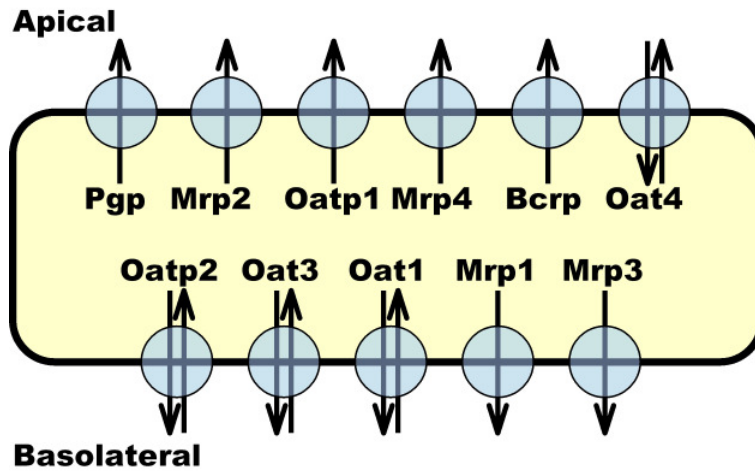
**Figure 6:** Localization of transport proteins in CP epithelium. Oat3 and Oatp3 are located to the apical membrane, whereas Oatp2, Mrp1 and Mrp4 are located to the basolateral site. Only transporters are shown that are clearly localized to one membrane by immunostaining.



The exchangers Oat3 and Oatp3 are located to the apical membrane of CP epithelial cells, Oatp2, Mrp1 and Mrp4 are located to the basolateral membrane.

Transporter distribution in CP epithelium is partially contrary to localization in kidney proximal tubulus epithelial cells. In Figure 7 an assortment of transport proteins in kidney proximal tubulus epithelium is shown. Contrary to the findings in CP epithelium, Mrp4 is located to the apical membrane of kidney proximal tubules epithelial cells whereas Oat3 is located to the basolateral membrane (Russel et al., 2002).

**Figure 7:** Localization of transport proteins in kidney proximal tubulus epithelial cells. Localization of Mrp4 and Oat3 is contrary to that in CP epithelium.



## **2 Purpose of the study**

Aim of the study were analyses of transport mechanisms for organic anions in different models, especially in CP tissue. Due to the difficult isolation and the low viability of rat CP tissue, different models for transport processes were used to get evidence for transport proteins involved in transport processes in rat CP.

### **2.1 Fluo-cAMP Transport in Killifish Proximal Tubulus**

Due to the possibility of visualization of transport processes by confocal microscopy, one purpose was the investigation of Mrp4 function using the fluorescent dye fluo-cAMP. As cAMP is a common substrate for Mrp4 used its fluorescent analog as model substance for transport processes mediated by Mrp4, which is localized to the apical membrane of killifish (*fundulus heteroclitus*) proximal tubules, as shown in the present study. To analyze these transport processes, we performed functional analyses using fluo-cAMP as substrate and different inhibitors of organic anion transport in killifish proximal tubules. Furthermore we investigated regulatory pathways which are involved in regulation of transport of the fluorescent compound. Killifish kidneys contain a high fraction of proximal tubules (Evans, Physiology of Fishes), which can be easily isolated and are stable at room temperature for a long period of time. Due to the similarity between kidney and CP, concerning function and transport proteins expressed (Breen et al., 2004; Kusuhara et al., 2004; Miller, 2004; Spector/Johanson, 1991), killifish proximal tubules seem to be a good model for transport processes in CP.

### **2.2 Fluo-cAMP Transport in Membrane Vesicles**

For analyses of specific transport processes mediated by MRP2 and MRP4, we used membrane vesicles of MRP2 and MRP4 overexpressing cells, respectively. Using this model, fluo-cAMP transport mediated by both MRPs could selectively be investigated. The advantage of using membrane vesicles of overexpressing cells is the possibility to study transport processes mediated by only one protein.

### **2.3 Fluo-cAMP Transport in Rat Choroid Plexus**

To examine the eligibility of the described methods as models for transport processes in CP tissue, we performed transport studies using fluo-cAMP as substrate in rat CP as well. Initially, we analyzed expression and localization of Mrp4 in rat CP and accomplished transport studies as described for the killifish model. For analyses of regulatory processes involved in transport of fluo-cAMP we researched into the effects of activators or inhibitors for different regulatory cascades including endothelin and mitogen-activated proteinkinase pathway.

### **2.4 Texas Red Transport in Rat and Shark CP**

Dogfish shark (*Squalus acanthias*) CP is easily accesible, of a large size and stable for a long period of time. These features are reasons for the use of shark CP as a model for mammalian CP. We analyzed transport of the fluorescent dye texas red (TR) in CPs of both species for comparison of transport processes. As described above, we incubated CP tissue with TR and different modulators of organic anion transport to specify transport proteins involved in TR transport in rat and shark CP, respectively.

### **2.5 Regulation of Fluorescein-Methotrexate Transport**

From previous studies we know that transport proteins involved in fluorescein-methotrexate (FL-MTX) transport in rat and dogfish shark are the same (Baehr et al., in press; Breen et al., 2004). For further comparison of FL-MTX transport we wanted to investigate into regulatory pathways driving transport of FL-MTX in both species. Baehr et al. (in press) analyzed regulation of FL-MTX transport in dogfish shark CP, here we determined regulation of FL-MTX transport in CPs of rats.

## 3 Materials and Methods

### 3.1 Materials

All chemicals were reagent grade or better and obtained from Sigma Chemical co. (St. Louis, MO/ Zwijndrecht, the Netherlands/ Steinheim, Germany) or other commercial sources.

MDCKII-MRP2 cells were obtained from P. Borst (Dutch Cancer Institute, Amsterdam, the Netherlands). For fluorescence measurements in membrane vesicle studies a Shimadzu RF-5301PC spectrofluorophotometer was used.

The RNeasy Kit® for RNA Isolation was obtained from Qiagen GmbH (Mannheim, Germany). Tissue was stored in RNAlater®, obtained from Sigma-Aldrich GmbH (Steinheim, Germany) before RNA-Isolation. RNA was quantified using a NanoDrop® ND-3300 fluorospectrophotometer obtained from Nanodrop Technologies (Wilmington, DE). The Promega Reverse Transcription System® was purchased from Promega GmbH (Mannheim, Germany). Ethidium Bromid was obtained from GibcoBRL (Karlsruhe, Germany). RiboLock ribonuclease inhibitor was purchased from Fermentas GmbH (St. Leon-Rot, Germany). Supertaq® was from MoBiTec GmbH (Freiburg, Germany). Primers were custom primers obtained from Invitrogen (Karlsruhe, Germany). Both, reverse transcription (RT) and polymerase chain reaction (PCR) were performed in a PCRSprint® cyclor from Thermo Hybaid (Heidelberg, Germany).

The used primary Mrp4 antibody in killifish experiments was a rat Mrp4 antibody (pAb rM4-pl) raised in rabbit at the Nijmegen Centre for Molecular Life Sciences (NCMLS, Rabound University, Nijmegen, the Netherlands) described in Van Aubel et al., 2002. Goat derived anti-rabbit IgG 488 was obtained from Molecular Probes (Eugene, OR). For immunocytological experiments in rats, Mab to Mrp4 (M<sub>4</sub>I-80) from Alexis (Grünberg, Germany) and rabbit derived FITC-labeld anti-rat IgG from DAKO A/S (Glostrup, Denmark) were used. The fluorescence enhancer Aqua Poly/Mount was obtained from Polysciences Inc. (Warrington, PA).

Male and female sprague-dawley and wistar rats were obtained from the animal faculty of the university of Heidelberg. TR<sup>-</sup> rats were a kind gift from Prof. Dr. Petzinger (University of Gießen, Germany).

Isofluran for anaesthetizing rats was obtained from Abbott (Wiesbaden, Germany). Fluo-cAMP and fluo-cGMP were purchased from Biolog Life Science institute (San Diego, CA/

Bremen, Germany). Fluorescein-Methotrexate (FL-MTX) and phorbol-12-myristate-13-acetate (PMA) were obtained from Molecular Probes (Eugene, OR). Texas Red (TR) was obtained from Sigma-Aldrich GmbH (Steinheim, Germany). MK571 was purchased from Biomol (Hamburg, Germany). Prostaglandin E<sub>2</sub> was a kind gift from the group of Prof. Dr. Offermanns (University of Heidelberg, Germany). The radioactive [<sup>3</sup>H]-cGMP was obtained from Moravek Biochemicals (Brea, CA) or Amersham Pharmacia Biotech (Freiburg, Germany). Ultima Gold MV Liquid Scintillation Cocktail was obtained from Canberra Packard (Frankfurt, Germany). Radioactivity analyses were carried out in a Tricarb 2000 CA Scintillation Counter from Canberra Packard (Frankfurt, Germany).

Fluorescence was visualized using Confocal Laser Scanning Microscopy. The used Confocal Laser Scanning microscopes were the Leica DM IRBE from Leica (Bensheim, Germany) and the Olympus Fluoview from Melville (NY, USA).

## **3.2 MDCKII and Sf9-Cells**

MDCKII (Madin-Darby Canine Kidney) cells overexpressing human MRP2 were obtained from P. Borst (Dutch Cancer Institute, Amsterdam, the Netherlands). Sf9 (*Spodoptera frugiperda*) cells expressing human MRP4 were generated by infection of cells using a recombinant baculovirus encoding MRP4 or, as a control, Opsine, as described previously (Van Aubel et al., 2002) at the NCMLS (Rabound University, Nijmegen, the Netherlands).

### **3.2.1 Cell Culture**

We carried out cell culture at 37°C, 5% CO<sub>2</sub> und 95% relative humidity. Culture medium was composed of Dulbecco's MEM 1x with 10 % fetal calf serum and 1 % penicillin/streptomycin added. Once a week cells were passaged and seeded in cell culture flasks with an area of 75 and 175 cm<sup>2</sup>. After seven days in culture, cells were used for membrane vesicle isolation.

### **3.2.2 Isolation of Crude Membrane Vesicles**

Infected Sf9 cells were resuspended in ice-cold homogenization buffer (0.5 mM sodium phosphate, 0.1 mM EDTA), supplemented with protease inhibitors (100 µM PMSF, 5 µg/ml aprotinin, 5 µg/ml leupeptin, 1 µg/ml pepstatin, 1 µM E64), and shaken on ice for 1 h. Lysed

cells were centrifuged at 100,000 x *g* and 4°C and the resulting pellet was homogenized in ice-cold TS buffer (10 mM Tris-HEPES, 250 mM sucrose, pH 7.4) with a tight-fitting Dounce glass tissue grinder. The homogenate was centrifuged at 500 x *g* and 4°C and the resulting supernatant was centrifuged at 100,000 x *g* at 4°C. The resulting pellet was resuspended in TS buffer and passed 30 times through a 27-gauge needle. Aliquots of crude membrane vesicles were frozen in liquid nitrogen and stored at -80°C until use. Sf9 membrane vesicles were prepared and characterized at the NCMLS (Nijmegen, the Netherlands).

MDCKII-MRP2 cells were directly scraped in homogenization buffer supplemented with protease inhibitors as described above, and centrifuged at 100,000 x *g* and 4°C to collect cells and debris. The pellet was homogenized in TS buffer, and the procedure, described for Sf9 cells, was followed to obtain vesicles. MDCKII-MRP2 membrane vesicles were prepared and characterized at the NCMLS (Nijmegen, the Netherlands). ~65% of the vesicles were orientated inside-out.

### **3.3 Tissues *Ex Vivo***

For functional and immunocytological analyses we used freshly isolated tissues from killifishes, rats and dogfish sharks. All animal studies were performed in accordance with the rules of the local authorities for animal protection.

#### **3.3.1 Killifish Proximal Tubulus *Ex Vivo***

Killifish (*fundulus heteroclitus*) were collected in the vicinity of Mount Desert Island, Maine. The fishes were held in tanks with natural flowing sea water at the Mount Desert Island Biological Laboratory (MDIBL). After dispatching the animals, renal tubules masses were extracted and carried over into petri dishes containing marine teleost saline buffer based on Forster and Taggart (1950) (140 mM NaCl, 2.5 mM KCl, 1.5 mM CaCl<sub>2</sub>, 1.0 mM MgCl<sub>2</sub> and 20 mM Tris at pH 8.0). All experiments were carried out at room temperature (18-25°C).

Under a dissecting microscope, we removed adherent haematopoietic tissue with fine no. 5 forceps and proximal tubules were transferred to a foil-covered Teflon chamber (Bionique) containing marine teleost saline buffer for functional or 2% (v/v) formaldehyde and 0.1% (v/v) glutaraldehyde for immunocytological analyses.

### **3.3.2 Rat Choroid Plexus *Ex Vivo***

CPs were isolated from male and female Wistar and Sprague Dawley rats and TR<sup>-</sup> rats which are deficient in Mrp2. Rats were narcotized by inhaling isofluran in an exsiccator and sacrificed by cervical dislocation. Skullcap was sliced, the brain removed and placed into pregassed (95% O<sub>2</sub>/5% CO<sub>2</sub>) artificial cerebrospinal fluid (aCSF) containing 103 mM NaCl, 4.7 mM KCl, 1.2 mM KH<sub>2</sub>PO<sub>4</sub>, 1.2 mM MgSO<sub>4</sub> x 7 H<sub>2</sub>O, 25 mM NaHCO<sub>3</sub>, 10 mM glucose, 1 mM sodium pyruvate, 2.5 mM CaCl<sub>2</sub> at pH 7.4. Brains were cut into halves and both lateral CPs were removed. Each CP was cut into two pieces and placed in pregassed aCSF for functional analyses or in 8% Paraformaldehyde (PFA) for immunocytological experiments. For gene expression experiments whole CP tissue was stored in RNAlater® at –80°C until use.

### **3.3.3 Dogfish Shark Choroid Plexus *Ex Vivo***

Adult male and female spiny dogfish sharks (*Squalus acanthias*) were collected in the vicinity of Mount Desert Island, Maine. Sharks were held in large tanks of flowing sea water for 1-4 days before use. After decapitation the cranial compartment was removed immediately and transferred into icecold, pregassed (99% O<sub>2</sub>/1% CO<sub>2</sub>) elasmobranch ringer (ER), containing 280 mM NaCl, 6 mM KCl, 4 mM CaCl<sub>2</sub>, 3 mM MgCl<sub>2</sub>, 1 mM NaH<sub>2</sub>PO<sub>4</sub>, 0.5 mM Na<sub>2</sub>SO<sub>4</sub>, 350 mM urea, 72 mM trimethylamine oxide, 2.5 mM glucose, and 8 mM NaHCO<sub>3</sub> at pH 7.8, and placed on ice. The brain was removed and lateral and IV CPs were extracted, adherent tissue was excised and CPs were given into icecold ER. Each CP was dissected in two pieces.

## **3.4 Gene Expression**

### **3.4.1 Total RNA Isolation**

CP tissue frozen in RNAlater® was defrosted and up to 30 mg were lysed with RLT-buffer containing β-mercaptoethanol in a glass-homogenizer. Total RNA was isolated from the samples according to the Qiagen RNeasy® manual. After homogenization with RLT-buffer an equal volume of EtOH 70% was added. Samples were transferred onto RNeasy® mini spin columns and centrifuged for 30 seconds. Samples were washed and centrifuged with different

buffers as described in the RNeasy® protocol. Total RNA was eluted in 30 µl of nuclease free H<sub>2</sub>O. The amount of total RNA in the samples was quantified using a NanoDrop® ND-3300.

### 3.4.2 Reverse Transcription

Total RNA was transcribed in complementary DNA (cDNA) using reverse transcriptase. Reverse transcription (RT) was performed using 1 µg of total RNA. The Promega Transcription System® was used according to the manufacturers protocol. RNA was preincubated at 70°C for 10 minutes. Afterwards reaction mixture, containing 4 µl 5x avian myeloblastosis virus reverse transcriptase (AMV-RT) buffer, 4 µl MgCl<sub>2</sub> (25mM), 2 µl dNTP mixture (10mM), 1 µl oligo(dT)<sub>15</sub> primer (500 µg/ml), 0.5 µl Rnasin® or Riboblock® ribonuclease inhibitor (2.5 units), nuclease free water and 1 µl (5 units) of AMV-RT, was added and samples incubated at 42°C for 60 minutes. For determining the reaction samples were incubated at 95°C for 5 minutes and afterwards cooled to 4°C. The originated cDNA product was not stored, but directly used for polymerase chain reaction (PCR).

### 3.4.3 Polymerase Chain Reaction

For amplifying special regions of engendered cDNA, polymerase chain reaction was used. A hot start method (described by D'Aquila et al., 1991) was performed to destroy potentially formed primer-template complexes and prevent extension of these complexes during annealing. For PCR 0.1 µg of RNA (accordant 2 µl of template) was used. Template was mixed with a reaction mixture (5 µl Supertaq® reaction buffer containing MgCl<sub>2</sub> (20 mM), 0.25 µl of forward and reverse primer (100 µM), 2 µl of dNTP mixture (10 mM) and nuclease free water) and incubated at 94°C. After 8 minutes incubation 0.5 units Supertaq® were added. 15 up to 50 cycles of denaturation (94°C for 30 seconds), annealing (53°C for 30 seconds) and extension (72°C for 30 seconds) were performed. After a final extension at 72°C for 10 minutes, PCR products were stored at 4°C. PCR products were separated in a 1.5% agarose gel, containing 10 µl ethidium bromide per 100 ml, at 100 V for 1 hour. Visualization was carried out using UV-light and the Quantity One® software in a ChemieDoc™ XRS (Biorad, München, Germany).

We used forward and reverse primer that are specific for the target sequence, nucleotide sequences are listed in Table 5.

**Table 5:** Specific primers for Mrp4 and Pbgd cDNA. Primers are custom primers, ascertained after a nucleotide-nucleotide BLAST.

| Target | Forward Primer (5' to 3') | Reverse Primer (3' to 5') | Product Size (bp) |
|--------|---------------------------|---------------------------|-------------------|
| Ppgd   | GTGATGAAGGATGGGCAACT      | TTAAGGAGCACAGGGCACTT      | 360               |
| Mrp4   | CCTGGTAAAATGGGACTGA       | CTGTTAAGGCACAAAACCTG      | 773               |

### 3.4.4 Semiquantitative RT-PCR

Specific PCR products were amplified according to the described methods. 15 up to 50 cycles of denaturation, annealing and extension were performed in 5-cycle intervals. For analyzing linear amplification density of PCR products, visualized by ethidium bromide binding, was compared. Scion Image software (NIH, USA) was used to analyze density. For semiquantitative RT-PCR a cycle number with linear amplification was chosen and expression of target gene and housekeeping gene were compared. The non-regulated, pseudogene free housekeeping gene, Porphobilinogen deaminase (Pbgd) was used as standard housekeeping gene.

### 3.4.5 Immunocytological Staining

Freshly isolated killifish proximal tubules and rat CP tissue were stained using different protocols. As described by Masereeuw et al. (2000), tubules were washed (10 mM PBS) and fixed for 10 min at room temperature. Fixation solution was composed of 2% (v/v) formaldehyde and 0.1% (v/v) glutaraldehyde. After washing 5 times with 10 mM PBS, tubules were permeabilized using Triton X-100 1% (v/v) in PBS for 30 min. Tubules were washed and incubated with the primary pAb rM4-pl antibody in PBS for 90 min at 37°C. After washing 5 times, tubules were incubated with the fluorescein-labeled anti-rabbit IgG 488 for 60 min at 37°C and washed 5 times. Mrp4 localization was viewed using the Olympus fluoview confocal microscope.

Rat CP tissue was fixed in 8% PFA for 30 minutes at room temperature, followed by permeation in Triton X-100 0.1% (v/v) for 15 minutes. After washing 3 times with aCSF CPs were incubated with blocking buffer (1% BSA, 1% milk powder and 5% rabbit serum) for 1 hour. Subsequently CPs were incubated with blocking buffer (control) or Mab to Mrp4 M<sub>4</sub>I-

80 (described in Leggas et al., 2004) diluted 1:5 in blocking buffer at 4°C overnight. CPs were washed 3 times with Triton X-100 0.05% and incubated with rabbit derived FITC-labeled anti-rat IgG and 1 μM propidium iodide (PI) for 2 hours at room temperature. After washing 3 times with Triton X-100 and aCSF, fluorescence was visualized using the Leica DM IRBE confocal microscope. CPs were embedded in Aqua Poly/Mount to enhance fluorescence.

### **3.5 Functional Analyses**

Functional analyses were performed to determine transport proteins and their function in different models. Transport of the fluorescent compounds fluo-cAMP, TR and FL-MTX as well as the radioactive-labeled substance [<sup>3</sup>H]-cGMP were examined in membrane vesicles, killifish proximal tubules and rat or dogfish shark CP.

#### **3.5.1 Uptake Studies in Membrane Vesicles**

Uptake studies were performed using fluo-cAMP and [<sup>3</sup>H]-cGMP as substrates as described in Smeets et al. (2004). Vesicles stored at -80°C were prewarmed for 1 min at 37°C and added to a mixture of TS-Buffer (10 mM Tris-HEPES, 250 mM Sucrose, pH 7.4), 10 mM MgCl<sub>2</sub>, an ATP-regenerating system (4 mM ATP, 10 mM creatine phosphate, 100 μg/ml creatine kinase) and fluo-cAMP or [<sup>3</sup>H]-cGMP, respectively. For control experiments ATP was replaced by 5'-AMP. At indicated time points samples were taken and diluted in 900 μl icecold TS-Buffer to stop transport processes. Samples were filtered through NC45 filters (Whatman, Maidstone, UK) with a sampling manifold (Millipore, Billerica, MA). For the fluorescent compound filters were incubated in SDS/HEPES-Puffer (1% SDS, 7.5 mM HEPES) for at least 30 min. Afterwards fluid fluorescence was measured using a Shimadzu RF-5301PC spectrofluorophotometer (EX: 480 nm, EM: 520 nm). In experiments with [<sup>3</sup>H]-cGMP, filters were put into vials, 4 ml Opti-fluor were added and vials were shaken. Radioactivity was counted in the Scintillation counter. All experiments were performed in triplicate.

ATP-dependent transport was calculated by subtracting values obtained in presence of 5'-AMP from those obtained in presence of ATP. To calculate MRP2 and MRP4 specific transport, respectively, values for ATP-dependent transport of control vesicles were subtracted from those of transfected cell membrane vesicles.

### 3.5.2 Transport Studies in Killifish Proximal Tubulus

As described above proximal tubules were transferred to Teflon chambers containing 1 ml of marine teleost solution with or without inhibitors added. Different inhibitors of organic anion transport were added as stock solutions in marine teleost saline or in dimethylsulfoxide (DMSO). The DMSO concentration did not exceed 0.5%. This DMSO concentration had no effect on fluo-cAMP or FL-MTX transport (present study, Breen et al., 2004). After 30 minutes preincubation the fluorescent compound (2  $\mu$ M fluo-cAMP or 2  $\mu$ M FL-MTX) was added and incubated for another 45 minutes at room temperature. For experiments with high potassium, KCl concentration in the marine teleost saline buffer was increased 10fold, NaCl was isoionic decreased. Tissue was preincubated in high K<sup>+</sup>-buffer and after 30 minutes the fluorescent compound was added as described above. After incubation tissue was viewed by means of an inverted confocal laserscanning microscope.

Images were taken from 10 different tubules and quantified using NIH Scion Image Software as described in Breen et al., 2004. Fluorescence levels in epithelial cells and lumens were analyzed after background subtraction. The diagrammed results are representatives of at least two different experiments.

### 3.5.3 Transport Studies in Rat and Dogfish Shark Choroid Plexus

Pieces of CP were incubated for 30 min in buffer or buffer with various inhibitors of organic anion transport. Then we incubated 90 min (rat) or 60 min (shark) with TR (control) or TR with inhibitors added. Substances were diluted in pregassed aCSF or ER, respectively. Stock solutions were prepared in water or DMSO, the final DMSO concentration was  $\leq 0.05\%$ . Plexuses were gassed with 95% O<sub>2</sub>/5% CO<sub>2</sub> (rat) or 99% O<sub>2</sub>/1% CO<sub>2</sub> (shark) in Ziplock bags under slightly positive pressure. Experiments were carried out at room temperature. For some experiments a modified aCSF (ER) was used: a) for low Na<sup>+</sup> aCSF (ER) NaCl was replaced by N-methyl-D-glucamine, b) for Na<sup>+</sup>-free aCSF (ER) NaCl was replaced by N-methyl-D-glucamine and NaHCO<sub>3</sub> was replaced by choline bicarbonate and c) for high K<sup>+</sup> aCSF (ER) KCl concentration was increased to 47 mM (NaCl was isoionic decreased).

To acquire images, tissue and incubation solution were transferred to covered teflon chambers with a glass coverslip bottom. Chambers were fixed on the stage of a leica DM IRBE or an Olympus Fluoview inverted confocal laser scanning microscope. Samples were viewed through transmitted light, a x 63 oil immersion objective, a 544 nm HeNe ion laser excitation

and a 488/544/633 nm triple dichroic filter. Photomultiplier (PMT) gain was set to yield an average fluorescence intensity, with tissue autofluorescence being undetectable. From each piece of CP at least 5 images were taken.

Fluorescence intensity was quantified using the NIH Scion Image software (Breen et al., 2002). Fluorescence levels in vascular/subepithelial spaces, the interior of blood vessels and epithelial cells were analyzed after background subtraction from 10 images. All presented values are representatives of at least two different experiments.

### **3.6 Statistics**

All values presented are means +/- SEM. Values of control and treated groups were compared with one-way ANOVA test and Dunetts Post test. For  $P > 0.05$  no statistical difference was observed. Differences were statistically significant for  $*P < 0.05$ , very significant for  $**P < 0.01$  and extremely significant for  $***P < 0.001$ . For statistical analyses Graphpad Prism 4 or Prism 3.0 software was used.

## 4 Results

In the present study we investigated into transport processes for organic anions in killifish proximal tubules, membrane vesicles of transfected cells and choroid plexus (CP) tissue. To study transport mediated by multidrug resistance-associated protein (Mrp) 4 we used the fluorescent compound fluo-cAMP. Before Mrp4 studies could be performed, expression and localization of the protein in rat CP tissue and killifish proximal tubules was analyzed.

### 4.1 Molecular Analyses

Using RT-PCR and indirect immunohistological staining, Mrp4 expression and localization could be demonstrated as described in the following chapters.

#### 4.1.1 Mrp4 Gene Expression in Rat Choroid Plexus

To analyze Mrp4 gene expression in rat CP, RNA expression levels of Mrp4 and the pseudogene free and non-regulated housekeeping gene Porphobilinogen deaminase (Pbgd) were compared in rat. For semiquantitative analyses linearity of PCR products was initially examined in rat CP. Different cycle numbers were tested and density of bands was measured as described in materials and methods. As shown in Figure 8, density of bands accumulated with increasing numbers of cycles and then remained static. In Figure 8 A linearity analyses of Pbgd are shown, a plateau of band density was reached after 45 cycles. Figure 8 B shows analyses of Mrp4, for Mrp4 the plateau was reached after 40 cycles.

To compare Mrp4 gene expression in rat CP with gene expression of the housekeeping gene, a cycle number in the linear area was chosen. For Mrp4 we used 35 cycles as well as for Pbgd, at an annealing temperature of 53°C. In Figure 9 PCR products are shown using specific primers for Mrp4 and PBGD, respectively. For the PCR product of Pbgd product size is 360 bp, PCR of Mrp 4 results in a product of 773 bp. Mrp4 mRNA expression was high in rat CP, band density of the PCR product for Mrp4 was comparable to that of Pbgd.

**Figure 8:** Density of bands of PCR products for Pbgd and Mrp4. Density was analyzed using the NIH software Scion Image. For Pbgd the linear area started at 30 cycles and reached plateau after 45 cycles. For Mrp4 PCR product linearity was reached after 30 cycles with a plateau after 40 cycles. For semiquantitative PCR analyses 35 cycles were used for Pbgd as well as for Mrp4.

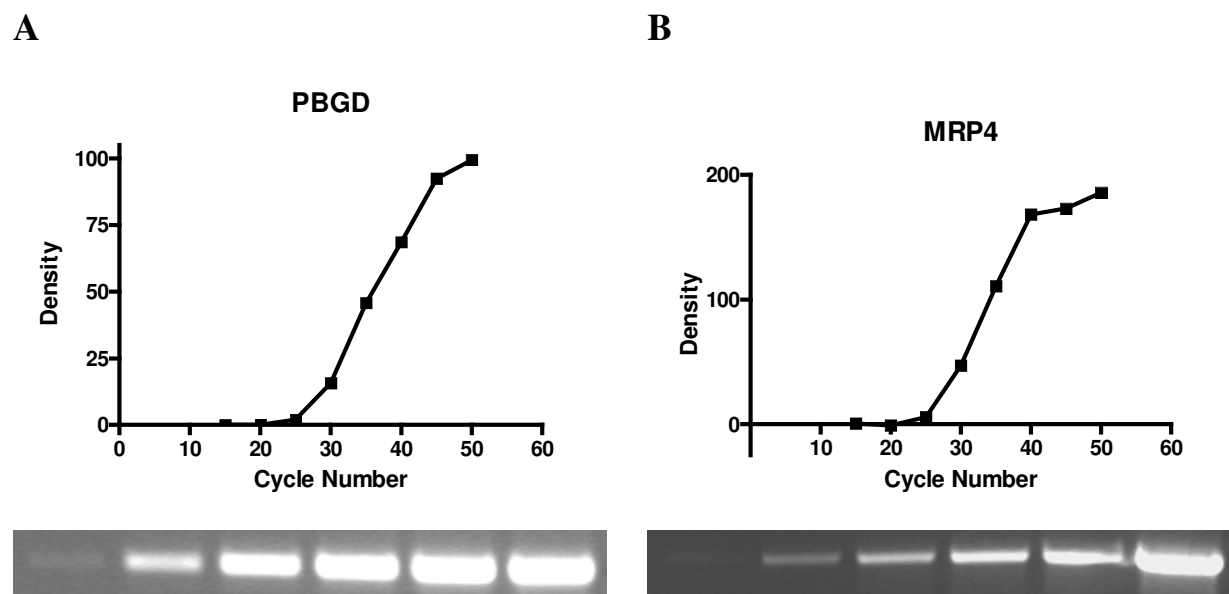
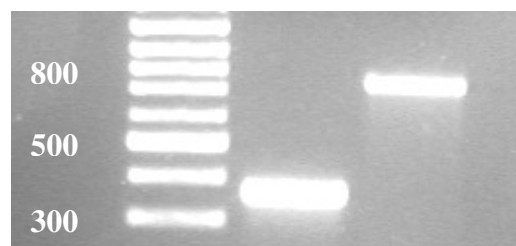


**Figure 9:** mRNA expression of Mrp4 compared to Pbgd in rat CP. PCR product size for Pbgd is 360 bp and for Mrp4 is 773 bp. Mrp4 mRNA expression was high in rat CP



#### 4.1.2 Immunostaining in Choroid Plexus and Proximal Tubulus

Following gene expression studies we examined localization of Mrp4 protein in rat CP. It is known that Mrp1 and Oatp2 are located to the basolateral, blood facing, membrane of rat CP epithelium, whereas Oatp3 and Oat3 are located to the apical membrane. Here, we show basolateral localization of Mrp4 in rat CP epithelial cells using indirect immunohistochemical analyses.

In Figure 10 A a control CP is shown. CP tissue was incubated with propidium iodide (PI) and secondary FITC-labeled antibody, only nuclei are stained with PI. Figure 10 B shows CP tissue after incubation with the specific Mab to MRP4 M<sub>4</sub>I-80 antibody, rabbit derived FITC-labeled anti-rat IgG and PI. The green staining is specific for Mrp4 and located to the

basolateral membrane of rat CP epithelium. Contemplating that, Mrp4 is colocalized to Mrp1 to the basolateral membrane of CP epithelial cells in rat. Thus, our results are in accordance with Leggas et al. (2004), who described a basolateral localization for Mrp4 in rat CP as well.

**Figure 10:** Indirect immunostaining of rat CP. In A a control CP is shown; only nuclei are stained with propidium iodide. B shows a CP after staining with the specific Mrp4 antibody and FITC-labeled anti-rat IgG. Basolateral staining of Mrp4 can be recognized.

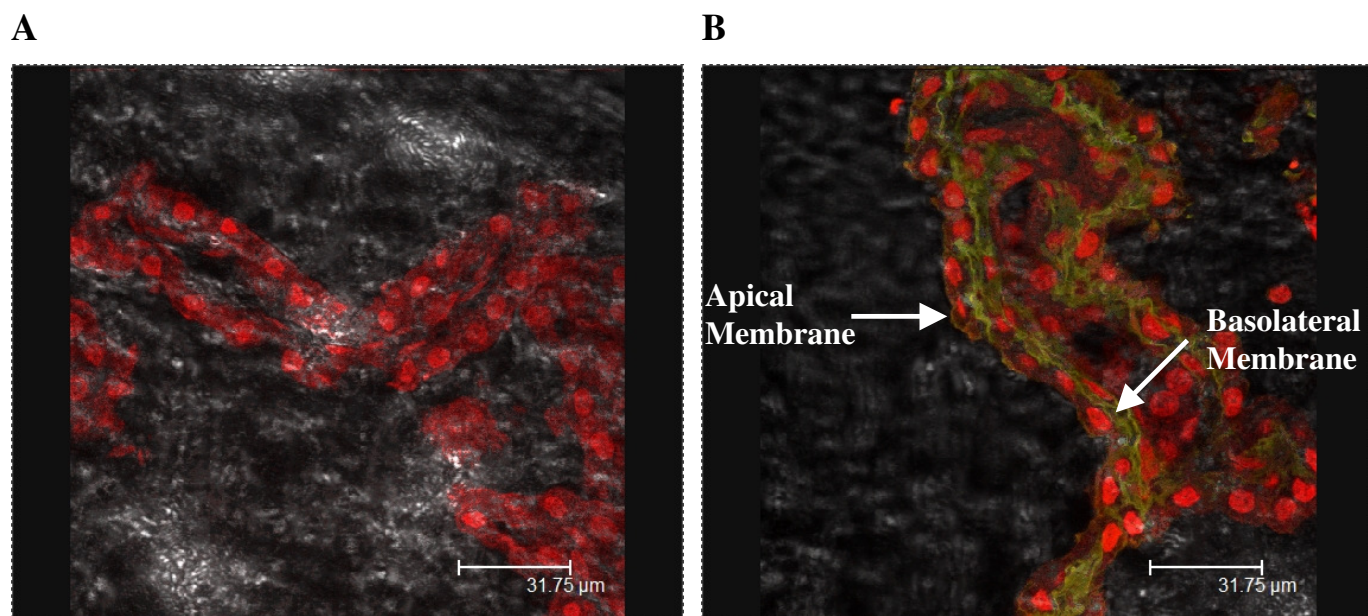


**Figure 11:** In killifish proximal tubules Mrp4 localisation was proved by indirect immunostaining. A tubulus stained with primary pAb rM4-pl antibody and the fluorescein-labeled secondary anti-rabbit IgG 488 antibody is shown. Mrp4 is clearly located to the luminal site of proximal tubules epithelial cells.



In a comparative study we examined localization of Mrp4 in killifish (*fundulus heteroclitus*) proximal tubules. Killifish represent an excellent model tissue, since most of its membrane transporters are expressed in analogy to mammalian tissue (Pritchard and Miller, 1991).

We found luminal localization of the teleost fish analog to Mrp4 (Figure 11) in killifish proximal tubules using the specific pAb rM4-pl antibody and indirect staining with

fluorescein-labeled anti-rabbit IgG 488. Mrp2 is located to the luminal site of proximal tubulus epithelial cells as well (Masereeuw et al., 2000).

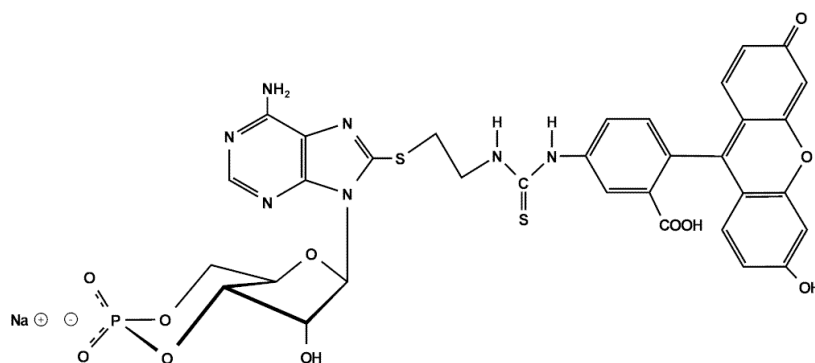
## 4.2 Functional Analyses

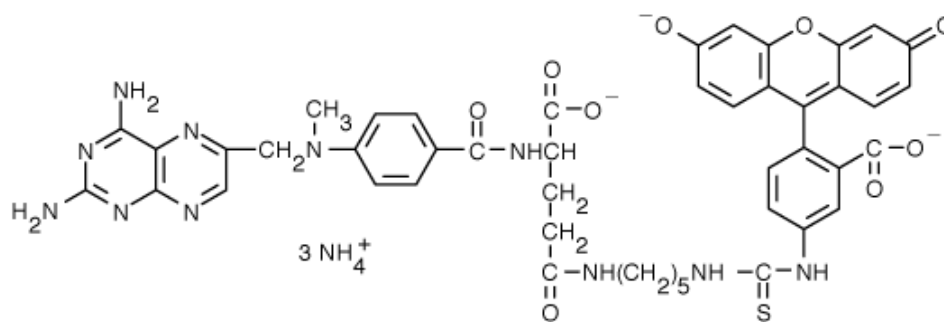
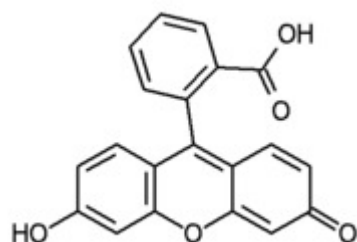
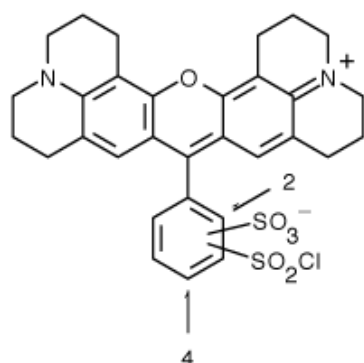
Functional analyses were carried out using membrane vesicles of MDCKII-MRP2 and Sf9-MRP4 cells, killifish renal proximal tubules and rat or dogfish shark CP. We used different fluorescent dyes as substrates, one of them was the fluorescent cAMP analog 8-[[2-[(fluoresceinylthioureido)amino]ethyl]thio]-cAMP (fluo-cAMP), which has a molecular weight of 815.7 Da (Figure 12 A). Schwede et al. (2000) tested binding of cAMP analogs, substituted at position 8 of the adenine moiety (C8), to the cAMP interaction sites of the regulatory subunits of cAMP dependent proteinkinase in comparison to cAMP. Fluo-cAMP is a lipophylic compound which has the bulkiest substituent of the tested cAMP analogs: fluorescein coupled to C8 via a six-atom-spacer. But even with this bulky substituent, fluo-cAMP was able to bind on two of the binding sites of cAMP dependent proteinkinase, indicating that features of the cAMP molecule are conserved.

Another fluorescent substance used for functional analyses was the fluorescent methotrexate analog FL-MTX with a molecular weight of 979.1 Da (Figure 12 B). Transport of fluo-cAMP and FL-MTX was compared to transport of the small-sized molecule FL (332.3 Da) (Figure 12 C) and the medium-sized organic anion TR (625 Da) (Figure 12 D). Different transport characteristics were found for all tested dyes.

**Figure 12:** Molecular structures of the fluorescent dyes fluo-cAMP (A), FL-MTX (B), FL (C) and TR (D).

**A**



**Figure 12:** Molecular structures of the fluorescent dyes fluo-cAMP (A), FL-MTX (B), FL (C) and TR (D).**B****C****D**

#### 4.2.1 Transport Studies in Killifish Proximal Tubulus

Transport studies analyzing transport of the fluorescent cAMP analog fluo-cAMP were carried out using freshly isolated killifish kidney proximal tubules. cAMP is a Mrp4 substrate (Chen et al., 2001; Van Aabel et al., 2002) and in transport studies we wanted to examine if the fluorescent analog is transported by Mrp4 as well.

Killifish kidneys contain a high fraction of proximal tubules (Physiology of Fishes, 1997), which can easily be isolated and are stable for a long period of time at room temperature. Furthermore, transport mechanisms in killifish proximal tubules seem to be similar to those in mammals to a large extent (Pritchard and Miller, 1991). Massereeuw, Notenboom and Miller researched into transport processes and their regulation in killifish proximal tubules

before. Especially transport processes mediated by Mrp2 were analyzed. As shown at page 34 Mrp4 is located to the luminal membrane of killifish proximal tubules as well as Mrp2, therefore we can use this model to investigate into transport of fluo-cAMP, presumably mediated by Mrp4.

**Figure 13:** Time course of fluo-cAMP transport from bath into proximal tubular lumen. Luminal fluorescence reached steady state after 25 minutes, cellular fluorescence was the same for the whole period of time. Luminal fluorescence exceeded cellular fluorescence by a factor 5-8. Data are expressed as mean  $\pm$  SE of 10 tubules from one representative isolation.

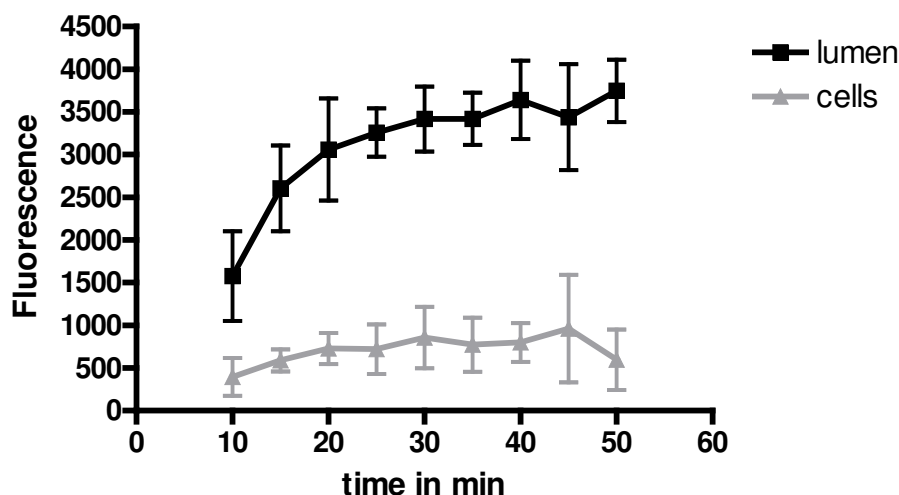


Figure 13 shows the time course of fluo-cAMP transport in killifish proximal tubules. Luminal fluorescence increased rapidly over the first 20 min, steady state was reached within 25 min, thus, subsequent experiments were carried out using incubation times of 45 minutes. At steady state luminal fluorescence exceeded cellular fluorescence by a factor 5-8. Cellular fluorescence was almost the same for the whole period of time. Fluorescence levels were highest in lumens of killifish proximal tubules, followed by epithelial cells. Bath fluorescence was the lowest. The high luminal fluorescence accumulation is a strong indication for an active, concentrative transport process in killifish proximal tubules. The distribution of fluo-cAMP with highest levels in lumen and lowest levels in the bath indicates a two-step mechanism composed of uptake from the bath at the basolateral membrane of proximal tubules epithelial cells and efflux into urine at the apical site.

Fluo-cAMP excretion into proximal tubular lumens was inhibited by addition of NaCN at a concentration of 1 mM. This result indicates a metabolism driven excretion of fluo-cAMP in killifish proximal tubules. Inhibition by metabolic poisons is typical for active transport processes (Figure 14).

**Figure 14:** Effects of NaCN on fluo-cAMP transport in killifish proximal tubules. Fluo-cAMP transport was clearly inhibited after NaCN treatment, luminal and cellular fluorescence were reduced. Data are expressed as mean  $\pm$  SE of 10 tubules from one representative isolation. (Significantly different from control values: \* for  $P < 0.05$ , \*\* for  $P < 0.01$  and \*\*\* for  $P < 0.001$ ).

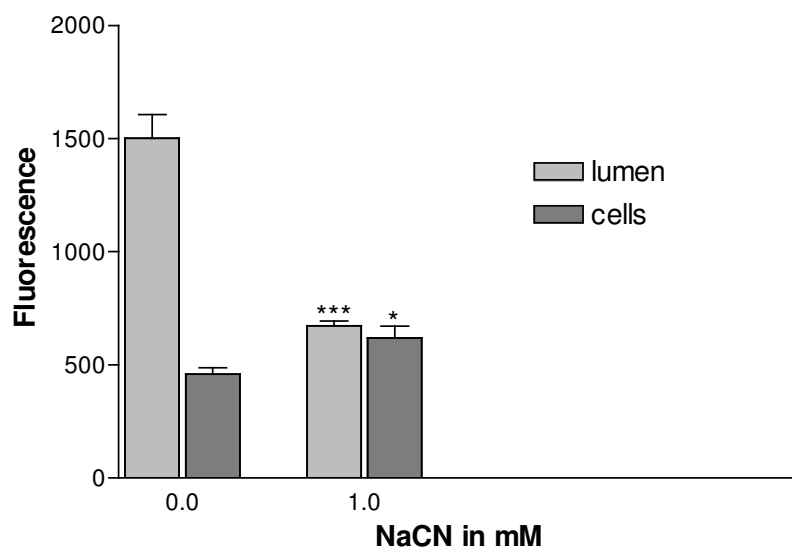


Figure 15 shows the basic characteristics of fluo-cAMP transport in killifish proximal tubules at steady state. High fluorescence intensity is recognizable in proximal tubular lumens, fluorescence in epithelial cells is lower and background fluorescence is the lowest.

**Figure 15:** Fluo-cAMP transport in killifish proximal tubules. Fluo-cAMP accumulated in tubular lumen and to a lower extent in epithelial cells, both fluorescence was very low.

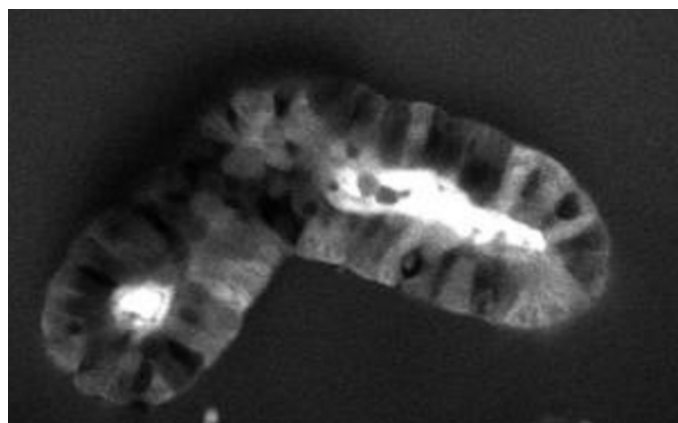
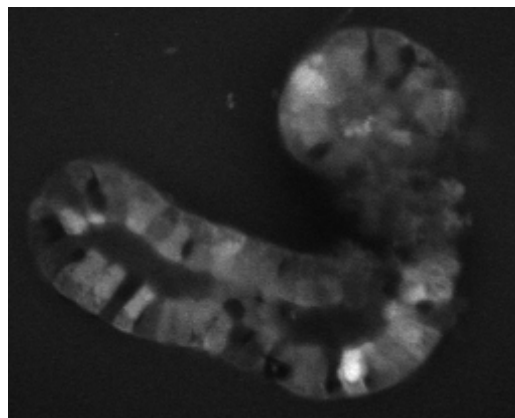


Figure 16 shows a proximal tubulus after treatment with the acyclic adenine derivative 9-(2-phosphonyl-methoxyethyl)adenine (PMEA, adefovir), which is a known substrate of Mrp4 (Dallas et al., 2004), at a concentration of 10  $\mu$ M. Compared to the proximal tubulus shown in Figure 15, luminal fluorescence was clearly decreased. As shown below, adefovir treatment also affected cellular fluorescence at higher concentrations.

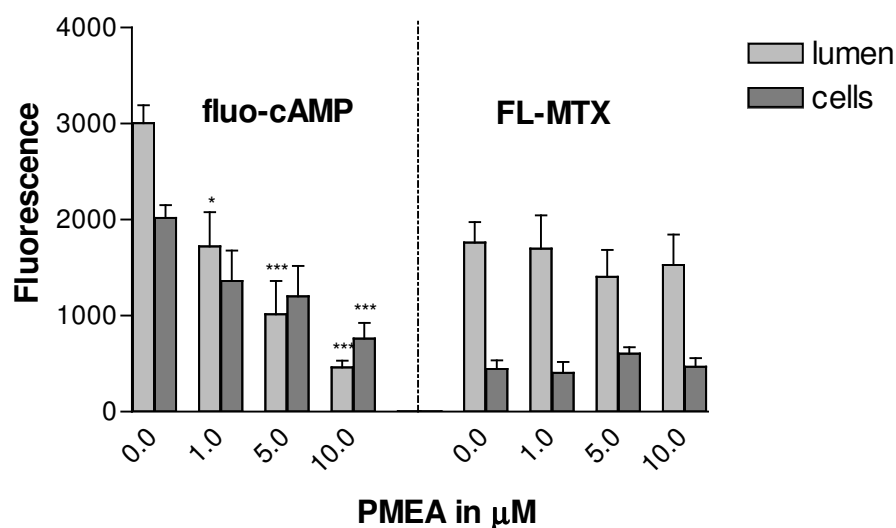
This known Mrp4 substrate was used at different concentrations to examine its effects on fluo-cAMP transport in killifish proximal tubules. After concomitant incubation with adefovir, fluo-cAMP accumulation was clearly affected. Luminal and cellular fluorescence

intensities were decreased when PMEAs were used at concentrations between 1 and 10  $\mu\text{M}$ , a dose dependent effect on fluo-cAMP accumulation could be recognized. Contrary to this result, accumulation of FL-MTX, a Mrp2 substrate, was not affected by treatment with PMEAs at the same concentrations (Figure 17).

**Figure 16:** A killifish proximal tubulus after incubation with fluo-cAMP and adefovir at a concentration of 10  $\mu\text{M}$ . Luminal fluorescence is clearly decreased compared to the control tubulus shown in Figure 15.

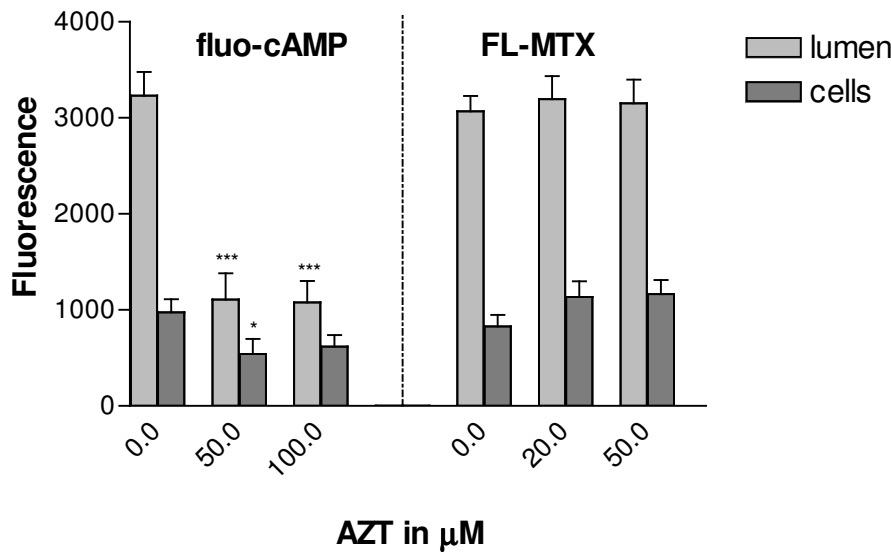


**Figure 17:** Effects of adefovir on fluo-cAMP and FL-MTX transport in killifish proximal tubules. Adefovir had a strong inhibitory effect on fluo-cAMP transport, FL-MTX transport was not affected. Data are expressed as mean  $\pm$  SE of 10 tubules from one representative isolation. (Significantly different from control values: \* for  $P < 0.05$ , \*\* for  $P < 0.01$  and \*\*\* for  $P < 0.001$ ).



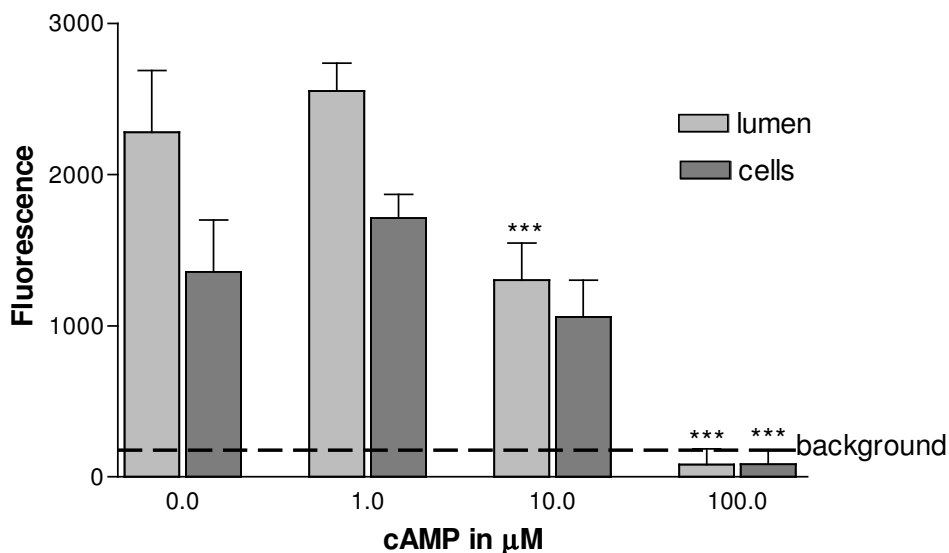
Incubation with another Mrp4 substrate, azidothymidine (AZT), led to similar effects. Fluo-cAMP transport was clearly inhibited at concentrations of 50 and 100  $\mu\text{M}$ , luminal fluorescence was stronger decreased than cellular fluorescence. FL-MTX transport was not affected at the same concentrations (Figure 18).

**Figure 18:** Effects of AZT treatment on fluo-cAMP and FL-MTX transport in killifish proximal tubules. AZT treatment reduced luminal accumulation of fluo-cAMP, cellular accumulation was barely affected. AZT had no effects on transport of FL-MTX. Data are expressed as mean  $\pm$  SE of 10 tubules from one representative isolation. (Significantly different from control values: \* for  $P < 0.05$ , \*\* for  $P < 0.01$  and \*\*\* for  $P < 0.001$ ).



Taken together the results obtained using adefovir and AZT as inhibitors give evidence for Mrp4 involvement in fluo-cAMP transport in killifish proximal tubules, because transport of FL-MTX, which is mediated by Mrp2, was not affected by the used inhibitors.

**Figure 19:** The effects on fluo-cAMP transport after incubation with the parent, non fluorescent molecule cAMP. A strong, dose-dependent effect was caused by cAMP treatment, assumably a comparative effect. Data are expressed as mean  $\pm$  SE of 10 tubules from one representative isolation. (Significantly different from control values: \* for  $P < 0.05$ , \*\* for  $P < 0.01$  and \*\*\* for  $P < 0.001$ ).



To investigate the effect of the non fluorescent molecule cAMP on transport of its analog fluo-cAMP we incubated tubules simultaneously with increasing concentrations of the parent, non fluorescent compound cAMP. A dose-dependent inhibitory effect at concentrations

between 1 and 100  $\mu\text{M}$  was the result. We assume a comparative effect of cAMP on fluo-cAMP transport (Figure 19).

8-Bromo-cGMP is a stable cGMP analogon, which inhibits a cAMP specific phosphodiesterase, causing intracellular cAMP levels to increase. 1  $\mu\text{M}$  of 8-Bromo-cGMP decreased luminal fluo-cAMP accumulation (Figure 20) in killifish proximal tubules, suggesting high intracellular cAMP levels as cause.

**Figure 20:** Effect of 8-Bromo-cGMP on fluo-cAMP transport in killifish proximal tubules. 8-Br-cGMP led to reduced luminal fluo-cAMP accumulation. 8-Br-cGMP causes high intracellular cAMP levels by inhibiting a cAMP specific phosphodiesterase, suggesting these cAMP levels as cause for the inhibition. Data are expressed as mean  $\pm$  SE of 10 tubules from one representative isolation. (Significantly different from control values: \* for  $P < 0.05$ , \*\* for  $P < 0.01$  and \*\*\* for  $P < 0.001$ ).

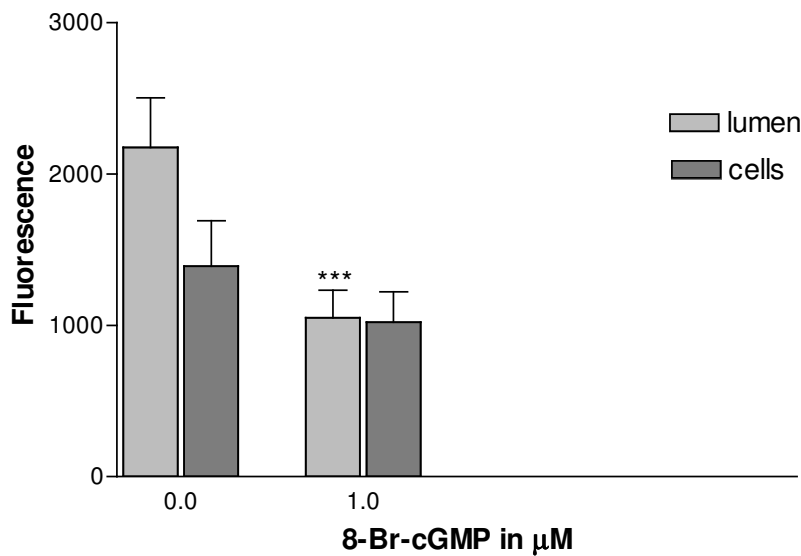
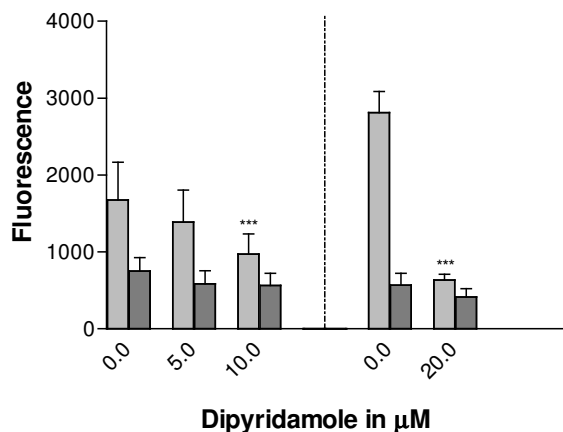
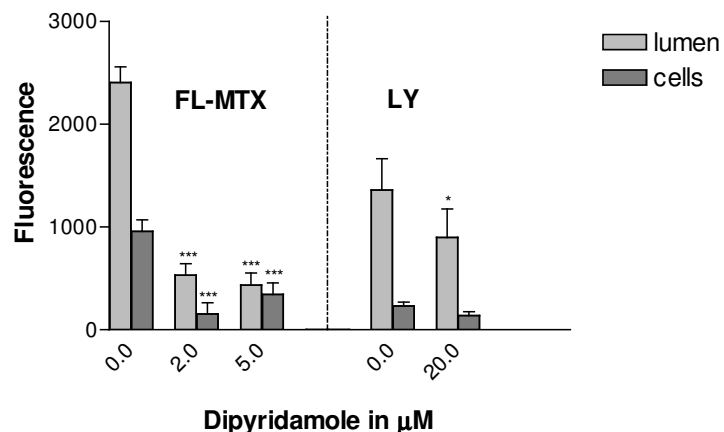


**Figure 21:** Effects of dipyrindamole on transport of fluo-cAMP, FL-MTX and LY in killifish proximal tubules. Dipyrindamole affected luminal fluorescence of all mentioned substrates, suggesting dipyrindamole as an inhibitor of Mrp2 and Mrp4 mediated transport processes. For FL-MTX cellular fluorescence was reduced as well. Data are expressed as mean  $\pm$  SE of 10 tubules from one representative isolation. (Significantly different from control values: \* for  $P < 0.05$ , \*\* for  $P < 0.01$  and \*\*\* for  $P < 0.001$ ).

**A**



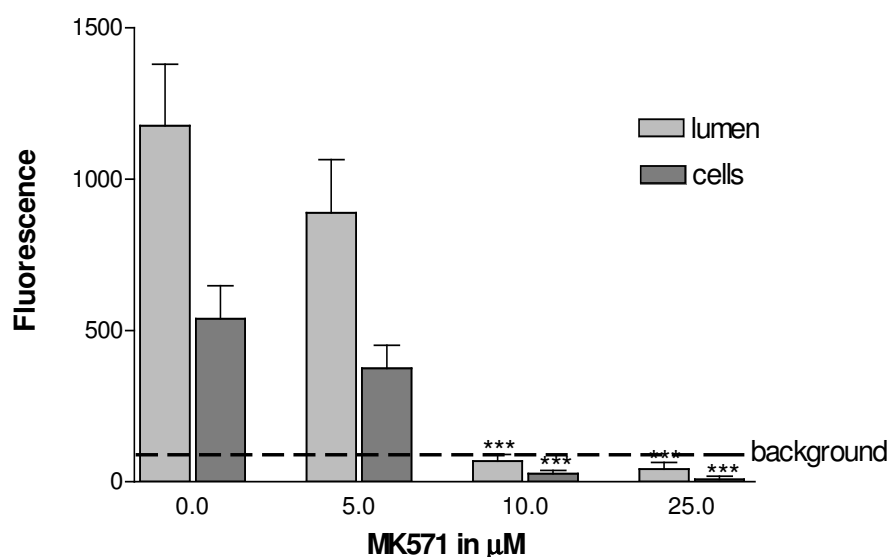
**B**



Dipyridamole is known to be a potent inhibitor of transport processes mediated by Mrp4 (Van Aubel et al., 2002). At concentrations of 5-20  $\mu\text{M}$  dipyridamole inhibited fluo-cAMP excretion in a dose-dependent manner (Figure 21 A). We also tested the effects of dipyridamole treatment on transport of FL-MTX, a Mrp2 substrate, and LY, another substrate of Mrp2 and Mrp4. Luminal efflux of FL-MTX and LY was inhibited as well (Figure 21 B). Therefore, dipyridamole seems not only to be an inhibitor for Mrp4 mediated transport, but also for transport processes mediated by Mrp2.

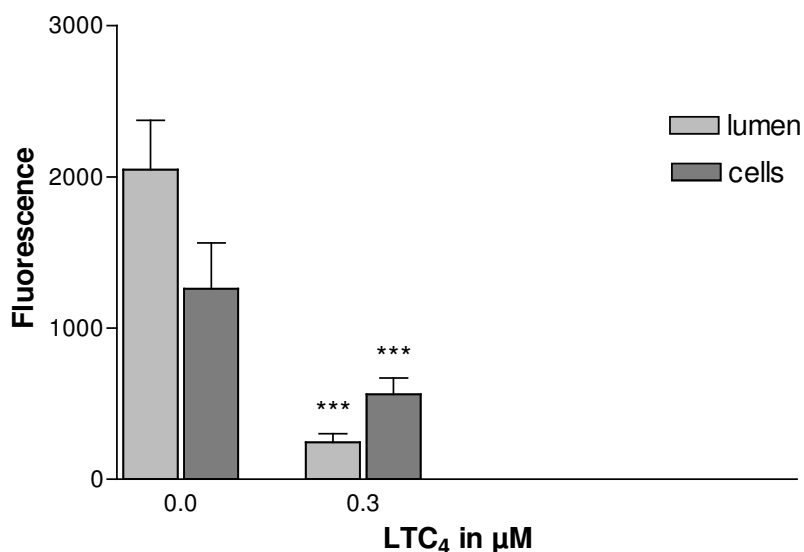
The Mrp inhibitor MK571 had a strong inhibitory effect on fluo-cAMP accumulation in proximal tubular cells and lumens at 10 and 25  $\mu\text{M}$  (Figure 22), suggesting one or more of the Mrps expressed in killifish proximal tubules to be involved in fluo-cAMP transport.

**Figure 22:** Effects of the Mrp inhibitor MK571 on fluo-cAMP transport in killifish proximal tubules. Luminal as well as cellular accumulation of fluo-cAMP were affected at concentrations of 10 and 25  $\mu\text{M}$ . Data are expressed as mean  $\pm$  SE of 10 tubules from one representative isolation. (Significantly different from control values: \* for  $P < 0.05$ , \*\* for  $P < 0.01$  and \*\*\* for  $P < 0.001$ ).



Leukotriene C<sub>4</sub> (LTC<sub>4</sub>) is a known inhibitor of Mrp1, Mrp2, Mrp3 (Russel et al., 2002) and Oatp (Li et al., 2000) mediated transport processes. FL-MTX transport in intact killifish proximal tubules was decreased in presence of 0.3  $\mu\text{M}$  LTC<sub>4</sub> (Gutmann et al., 2000). LTC<sub>4</sub> decreased transport of fluo-cAMP in killifish proximal tubules as well (Figure 23), lumen and epithelial cells were affected. Therefore, Mrp1,2,3 or Oatps seem also to be involved in fluo-cAMP transport in killifish proximal tubules, the strong inhibitory effect on cellular fluorescence leads to the suggestion, that the basolateral uptake step is inhibited as well as possibly the efflux step at the apical membrane. Thus, involvement of an Oatp in fluo-cAMP uptake is likely.

**Figure 23:** LTC<sub>4</sub> effect on fluo-cAMP transport in killifish proximal tubules. The effect on luminal fluorescence was very strong, cellular fluorescence was affected as well. Data are expressed as mean  $\pm$  SE of 10 tubules from one representative isolation. (Significantly different from control values: \* for P<0.05, \*\* for P<0.01 and \*\*\* for P<0.001).



This assumption was supported by inhibition experiments using probenecid which affects transport processes mediated by Mrps, Oats and Oatps. Probenecid inhibited transport of fluo-cAMP (Figure 24). This also leads to the suggestion that one or more transport proteins of the mentioned transport families are involved in mediation of fluo-cAMP transport in killifish proximal tubules.

**Figure 24:** Effects of probenecid on fluo-cAMP transport in killifish proximal tubules. Luminal fluo-cAMP accumulation was affected at concentrations of 10 and 50  $\mu$ M, cellular fluorescence was only affected at 50  $\mu$ M. Data are expressed as mean  $\pm$  SE of 10 tubules from one representative isolation. (Significantly different from control values: \* for P<0.05, \*\* for P<0.01 and \*\*\* for P<0.001).

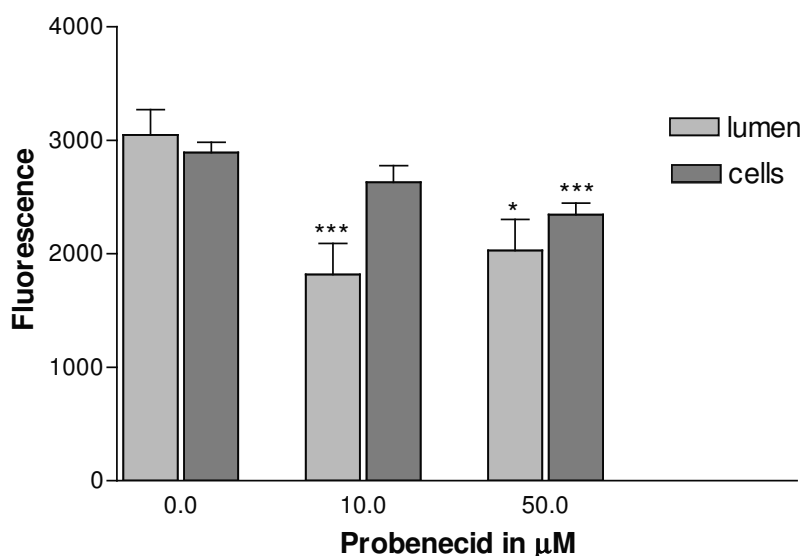
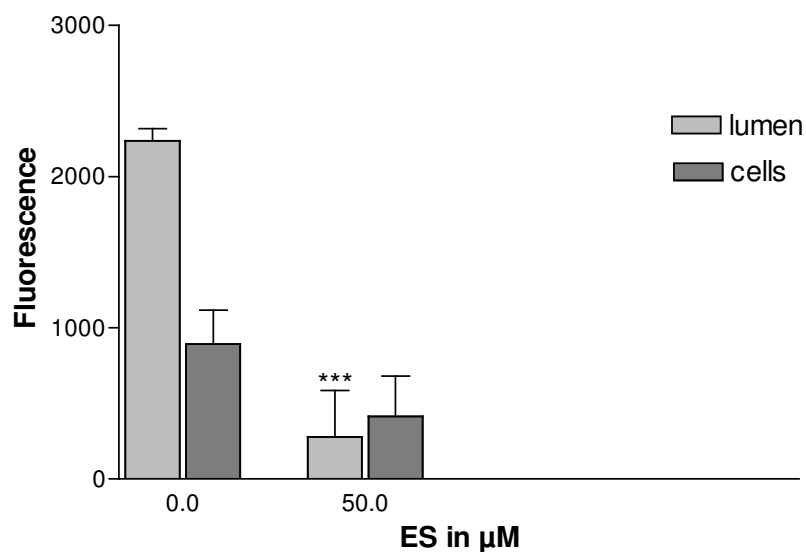
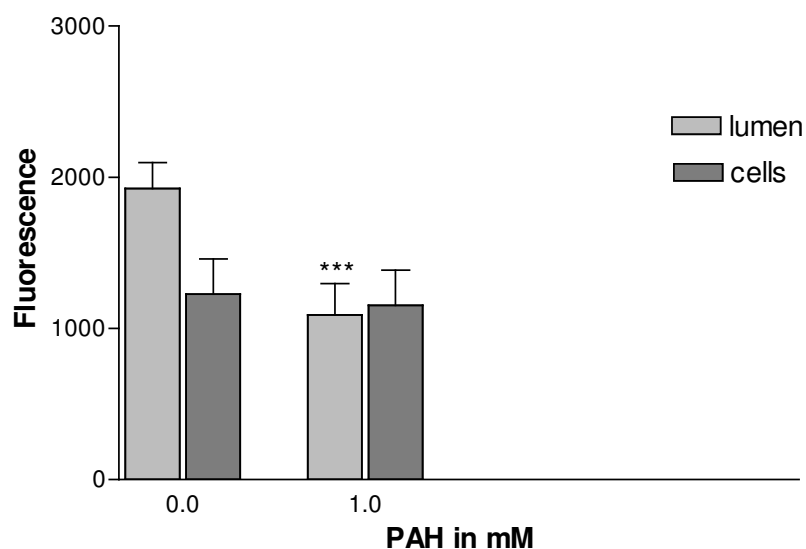


**Figure 25:** Effect of ES on fluo-cAMP transport in killifish proximal tubules. At 50  $\mu$ M luminal fluorescence was clearly reduced, changes in cellular accumulation were not statistically significant. Data are expressed as mean  $\pm$  SE of 10 tubules from one representative isolation. (Significantly different from control values: \* for  $P < 0.05$ , \*\* for  $P < 0.01$  and \*\*\* for  $P < 0.001$ ).



Estrone sulfate (ES) is a substrate for Oats, Oatps and Mrps. Incubation with fluo-cAMP and ES led to a significant decrease of luminal fluorescence intensity at 20 and 50  $\mu$ M (Figure 25). Oats, Oatps or Mrps seem to play a role in transport of the fluorescent compound fluo-cAMP in killifish proximal tubules.

**Figure 26:** Effect of PAH on fluo-cAMP transport in killifish proximal tubules. PAH only had an effect at a high concentration (1 mM), luminal but not cellular fluorescence was decreased. Data are expressed as mean  $\pm$  SE of 10 tubules from one representative isolation. (Significantly different from control values: \* for  $P < 0.05$ , \*\* for  $P < 0.01$  and \*\*\* for  $P < 0.001$ ).



p-Aminohippurate (PAH), a substrate of Oats, Mrp2 and Mrp4 (Smeets et al., 2004), had no effect on fluo-cAMP transport in killifish proximal tubules at lower concentrations (10-50  $\mu$ M). At the higher concentration of 1 mM it reduced luminal accumulation of fluo-cAMP,

cellular accumulation was not reduced (Figure 26). These results indicate inhibition of the efflux step for fluo-cAMP from epithelial cells into lumen at the apical membrane, presumably mediated by Mrp4 and Mrp2.

**Figure 27:** Effect of increasing medium  $K^+$  by an order of magnitude. High  $K^+$  levels lead to depolarisation of epithelial cells and changes in the electrical potential. This treatment had no effect on fluo-cAMP transport in killifish proximal tubules, suggesting independency of fluo-cAMP transport from PD. Data are expressed as mean  $\pm$  SE of 10 tubules from one representative isolation.

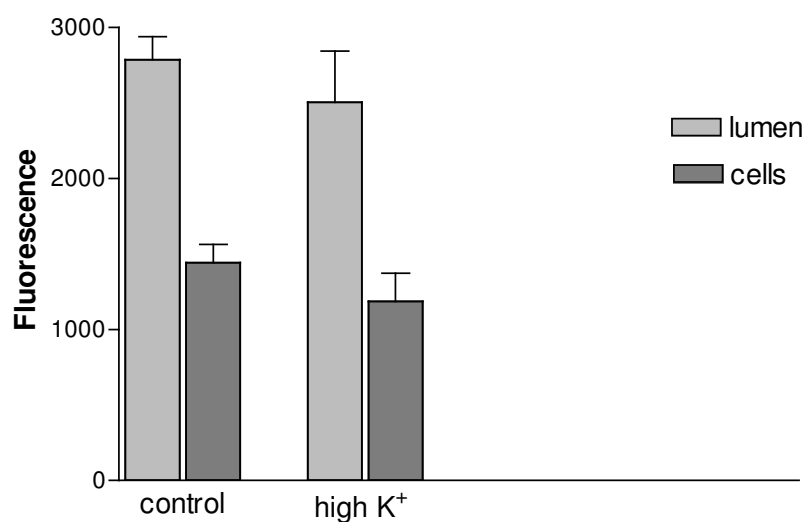
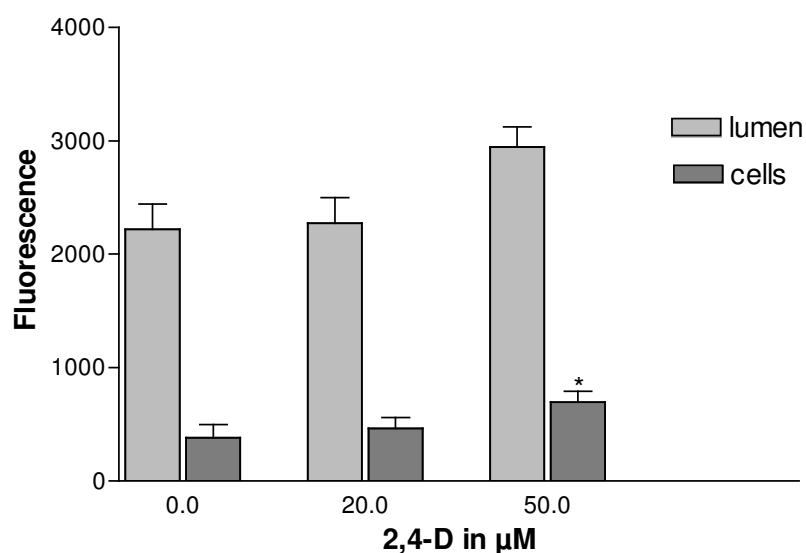


**Figure 28:** Effects of the herbicide 2,4-D on fluo-cAMP transport. 2,4-D treatment had no effect on distribution of fluo-cAMP within the tissue. Data are expressed as mean  $\pm$  SE of 10 tubules from one representative isolation.



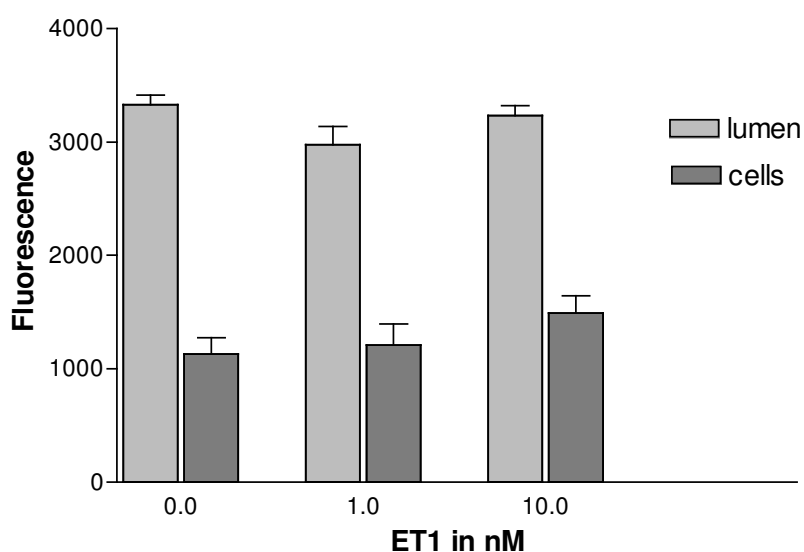
At an increased KCl concentration of 47 mM (isotonic NaCl replacement), we found no effects on fluo-cAMP accumulation (Figure 27). Increasing  $K^+$ -levels in the incubation

solution lead to depolarisation of epithelial cells. Thus, fluo-cAMP transport in killifish proximal tubules seems to be insensitive to changes in electrical potential differences (PD).

The herbicide 2,4-dichlorophenoxyacetic acid (2,4-D) which is a modulator of Oat3 mediated FL transport in rat and shark CP (Breen et al., 2002; Villalobos et al., 2002), had no effect on fluo-cAMP transport in killifish proximal tubules (Figure 28). Therefore, fluo-cAMP seems to be transported by different transport proteins than FL.

Since the overlapping substrate specificity of Mrp2 and Mrp4 makes a functional distinction of the two transport proteins difficult, further insights into the regulatory pathways may be helpful to discriminate their impact on fluo-cAMP transport. Masereeuw et al. (2000) showed that organic anion transport in killifish proximal tubules is regulated by an Endothelin (ET) pathway signaling through protein kinase C [PKC], starting with the binding of Endothelin 1 (ET1) to the Endothelin B (ET<sub>B</sub>) receptor and a subsequent cascade via NO-synthase and PKC which ends in a functional downregulation of Mrp2 (Notenboom et al., 2002).

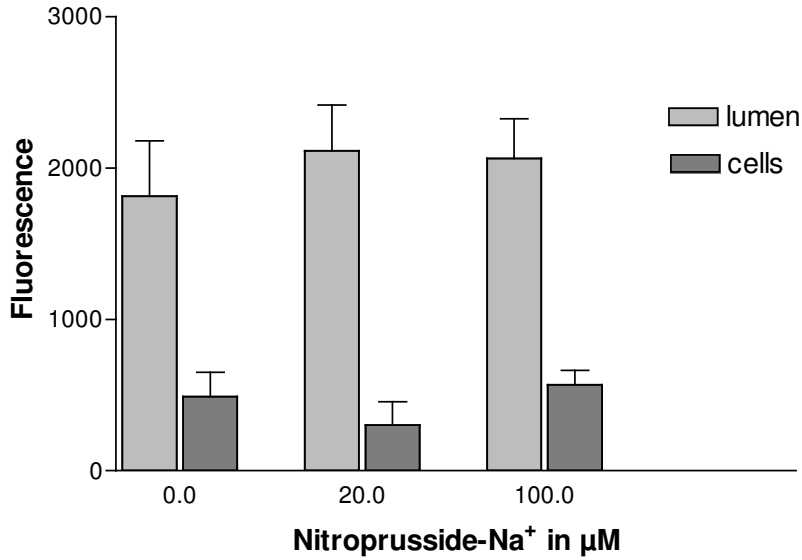
**Figure 29:** Effect of ET1 on fluo-cAMP transport in killifish proximal tubules. ET1 had nor an effect on luminal neither on cellular accumulation. Data are expressed as mean  $\pm$  SE of 10 tubules from one representative isolation.



ET1 has a dose dependent inhibitory effect on transport processes mediated by Mrp2 at nanomolar concentrations. As shown in shark rectal gland tubules, luminal accumulation of sulforhodamine 101 (Texas Red, TR), another Mrp2 substrate, was decreased by ET1, but it had no effect on cellular accumulation of sulforhodamine 101 (Miller et al., 2002). FL-MTX excretion into the lumen of killifish proximal tubules was significantly reduced in presence of ET1 at nanomolar concentrations. ET1 had no effect on cellular accumulation of FL-MTX (Masereeuw et al., 2000).

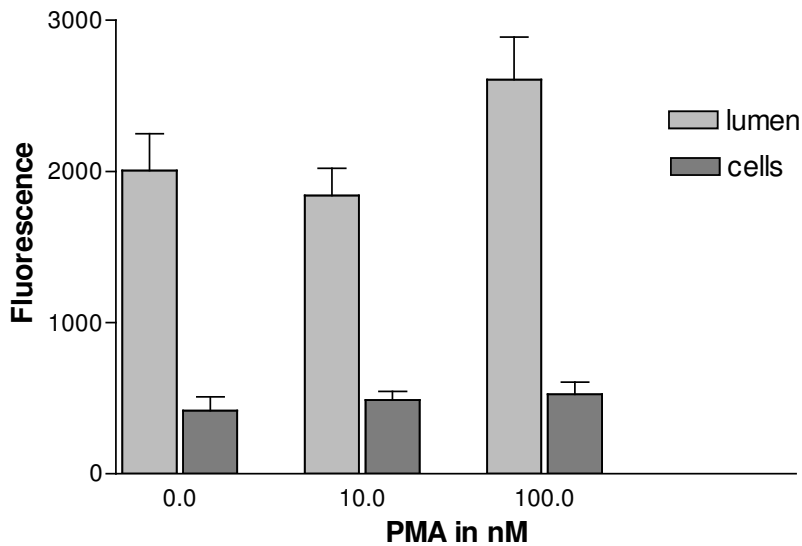
ET1, at 1 and 10 nM, had no effect at all on luminal or cellular accumulation of fluo-cAMP in killifish kidney proximal tubules (Figure 29), suggesting the ET signal cascade not to be involved in regulation of fluo-cAMP transport in killifish proximal tubules.

**Figure 30:** Effect of nitroprusside- $\text{Na}^+$  on transport of fluo-cAMP in killifish proximal tubules. The NO-donor did not affect distribution of fluo-cAMP. Data are expressed as mean  $\pm$  SE of 10 tubules from one representative isolation.



Nitroprusside- $\text{Na}^+$  leads to rapid NO release. The NO-donor had no effect on luminal and cellular fluo-cAMP accumulation (Figure 30), suggesting that NO release is no crucial factor for regulation of fluo-cAMP transport.

**Figure 31:** Effect of the phorbol ester PMA on fluo-cAMP transport in killifish proximal tubules. PMA leads to activation of PKC, this activation had no effect on fluo-cAMP transport. Data are expressed as mean  $\pm$  SE of 10 tubules from one representative isolation.



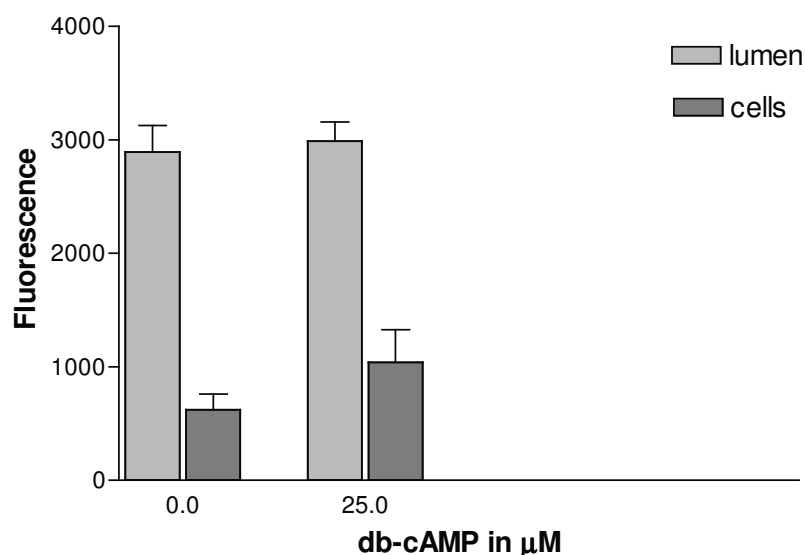
ET signaling involves activation of an ET receptor-coupled G protein which in turn activates

phospholipase C and PKC. FL-MTX transport into lumen in killifish proximal tubules was reduced when PKC was activated. PKC can be activated by phorbol ester. Incubation with PMA (phorbol-12-myristate-13-acetate) at 50 nM and 100 nM led to reduced FL-MTX accumulation in proximal tubular lumens (Masereeuw et al., 2000). However, in the present study, 10 nM and 100 nM PMA had no effects on fluo-cAMP distribution (Figure 31), suggesting that this regulatory cascade is of no relevance for transport of fluo-cAMP in killifish proximal tubules.

Soodvilai et al. (2004) investigated regulation of transport mechanisms mediated by Oat3. They showed that activation of PKC downregulates the action of Oat3. In contrast, activation of PKA leads to upregulation of Oat3 mediated transport.

To examine if PKA activation increases fluo-cAMP excretion in killifish proximal tubules we used the direct PKA activator dibutyryl cAMP (db-cAMP). At the used concentrations 5  $\mu$ M and 25  $\mu$ M db-cAMP had no effects on fluo-cAMP distribution within the tissue (Figure 32) which indicates that activation of PKA is not involved in regulation of fluo-cAMP transport in killifish proximal tubules.

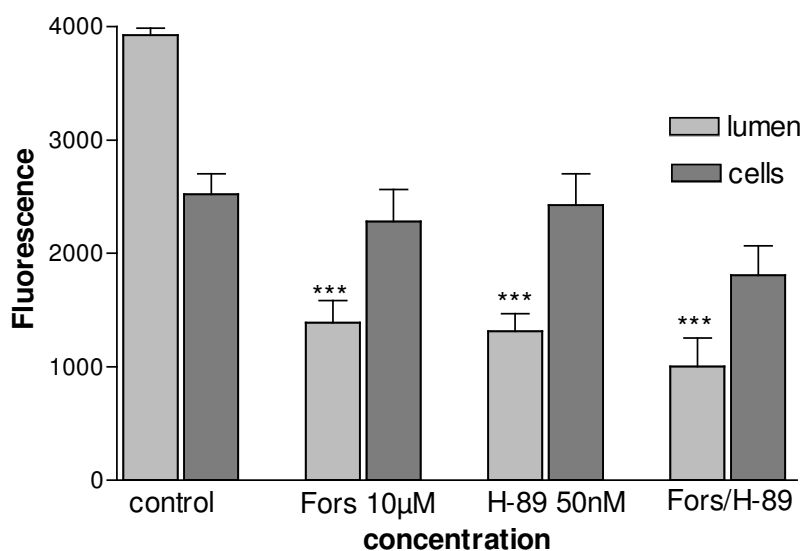
**Figure 32:** Effect of db-cAMP on transport of fluo-cAMP in killifish proximal tubules. The direct PKA activator did not affect fluo-cAMP transport. Data are expressed as mean  $\pm$  SE of 10 tubules from one representative isolation.



We tested another PKA activator which indirectly activates PKA due to an inhibition of phosphodiesterase and, subsequently, increasing intracellular cAMP concentration, forskolin. Forskolin treatment led to reduced fluo-cAMP transport in killifish proximal tubules in a dose-dependent manner at micromolar concentrations. To analyze whether this inhibition is caused by PKA activation, the PKA inhibitor H-89 was used concomitantly. We incubated

with 1) forskolin 10  $\mu$ M, 2) H-89 50 nM or 3) forskolin 10  $\mu$ M and H-89 50 nM. Figure 33 shows that H-89 decreased fluo-cAMP accumulation, but did not alter the forskolin effect. Similar results were found by Miller et al. (2002) in shark rectal gland tubules. We suggest that the inhibitory effect caused by forskolin treatment is caused by increased intracellular cAMP levels and not by PKA activation, because H-89 could not affect the inhibition caused by forskolin treatment.

**Figure 33:** Effects of forskolin and H-89 on fluo-cAMP transport in killifish proximal tubules. The indirect PKA activator forskolin led to reduced fluorescence levels in the lumen as well as H-89. H-89 could not alter the forskolin effect. Data are expressed as mean  $\pm$  SE of 10 tubules from one representative isolation. (Significantly different from control values: \* for  $P < 0.05$ , \*\* for  $P < 0.01$  and \*\*\* for  $P < 0.001$ ).



#### 4.2.2 Uptake Studies in Membrane Vesicles

To approve the presumptions found by analyses of fluo-cAMP transport in killifish proximal tubules, we used membrane vesicles of overexpressing MDCKII-MRP2 and Sf9-MRP4 cells for specific uptake studies and found evidences for fluo-cAMP transport mediated by MRP2 and MRP4. Western Blot studies performed at the NCMLS (Nijmegen, the Netherlands) demonstrated presence of the studied transport proteins (data not shown).

Initially, uptake of the common MRP4 substrate [ $^3$ H]-cGMP (Van Aubel et al., 2002) was analyzed. Uptake of [ $^3$ H]-cGMP at a concentration of 7  $\mu$ M into Sf9-MRP4 membrane vesicles was a specific transport process that was dependent on ATP hydrolysis (Figure 34). As described in materials and methods, we measured uptake of fluo-cAMP into membrane vesicles in presence of 5'-AMP or ATP (Figure 34 A). ATP-dependent transport was calculated by subtracting values obtained in presence of 5'-AMP from those obtained in

presence of ATP (Figure 34 B). To calculate MRP2 or MRP4 specific transport, values for ATP-dependent transport of control vesicles were subtracted from those of transfected cell membrane vesicles (Figure 34 C).

**Figure 34:** ATP-dependent, specific uptake of [<sup>3</sup>H]-cGMP by MRP4 into membrane vesicles. In A uptake of fluo-cAMP into membrane vesicles in presence of 5'-AMP or ATP is shown. B shows active, ATP-dependent transport, in C specific uptake of fluo-cAMP into membrane vesicles mediated by MRP4 is shown. Data are expressed as mean ± SE of three samples from one representative experiment. Ops: Opsine (control), Sf9-MRP4 93: MRP4 vesicles, batch 93.

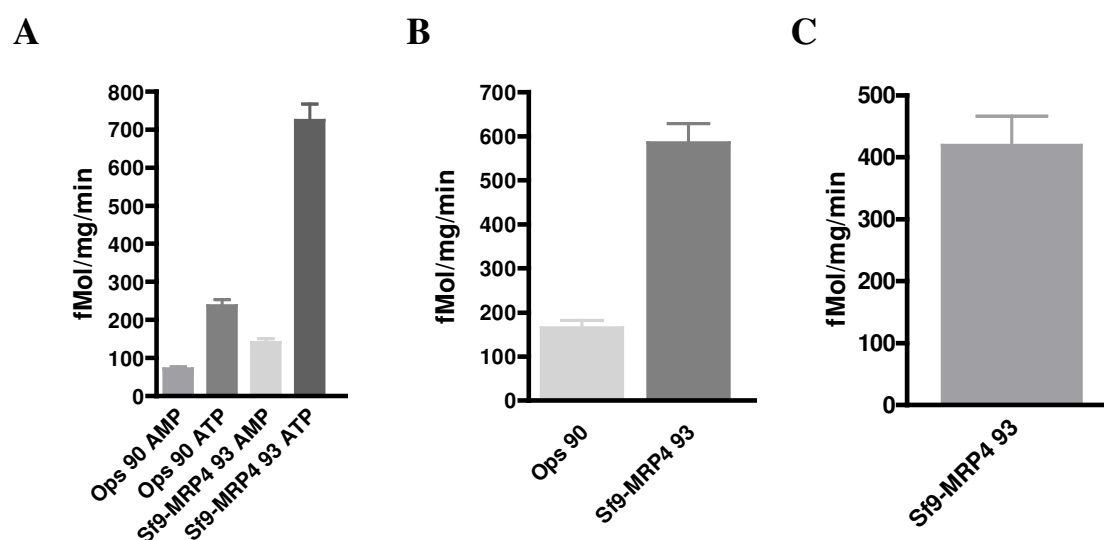
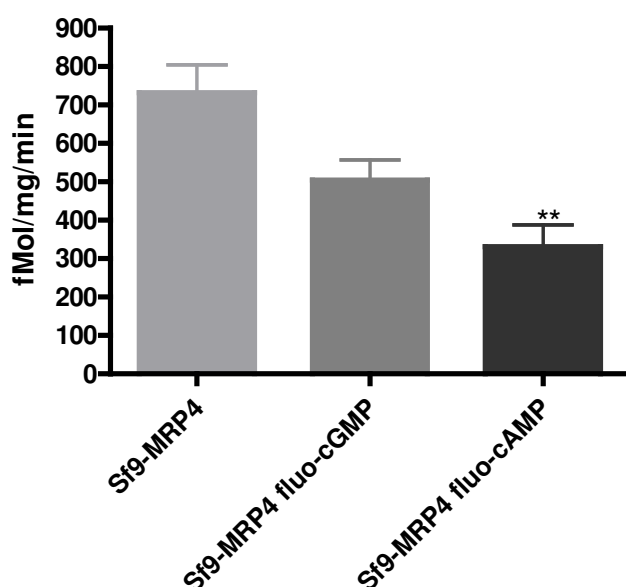


**Figure 35:** Effects of fluo-cGMP and fluo-cAMP on specific transport of [<sup>3</sup>H]-cGMP mediated by MRP4. Uptake of [<sup>3</sup>H]-cGMP into membrane vesicles was significantly reduced after fluo-cAMP treatment. Data are expressed as mean ± SE from three samples of one representative experiment.

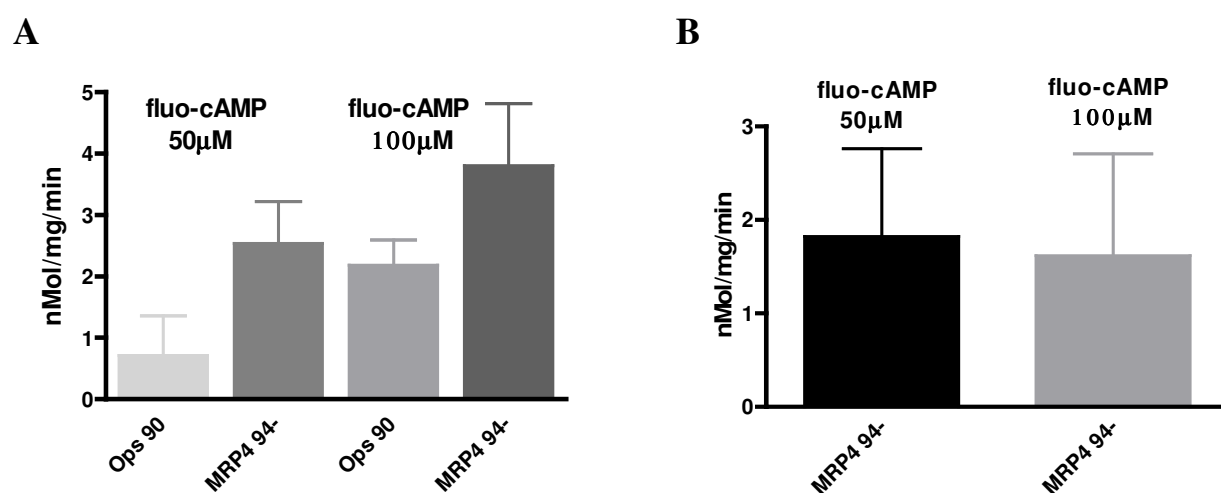


To test whether the fluorescent compounds fluo-cAMP and fluo-cGMP may be substrates for human MRP4 expressed in Sf9 cells, their effect on transport of [<sup>3</sup>H]-cGMP at a concentration

of 7  $\mu\text{M}$  in Sf9-MRP4 vesicles was studied. Concentrations of 20  $\mu\text{M}$  fluo-cAMP and fluo-cGMP were used. Incubation with fluo-cAMP led to significantly reduced uptake of [ $^3\text{H}$ ]-cGMP into Sf9-MRP4 vesicles, whereas the effect of fluo-cGMP was not statistically significant (Figure 35).

Further investigations regarded fluo-cAMP uptake into Sf9-MRP4 membrane vesicles. Fluo-cAMP uptake into Sf9-MRP4 vesicles was specific and ATP-dependent as shown in Figure 36 for 50 and 100  $\mu\text{M}$  fluo-cAMP. At these concentrations fluo-cAMP transport by MRP4 seems to be saturated, no differences between transport rates were obtained.

**Figure 36:** Fluo-cAMP uptake into Sf9-MRP4 membrane vesicles was a ATP-dependent, specific transport process. At 50 and 100  $\mu\text{M}$  fluo-cAMP no differences of transport rates were obtained. In A active transport of fluo-cAMP in control (Ops) and MRP4 membrane vesicles is shown. B shows specific uptake of fluo-cAMP mediated by MRP4. Data are expressed as mean  $\pm$  SE of three samples from one representative experiment.



Characteristics of fluo-cAMP transport including time and concentration course were studied. In Figure 37 the time course of fluo-cAMP into Sf9-MRP4 membrane vesicles is diagrammed. To analyze time course we measured fluorescence levels after different incubation times for 20  $\mu\text{M}$  fluo-cAMP. Amount of fluo-cAMP transported by MRP4 in Sf9-MRP4 membrane vesicles increased for the first 20 minutes and reached steady state after 20-30 min. To analyze fluo-cAMP transport in the increasing domain, following experiments were carried out with incubation times of 10 minutes.

To analyze kinetics of fluo-cAMP transport by human MRP4 expressed in Sf9 cells, we tested fluo-cAMP concentrations between 1 and 25  $\mu\text{M}$ . Fluo-cAMP transport in Sf9-MRP4 vesicles was concentration dependent with a  $V_{\text{max}}$  value of 1.1  $\pm$  0.2 nMol/mg/min and an apparent  $K_{\text{m}}$  value of 5.3  $\pm$  2  $\mu\text{M}$  (Figure 38).

**Figure 37:** Time course of fluo-cAMP (20  $\mu$ M) uptake mediated by MRP4 expressed in Sf9 cells. Accomodated fluo-cAMP amount per milligramm protein increased for the first 20 minutes and than reached steady state. Data are expressed as mean  $\pm$  SE from 3 independent experiments. MRP4 94-: batch 94-.

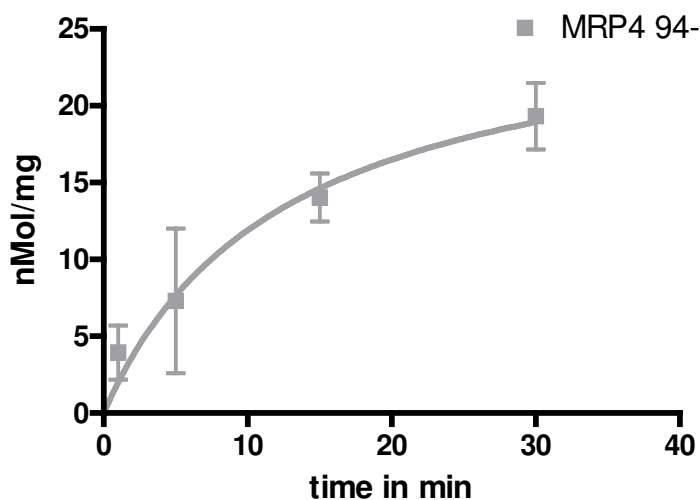
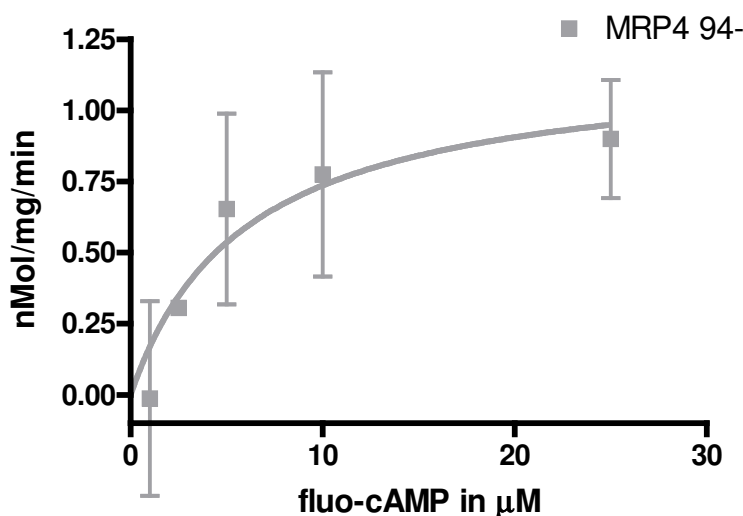
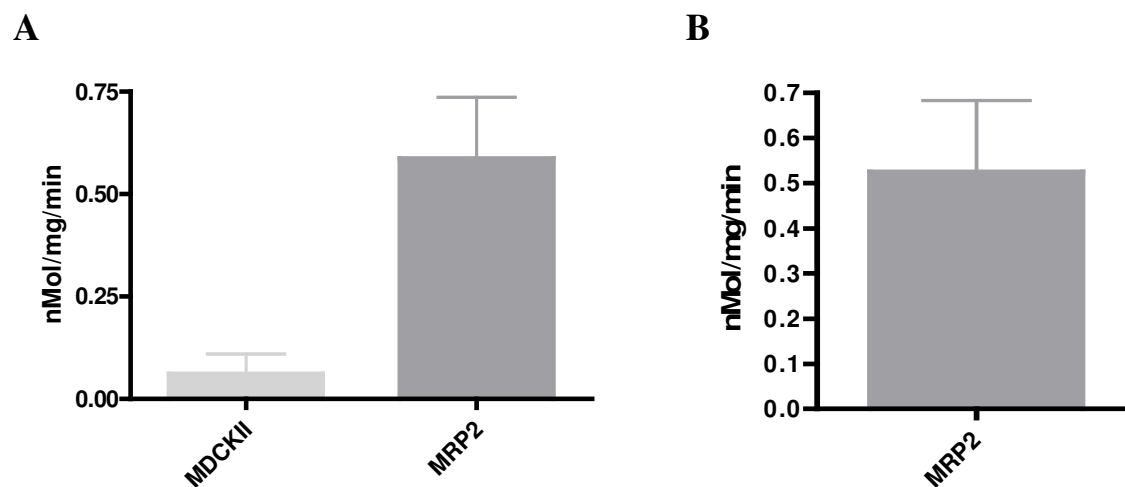


**Figure 38:** Concentration course of fluo-cAMP uptake into Sf9-MRP4 membrane vesicles. Fluo-cAMP transport was concentration dependent and saturable with a  $V_{max}$  of 1.1  $\pm$  0.2 nMol/mg/min and an apparent  $K_m$  value of 5.3  $\pm$  2  $\mu$ M. Data are expressed as mean  $\pm$  SE from 3 independent experiments. MRP4 94-: batch 94-.



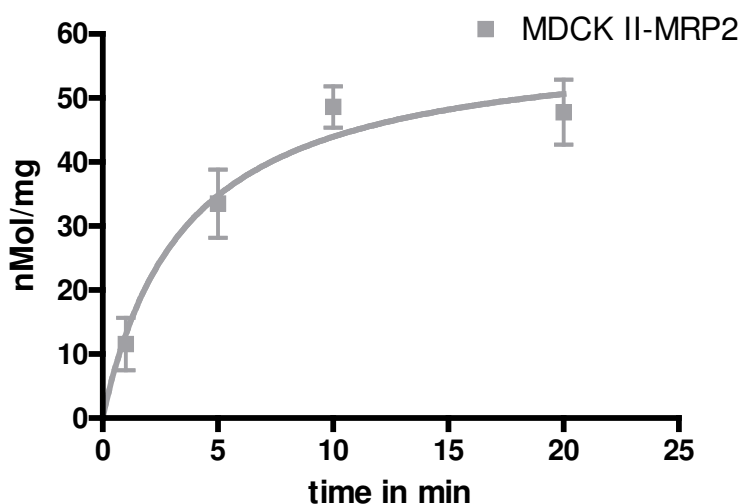
To test whether fluo-cAMP is transported by human MRP2 as well, we investigated into fluo-cAMP transport in MDCKII-MRP2 vesicles. Uptake into membrane vesicles mediated by MRP2 was a ATP-dependent, specific transport process as shown in Figure 39. Transport rate was 0.503 nMol/mg/min for fluo-cAMP transport at a concentration of 20  $\mu$ M.

**Figure 39:** ATP-dependent, specific transport of fluo-cAMP 20  $\mu$ M into MDCKII-MRP2 membrane vesicles. Fluo-cAMP was transported by a rate of 0.503 nMol/mg/min. In A active transport processes are shown in control (MDCKII) and MRP2 membrane vesicles. B shows specific uptake of fluo-cAMP mediated by MRP2. Data are expressed as mean  $\pm$  SE of three samples from one representative experiment.



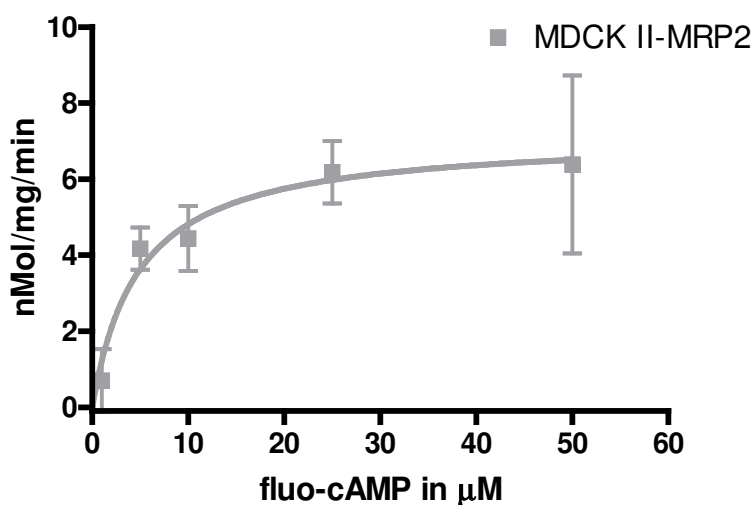
To research into transport characteristics for fluo-cAMP uptake by MRP2 in MDCKII-MRP2 vesicles, time and concentration dependency were analyzed. At a concentration of 20  $\mu$ M fluo-cAMP transport reached steady state after 10-20 minutes (Figure 40).

**Figure 40:** Fluo-cAMP transport into MDCKII-MRP2 membrane vesicles reached steady state after 10-20 minutes incubation with fluo-cAMP at 20  $\mu$ M. Data are expressed as mean  $\pm$  SE from 3 independent experiments.



For further experiments we used incubation times of 5 minutes. An apparent  $K_m$  value of 4.8  $\pm$  1.5  $\mu$ M was determined for ATP-dependent transport of fluo-cAMP mediated by MRP2 expressed in MDCKII cells. The  $V_{max}$  value was 7.2  $\pm$  0.6 nMol/mg/min (Figure 41).

**Figure 41:** Concentration course of fluo-cAMP uptake into MDCKII-MRP2 membrane vesicles. The apparent  $K_m$  was  $4.8 \pm 1.5 \mu\text{M}$  with a  $V_{\text{max}}$  value of  $7.2 \pm 0.6 \text{ nMol/mg/min}$ . Data are expressed as mean  $\pm$  SE from 3 independent experiments.



Taken together, these results indicate that affinities of fluo-cAMP to MRP4 ( $5.3 \pm 2 \mu\text{M}$ ) and MRP2 ( $4.8 \pm 1.5 \mu\text{M}$ ) are not statistically different. Maximum speed was 7-fold higher for transport mediated by MRP2, but due to the different expression system and expression rate, this value is of no relevance.

### 4.2.3 Transport Studies in Rat and Shark Choroid Plexus

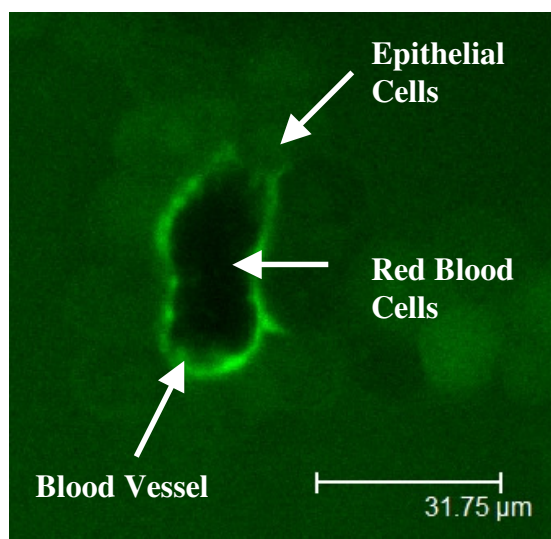
#### 4.2.3.1 Fluo-cAMP Transport in Rat Choroid Plexus

Different substances and their transport characteristics were investigated in rat and dogfish shark CP. Transport of the fluorescent compound fluo-cAMP was analyzed in rat CP and results were compared to results obtained from transport studies in killifish renal proximal tubules and Sf9-MRP4 and MDCKII-MRP2 membrane vesicles.

In Figure 42 basic characteristics of fluo-cAMP transport ( $2 \mu\text{M}$ ) in intact rat CP are shown. Steady state fluorescence in vascular/perivascular spaces and in the interior of blood vessels was much higher than in epithelial cells. Cellular fluorescence levels were higher than fluorescence levels in the bath, but fluorescence levels in the bath were quite high compared to bath fluorescence obtained using different fluorescent compounds or fluo-cAMP distribution in killifish proximal tubules. Accumulation of fluo-cAMP in vascular/perivascular spaces and in the interior of blood vessels indicate an active transport

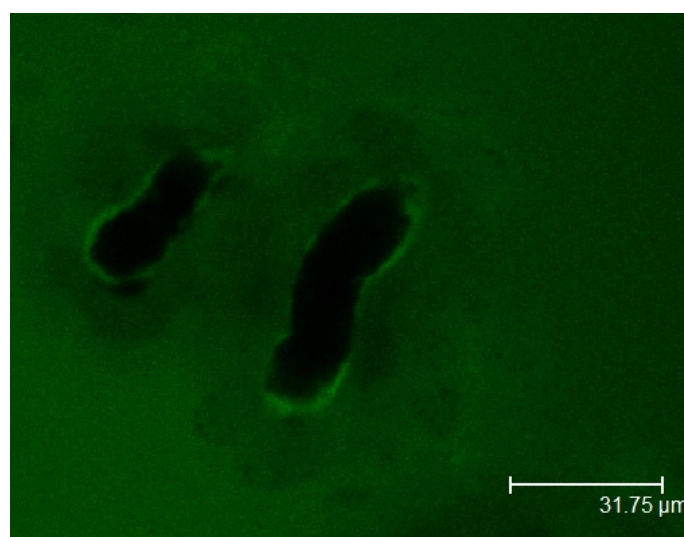
process, allocation of fluorescence levels between lumen, epithelial cells and bath are a sign of an active two-step mechanism.

**Figure 42:** Basic characteristics of fluo-cAMP ( $2\ \mu\text{M}$ ) transport in rat CP. Fluo-cAMP accumulated in perivascular/subepithelial spaces and the interior of the blood vessel and to a lower extent in epithelial cells. Cellular fluorescence barely exceeded cellular fluorescence. In the blood vessel an area of low fluorescence can be recognized where red blood cells are located.



To learn more about characteristics of fluo-cAMP transport in rat CP and transport proteins involved, different inhibitors of organic anion transport were added and their effects were measured.

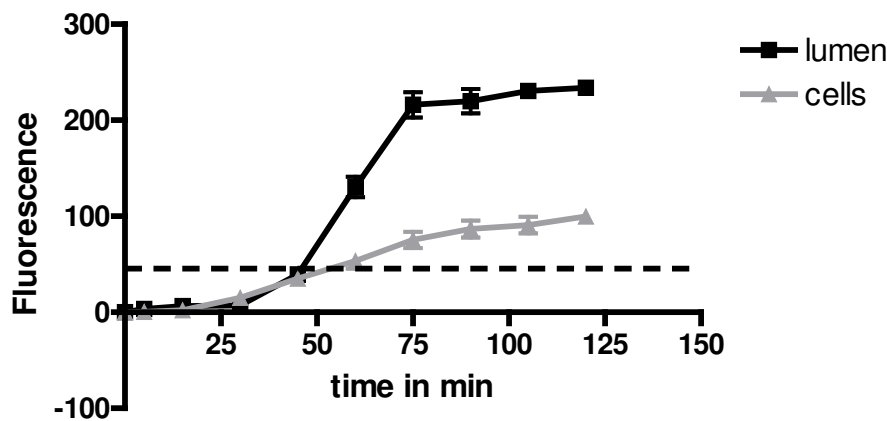
**Figure 43:** Effect of methotrexate on fluo-cAMP transport ( $2\ \mu\text{M}$ ) in rat CP. Compared to the control CP in Figure 42 fluorescence levels were clearly decreased after incubation with methotrexate.



In Figure 43 the effect of methotrexate ( $200\ \mu\text{M}$ ) on fluo-cAMP transport is pictured, to show an exemplary effect of an inhibitor of organic anion transport. In comparison to Figure 42, fluo-cAMP accumulation is clearly affected by methotrexate treatment.

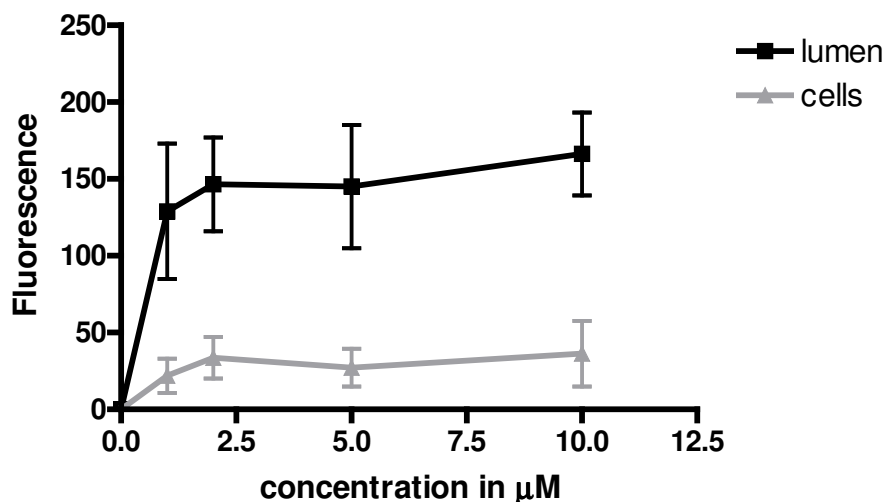
In Figure 44 the time course of fluo-cAMP accumulation in vascular/subepithelial spaces, the interior of blood vessels and epithelial cells in rat CP is shown. Steady state was reached after 75 minutes. Cellular fluorescence was approximately 40% of luminal fluorescence, both fluorescence was relatively high. Further experiments were carried out using incubation times of 90 minutes.

**Figure 44:** Time course of fluo-cAMP transport in rat CP. Steady state was reached after 75 minutes with cellular fluorescence being ~ 40% of luminal fluorescence. Data are expressed as mean  $\pm$  SE of 10 CP blood vessels from one representative isolation.



Fluo-cAMP accumulation in vascular/perivascular spaces and the interior of blood vessels as well as in epithelial cells was saturated using increasing concentrations of fluo-cAMP. Concentrations between 1 and 10  $\mu$ M were used. At concentrations  $> 2 \mu$ M luminal and cellular saturations were reached (Figure 45). All other experiments were carried out using a concentration of 2  $\mu$ M fluo cAMP.

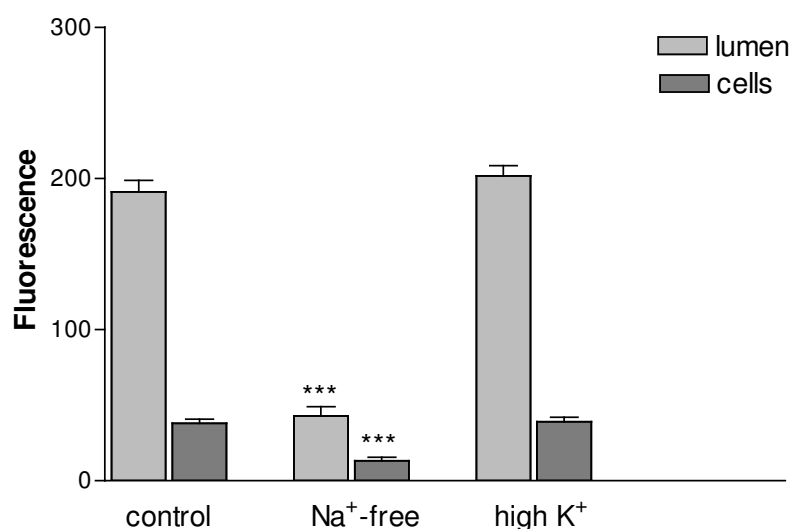
**Figure 45:** Concentration course of fluo-cAMP transport in rat CP. Saturation was reached at concentrations  $> 2 \mu$ M. Data are expressed as mean  $\pm$  SE of 10 CP blood vessels from one representative isolation.



Fluo-cAMP transport is  $\text{Na}^+$ -dependent as shown in Figure 46. Fluorescence levels in lumen and epithelial cells were decreased after incubation with  $\text{Na}^+$ -free aCSF. Concomitant reduction of luminal and cellular fluorescence indicates inhibition of uptake at the apical membrane of rat CP epithelium. A  $\text{Na}^+$ -dependent uptake transporter seems to be involved in fluo-cAMP uptake into CP epithelial cells.

Membrane depolarisation accomplished by increasing  $\text{K}^+$  concentration 10 fold had no effect on fluo-cAMP transport in rat CP (Figure 46). Therefore fluo-cAMP transport in rat CP seems to be insensitive from changes in membrane potential.

**Figure 46:** Effects of incubation with  $\text{Na}^+$ -free and high  $\text{K}^+$  aCSF on fluo-cAMP transport in rat CP. Removing  $\text{Na}^+$  had a strong inhibitory effect on fluo-cAMP accumulation in vascular/perivascular spaces, the interior of blood vessels and epithelial cells. Increasing  $\text{K}^+$  tenfold did not affect fluo-cAMP transport. Data are expressed as mean  $\pm$  SE of 10 CP blood vessels from one representative isolation. (Significantly different from control values: \* for  $P < 0.05$ , \*\* for  $P < 0.01$  and \*\*\* for  $P < 0.001$ ).

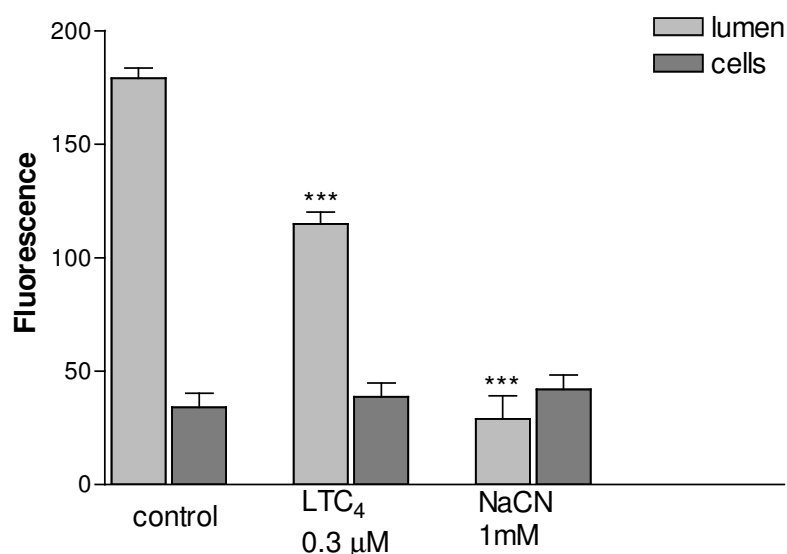


The inhibitory effect obtained using the metabolic poison NaCN indicates a metabolism driven transport of fluo-cAMP in rat CP. But NaCN treatment only affected luminal fluo-cAMP accumulation (Figure 47). Metabolism driven transport is characteristic for active transport processes.

To figure out which transport proteins are involved in fluo-cAMP transport in rat CP different specific inhibitors were used.  $\text{LTC}_4$  had an inhibitory effect on luminal fluo-cAMP accumulation, but not on cellular accumulation (Figure 47), suggesting inhibition of one or more basolateral efflux transporters.

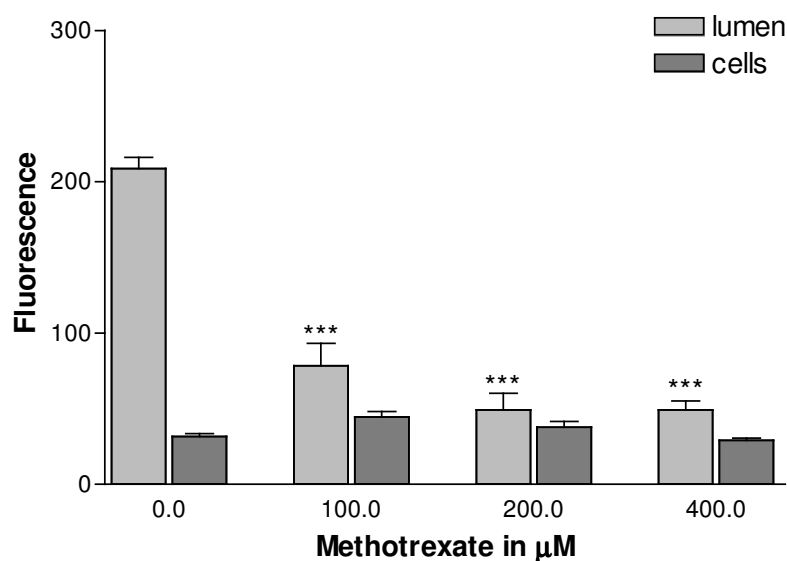
## Results

**Figure 47:** Effects of LTC<sub>4</sub> and NaCN on fluo-cAMP transport in rat CP. Both substances only affected luminal fluorescence, epithelial cell fluorescence was not concerned. Data are expressed as mean ± SE of 10 CP blood vessels from one representative isolation. (Significantly different from control values: \* for P<0.05, \*\* for P<0.01 and \*\*\* for P<0.001).



Methotrexate is a substrate for different Mrps. Inhibition of fluo-cAMP transport caused by methotrexate treatment is an evidence for involvement of one or more Mrps in mediation of fluo-cAMP transport in rat CP. The effect of methotrexate addition at different micromolar concentrations is diagrammed in Figure 48. Only luminal accumulation of fluo-cAMP was affected by methotrexate at concentrations between 100 and 400 μM.

**Figure 48:** Effects of methotrexate on fluo-cAMP transport in intact rat CP. Methotrexate had a strong inhibitory effect on basolateral efflux of fluo-cAMP. Data are expressed as mean ± SE of 10 CP blood vessels from one representative isolation. (Significantly different from control values: \* for P<0.05, \*\* for P<0.01 and \*\*\* for P<0.001).



MK 571, a potent inhibitor of Mrp mediated transport processes, led to reduced fluorescence levels in vascular/perivascular spaces, the interior of blood vessels and, at a higher concentration, also in epithelial cells. These effects were dose dependent (Figure 49). The effects indicate involvement of one or more Mrps in fluo-cAMP transport in rat CP.

**Figure 49:** Effects of MK571 on fluo-cAMP transport in rat CP. At 10  $\mu$ M only luminal fluorescence was affected, at a higher concentration cellular fluorescence was decreased as well. Data are expressed as mean  $\pm$  SE of 10 CP blood vessels from one representative isolation. (Significantly different from control values: \* for  $P < 0.05$ , \*\* for  $P < 0.01$  and \*\*\* for  $P < 0.001$ ).

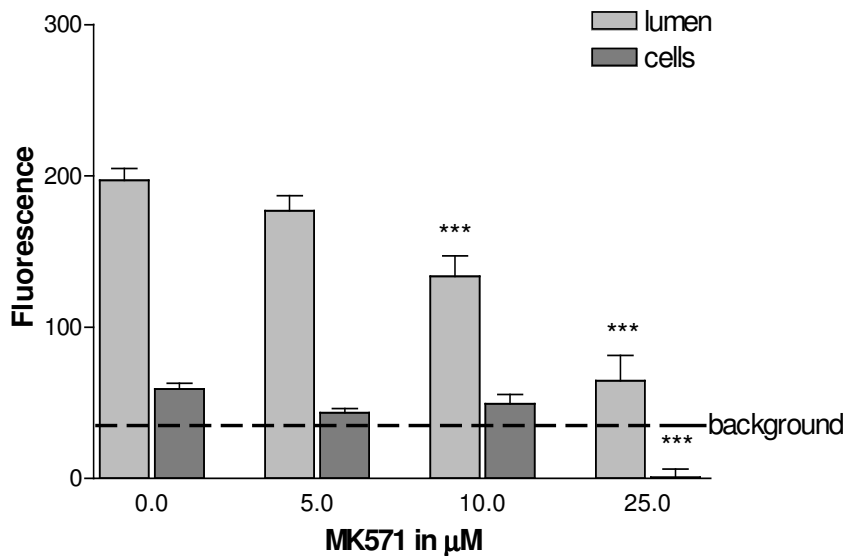
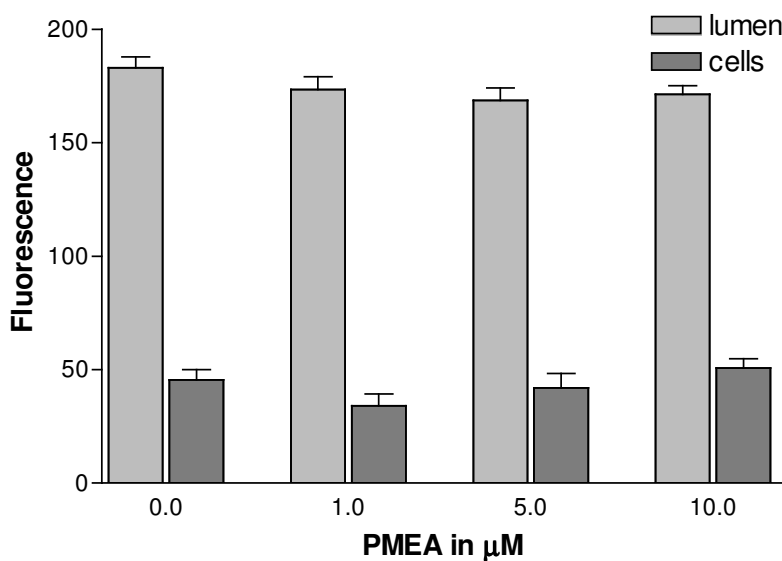


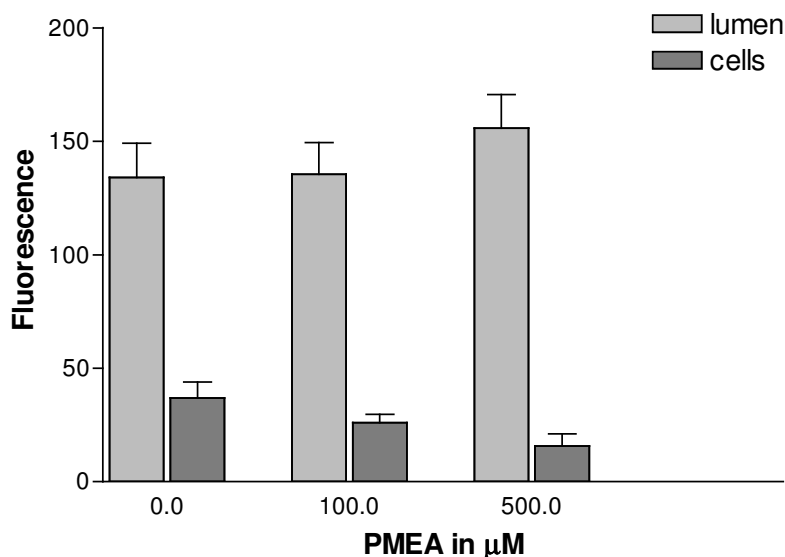
**Figure 50:** Effects of adefovir on fluo-cAMP transport. Adefovir had no effect on fluo-cAMP accumulation within the tissue at concentrations between 1 and 10  $\mu$ M. Data are expressed as mean  $\pm$  SE of 10 CP blood vessels from one representative isolation.



To detect which transport proteins of the Mrp family are involved in mediation of fluo-cAMP transport in rat CP, different Mrp4 substrates were tested. Adefovir did not affect fluo-cAMP

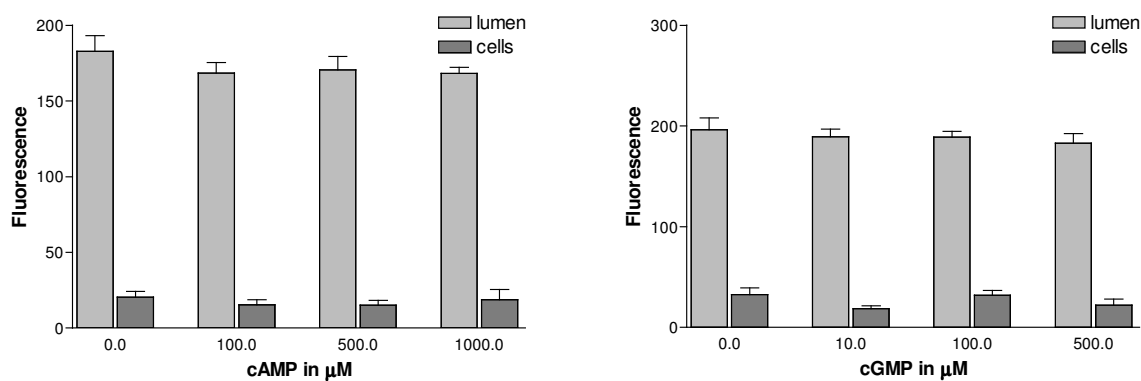
transport in rat CP at the same concentrations (1-10  $\mu\text{M}$ ) we used in killifish proximal tubules (Figure 50). We tested higher concentrations as well, but even at a concentration of 500  $\mu\text{M}$  adefovir did not affect fluo-cAMP transport in rat CP (Figure 51).

**Figure 51:** Effects of adefovir on fluo-cAMP transport in rat CP. Even at concentrations up to 500  $\mu\text{M}$  adefovir did not effect distribution of fluo-cAMP. Data are expressed as mean  $\pm$  SE of 10 CP blood vessels from one representative isolation.



The cyclic nucleotides cAMP and cGMP are known substrates of Mrp4 (Van Aubel et al., 2002). Both were used at high micromolar concentrations, but no effects on fluo-cAMP transport were obtained (Figure 52). Interestingly even the unlabeled cAMP had no effect on transport of its fluorescent analog. In rat CP cAMP and fluo-cAMP seem to be transported by different transport proteins.

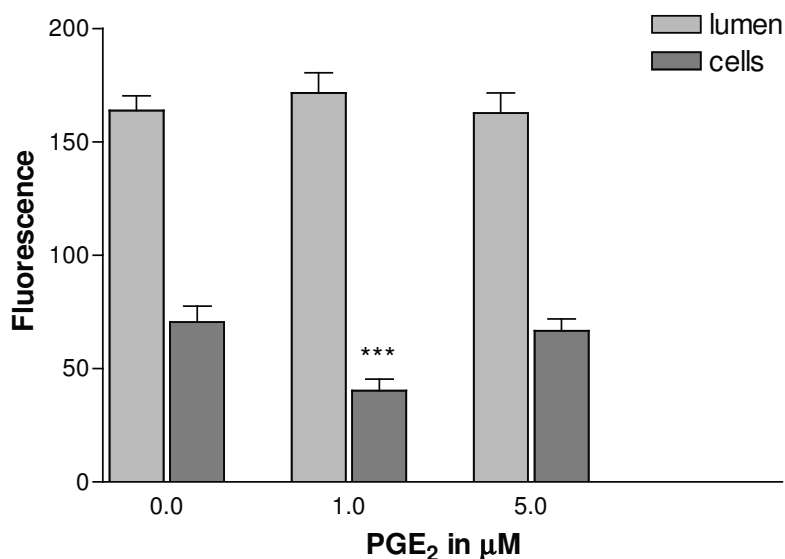
**Figure 52:** Effects of the cyclic nucleotides cAMP and cGMP on fluo-cAMP transport in rat CP. Neither cAMP nor cGMP had any effects on fluo-cAMP transport at high concentrations up to 500 or 1000  $\mu\text{M}$ . Data are expressed as mean  $\pm$  SE of 10 CP blood vessels from one representative isolation.



Prostaglandin E<sub>2</sub> (PGE<sub>2</sub>) is known as Mrp4 substrate as well (Reid et al., 2003). It had no effect on fluo-cAMP accumulation within vascular/perivascular spaces and the interior of

blood vessels. Epithelial cell fluorescence was affected, but only at a concentration of 1  $\mu\text{M}$  and not at 5  $\mu\text{M}$  of  $\text{PGE}_2$  (Figure 53), suggesting an unspecific effect.

**Figure 53:** Effects of  $\text{PGE}_2$  on fluo-cAMP transport in rat CP.  $\text{PGE}_2$  did not affect luminal accumulation but reduced cellular fluorescence at a concentration of 1  $\mu\text{M}$ . Data are expressed as mean  $\pm$  SE of 10 CP blood vessels from one representative isolation.



Summarizing the effects of adefovir, the cyclic nucleotides cAMP and cGMP and  $\text{PGE}_2$ , involvement of Mrp4 in fluo-cAMP efflux at the basolateral membrane of CP epithelial cells can be ruled out.

Mrp2 expression is low in rat CP, analyzed by Choudhuri et al. (2003) on RNA level. To exclude an involvement of Mrp2 on fluo-cAMP transport,  $\text{TR}^-$  rats were used.  $\text{TR}^-$  rats are wistar rats, deficient of Mrp2. The  $\text{TR}^-$  or GY rats were first established in Groningen (the Netherlands). Those *Mrp2-deficient Groningen Yellow/Transport deficient wistar rats* have a Mrp2 deformity. In  $\text{TR}^-$  rats mRNA levels of Mrp2 are very low and the protein is absent. This is due to a single nucleotide deletion in the gene resulting in a frame shift, which leads to an early stop codon. A human analog to  $\text{TR}^-$  rats is the Dubin-Johnson syndrome patient. Dubin-Johnson patients are lacking MRP2 causing a deficiency in the biliary excretion of several glutathione conjugates, glucuronides and other MRP2 substrates (Masereeuw et al., 2003).

Fluo-cAMP transport in  $\text{TR}^-$  rats was compared with its transport in wistar wildtype rats. No differences were obtained for the different rat strains (Figure 54). This means that Mrp2 is not involved in fluo-cAMP transport in rat CP.

Incubation with probenecid at 10-100  $\mu\text{M}$  led to reduced fluorescence levels in vascular/perivascular spaces, the interior of blood vessels and CP epithelial cells. 10  $\mu\text{M}$  did

not affect fluo-cAMP transport in rat CP, but the higher concentrations did. Cellular fluorescence was only affected by probenecid at the highest used concentration of 100  $\mu\text{M}$  (Figure 55). These effects allude participation of Mrps different from Mrp2 and Mrp4, Oatps or Oats in fluo-cAMP transport in rat CP.

**Figure 54:** Fluo-cAMP transport in CP of wistar rats as control or TR<sup>-</sup> rats. No differences in luminal or cellular fluorescence were obtained. Data are expressed as mean  $\pm$  SE of 10 CP blood vessels from one representative isolation.

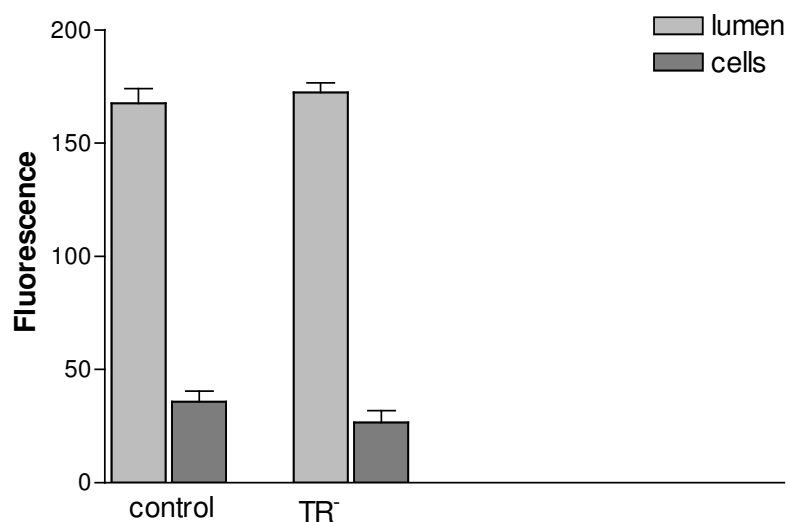
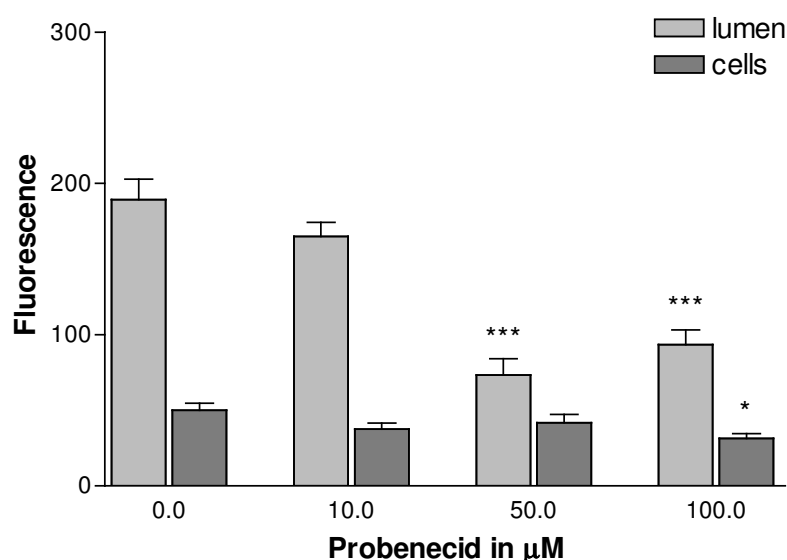


**Figure 55:** Effects of probenecid on fluo-cAMP transport in rat CP. Luminal fluorescence was affected by probenecid at a concentration of 50 and 100  $\mu\text{M}$ , cellular fluorescence was only reduced at 100  $\mu\text{M}$ . Data are expressed as mean  $\pm$  SE of 10 CP blood vessels from one representative isolation.



Na<sup>+</sup>-taurocholate, a substrate for Oats and Oatps (Miller, 2004), was used at concentrations between 10 and 100  $\mu\text{M}$ . The result was a dose-dependent inhibitory effect on luminal and, at 100  $\mu\text{M}$ , cellular fluo-cAMP accumulation. The inhibitory effect was strong and reduced

luminal and cellular fluorescence levels below background fluorescence at 100  $\mu\text{M}$  (Figure 56). This is evidence for an Oat or Oatp involved in fluo-cAMP transport in rat CP.

**Figure 56:** Effects of  $\text{Na}^+$ -taurocholate on fluo-cAMP transport in rat CP. Luminal and cellular fluorescence were decreased by  $\text{Na}^+$ -taurocholate treatment in a dose-dependent manner. Data are expressed as mean  $\pm$  SE of 10 CP blood vessels from one representative isolation. (Significantly different from control values: \* for  $P < 0.05$ , \*\* for  $P < 0.01$  and \*\*\* for  $P < 0.001$ ).

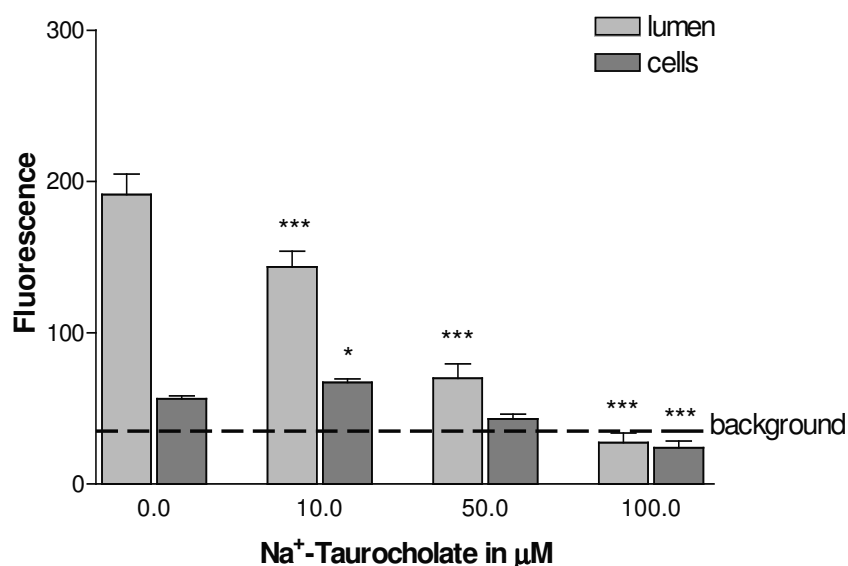
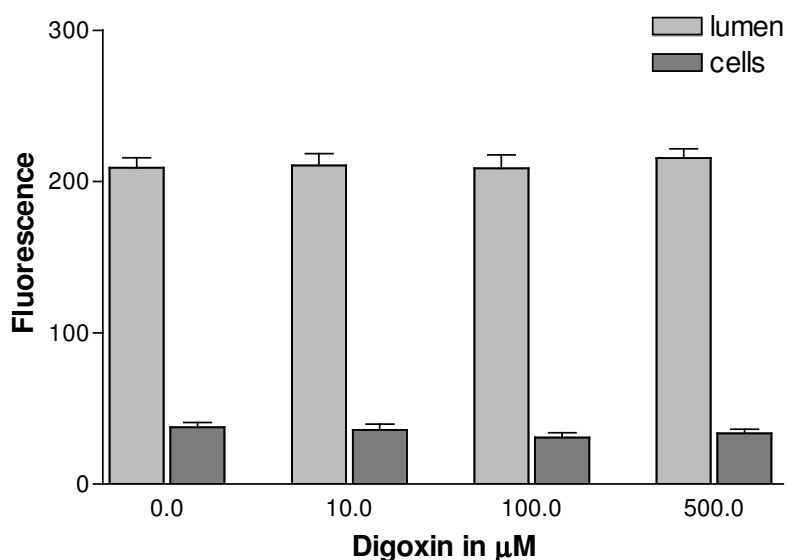


**Figure 57:** Effects of digoxin on fluo-cAMP transport in rat CP. Digoxin did not affect luminal or cellular fluorescence at concentrations between 10 and 500  $\mu\text{M}$ . Data are expressed as mean  $\pm$  SE of 10 CP blood vessels from one representative isolation. (Significantly different from control values: \* for  $P < 0.05$ , \*\* for  $P < 0.01$  and \*\*\* for  $P < 0.001$ ).



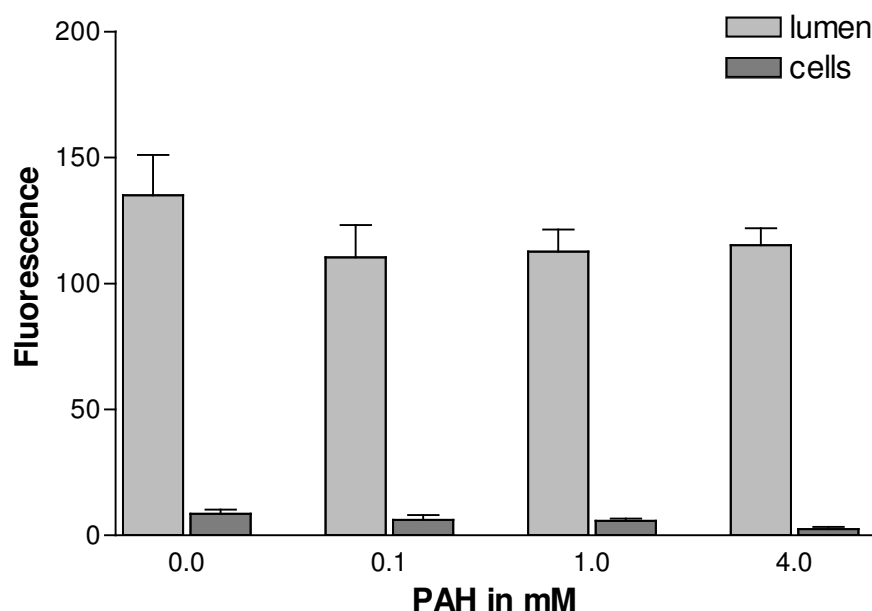
To examine whether the exchanger Oatp2, which is located to the basolateral membrane of CP epithelium (Kusuhara et al., 2004), is involved in fluo-cAMP transport in rat CP, digoxin was used. The cardiac glykoside digoxin has a higher affinity to Oatp2 than to the other

members of the Oatp family (Kusuhara et al., 2004). Digoxin had no effect on distribution of fluo-cAMP within CP tissue, even though high concentrations up to 500  $\mu$ M digoxin were used (Figure 57). Therefore Oatp2 seems not to be involved in active efflux of fluo-cAMP on the basolateral membrane of CP epithelium in rats.

$\text{Na}^+$ -dependency indicates involvement of an Oat, because transport processes mediated by Oats are affected by changes in  $\text{Na}^+$  concentration. rOat3 is the most abundant isoform expressed in CP epithelium and located to the apical membrane (Miller, 2004). rOat1 is only expressed to a lower extent in rat CP. This transporter could only be detected at mRNA level and protein expression could not be demonstrated (Kusuhara et al., 2004).

PAH, used at concentrations up to 4 mM, did not affect fluo-cAMP distribution in rat CP (Figure 58). Since PAH is an inhibitor of Oat1 and Oat3, the results obtained after incubation with PAH lead to the assumption that rOat1 and rOat3 seem not to be transporter involved in fluo-cAMP uptake at the apical membrane of epithelial cells. As PAH is a low affinity substrate for Mrp2 and Mrp4 as well, this result is one more evidence for mediation of fluo-cAMP transport independent from Mrp2 and Mrp4.

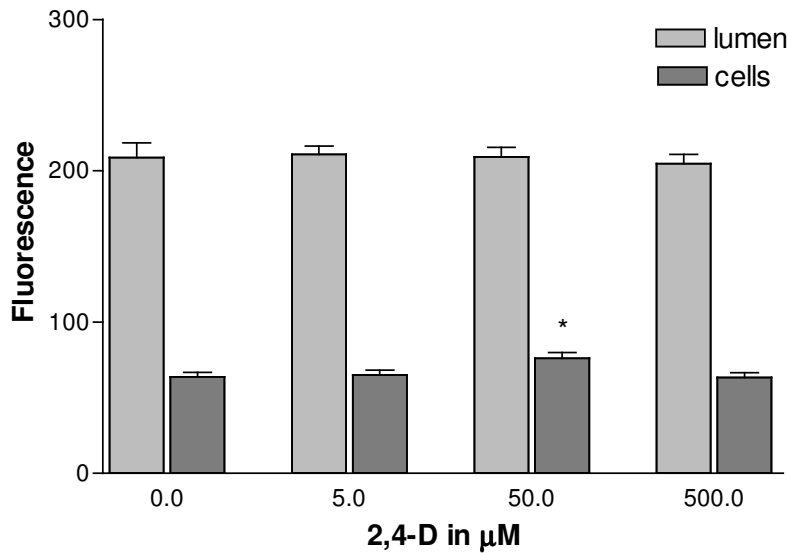
**Figure 58:** Effects of PAH on fluo-cAMP transport in rat CP. PAH at concentrations between 0.1 and 4 mM had no effects on fluo-cAMP transport. Data are expressed as mean  $\pm$  SE of 10 CP blood vessels from one representative isolation.



2,4-D, a substance that has an inhibitory effect on Oat3 mediated transport of FL in rat CP (Breen et al., 2002), had no effects on fluo-cAMP transport (Figure 59). Fluo-cAMP transport seems to be mediated by transport proteins being different from those involved in FL transport in rat CP.

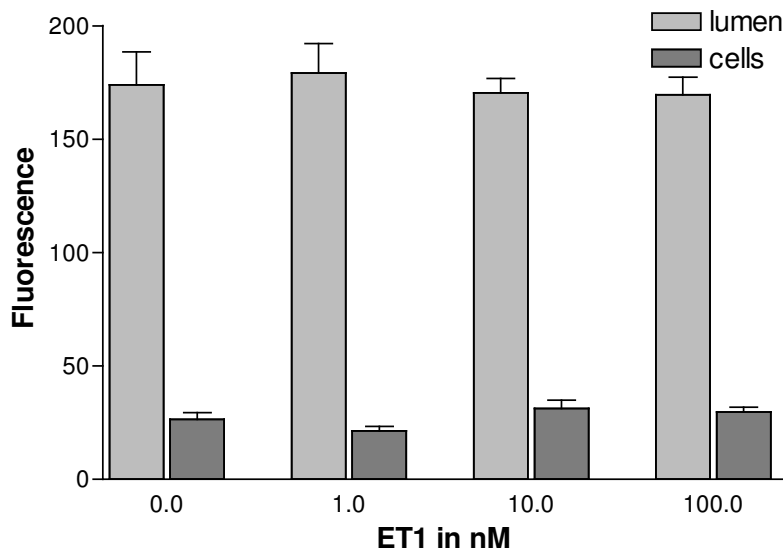
## Results

**Figure 59:** Effects of 2,4-D on fluo-cAMP transport in rat CP. 2,4-D affected fluo-cAMP transport only unspecific, at a concentration of 50  $\mu\text{M}$  cellular fluorescence was increased. At concentrations between 5 and 500  $\mu\text{M}$  no other effect was obtained. Data are expressed as mean  $\pm$  SE of 10 CP blood vessels from one representative isolation. (Significantly different from control values: \* for  $P < 0.05$ , \*\* for  $P < 0.01$  and \*\*\* for  $P < 0.001$ ).



To examine regulatory processes controlling fluo-cAMP transport in rat CP we investigated into different pathways. Initially, an endothelin pathway was studied.

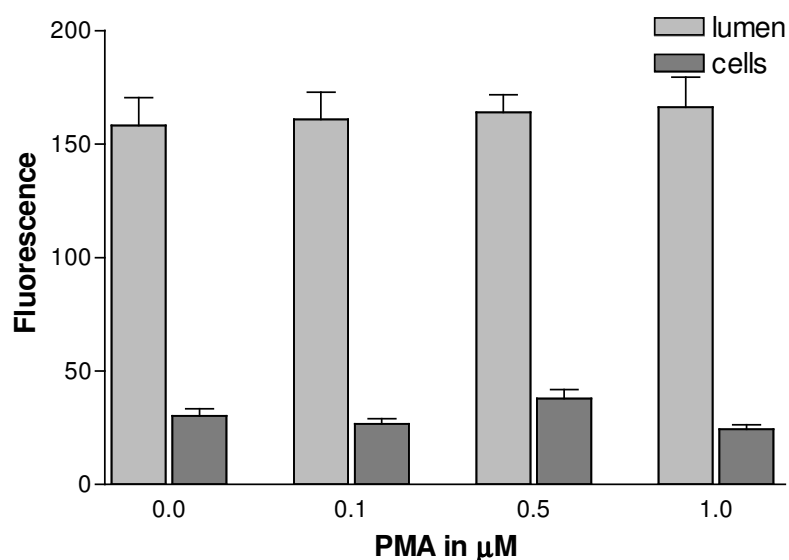
**Figure 60:** Effects of ET1 on fluo-cAMP transport in rat CP. ET1 had no effect at all on fluo-cAMP accumulation in vascular/perivascular spaces, the interior of blood vessels or epithelial cells. Data are expressed as mean  $\pm$  SE of 10 CP blood vessels from one representative isolation.



ET1 binding on  $\text{ET}_B$  receptor leads to a subsequent cascade via NO-synthase and activation of PKC. To research into this cascade we incubated rat CP with ET1 at nanomolar concentrations and fluo-cAMP. ET1 treatment did not affect fluo-cAMP transport in rat CP (Figure 60). This result leads to the suggestion that no ET pathway is involved in regulation of fluo-cAMP transport in rat CP.

To analyze whether PKC, activated by a different cascade than via ET1 signaling, is involved in regulation of fluo-cAMP transport, the phorbol ester phorbol-12-myristate-13-acetate (PMA) was used. PMA had no effects on fluorescence intensities in vascular/perivascular spaces, the interior of blood vessels or epithelial cells in rat CP as shown in Figure 61. Therefore, ET1 and PKC seem not to be involved in regulatory processes concerning fluo-cAMP transport in rat CP.

**Figure 61:** Effects of the phorbol ester PMA on fluo-cAMP transport in rat CP. PMA did not affect luminal or cellular fluorescence. Data are expressed as mean  $\pm$  SE of 10 CP blood vessels from one representative isolation.



To verify whether activation of PKA affects fluo-cAMP transport in rat CP, the indirect PKA activator forskolin was added. We incubated tissue with forskolin and H-89 as described above. Forskolin had no effect on fluo-cAMP transport at micromolar concentrations, nor had the PKA inhibitor H-89 (Figure 62).

Another pathway which may be involved in regulation of fluo-cAMP transport in rat CP is the mitogen-activated protein kinase (MAPK) pathway. Epidermal growth factor (EGF) leads to phosphorylation of mitogen-activated/extracellular signal-regulated kinase (MEK), extracellular signal-regulated kinase 1 and 2 (ERK1/2) and phospholipase A<sub>2</sub> (PLA<sub>2</sub>). PLA<sub>2</sub> activation leads to increased release of arachidonic acid which is metabolised to prostaglandin via cyclooxygenase 1 (COX1). Prostaglandin leads to PKA activation via adenylate cyclase activation (Soodvilai et al., 2004).

## Results

**Figure 62:** Effects of forskolin and H-89 on fluo-cAMP transport in rat CP. Neither the PKA activator forskolin nor the PKA inhibitor H-89 affected distribution of fluo-cAMP in vascular/perivascular spaces, the interior of blood vessels and epithelial cells. Data are expressed as mean  $\pm$  SE of 10 CP blood vessels from one representative isolation.

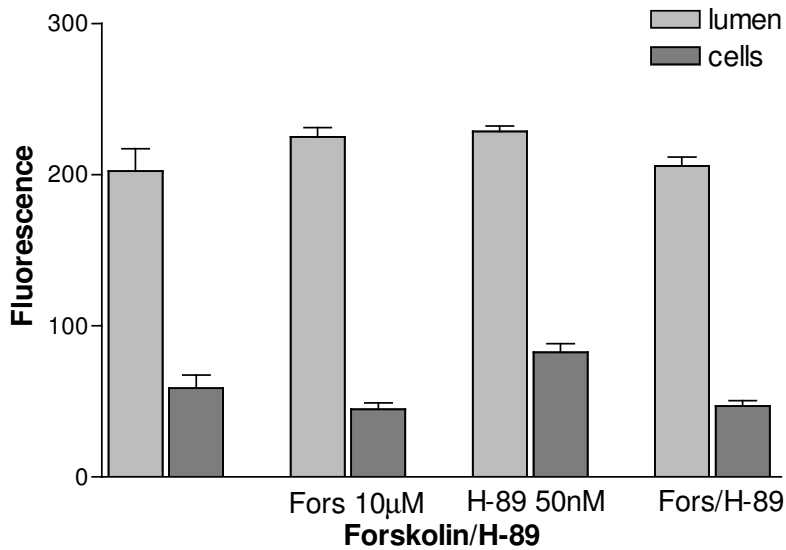
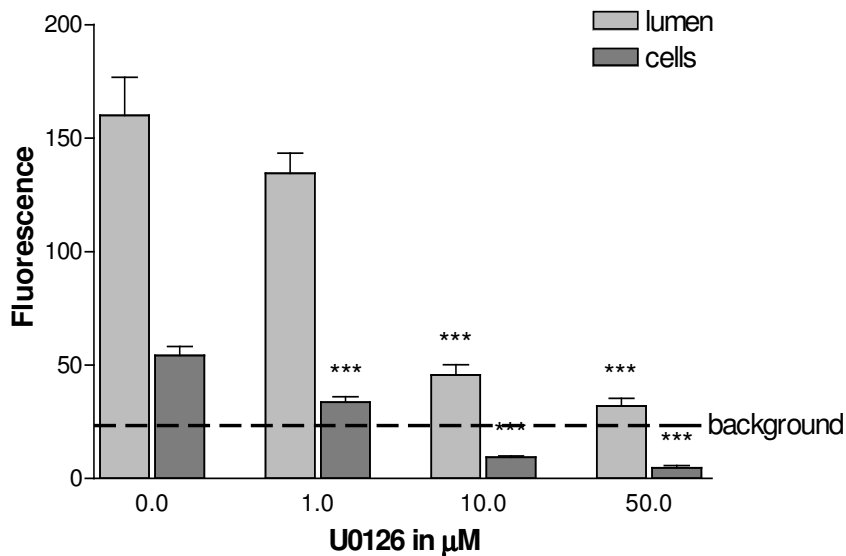


**Figure 63:** Effects of U0126 on fluo-cAMP transport in rat CP. U0126 had a strong inhibitory effect on cellular fluorescence, fluorescence in vascular/perivascular spaces and the interior of blood vessels were only affected at concentrations of 10 and 50 µM. Data are expressed as mean  $\pm$  SE of 10 CP blood vessels from one representative isolation. (Significantly different from control values: \* for  $P < 0.05$ , \*\* for  $P < 0.01$  and \*\*\* for  $P < 0.001$ ).

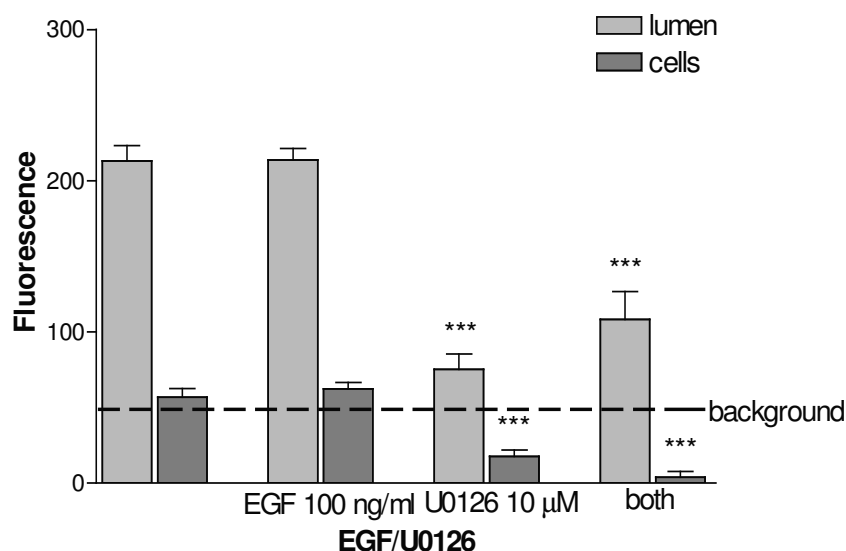


Effects provoked by the MEK1/2 specific inhibitor U0126 were analyzed. U0126 had a strong inhibitory effect on fluo-cAMP accumulation in vascular/perivascular spaces, the interior of blood vessels and epithelial cells in rat CP at 10 and 50 µM. At 1 µM U0126 only cellular fluorescence was reduced (Figure 63). These results indicate an inhibition of apical uptake

into CP epithelial cells and hence decreased accumulation of fluo-cAMP in vascular/perivascular spaces and the interior of blood vessels.

EGF activates the MAPK pathway. If this pathway is involved, EGF should alter the inhibitory effect triggered by U0126.

**Figure 64:** Effects of EGF and U0126 on fluo-cAMP transport in rat CP. EGF had no effect and could not alter the inhibitory effect of U0126. Data are expressed as mean  $\pm$  SE of 10 CP blood vessels from one representative isolation. (Significantly different from control values: \* for  $P < 0.05$ , \*\* for  $P < 0.01$  and \*\*\* for  $P < 0.001$ ).



We incubated CPs with fluo-cAMP and 1) EGF 100 ng/ml or 2) U0126 10  $\mu$ M or 3) EGF 100 ng/ml and U0126 10  $\mu$ M. EGF alone had no effect, MAPK is not activated. As described above U0126 had a strong inhibitory effect which cannot be altered by EGF addition (Figure 64). The inhibitory effect of U0126 should be altered by EGF in case MAPK pathway was involved. But regarding the results obtained from inhibitor studies using EGF and U0126, the MAPK pathway seems not to be involved in regulation of fluo-cAMP transport in rat CP. The U0126 effect seems to be independent from MAPK pathway activation.

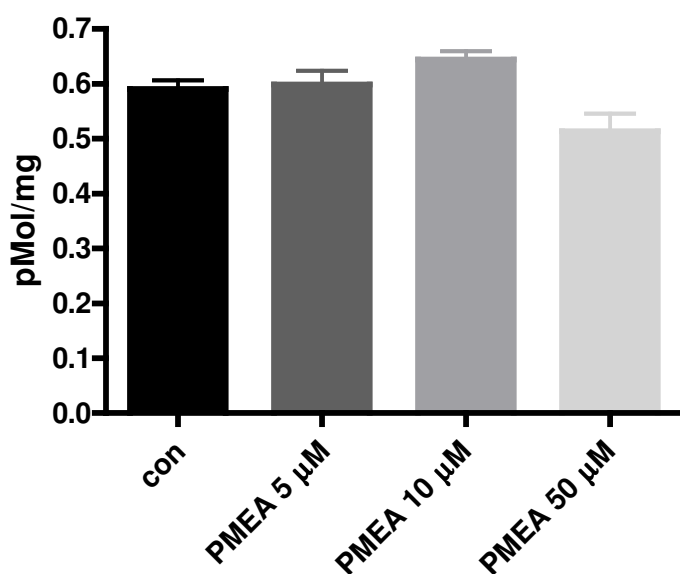
#### 4.2.3.2 [ $^3$ H]-cGMP transport in rat CP

As mentioned above cGMP is a known substrate of Mrp4, which we localized to the basolateral membrane of rat CP epithelium using indirect immunohistochemistry (Figure 10 B). To verify this localization, we carried out functional analyses using the radioactive labeled compound [ $^3$ H]-cGMP, which is a specific substrate for Mrp4. Using radioactive compounds we can only detect changes in accumulation within whole CP tissue, reflecting inhibition or activation of transport processes at the apical membrane of CP epithelium. If Mrp4 is localized to the apical membrane of CP epithelium, an inhibition caused by adefovir would

lead to increased radioactivity in the tissue. Inhibition of a basolateral localized Mrp4 would cause reduced radioactivity in epithelial/subepithelial spaces and the interior of blood vessels, cellular fluorescence would be increased, but total radioactivity in CP tissue would remain stable.

For functional analyses CPs were incubated with [ $^3\text{H}$ ]-cGMP and the Mrp4 inhibitor adefovir at concentrations between 5 and 50  $\mu\text{M}$ . Amount of [ $^3\text{H}$ ]-cGMP in the tissue was measured afterwards. After incubation with adefovir extent of radioactivity in the tissue was not affected significantly in comparison to a control (Figure 65).

**Figure 65:** Effects of adefovir on [ $^3\text{H}$ ]-cGMP transport in rat CP. No statistically different changes compared to control were obtained. Data are expressed as mean  $\pm$  SE of three independent isolations



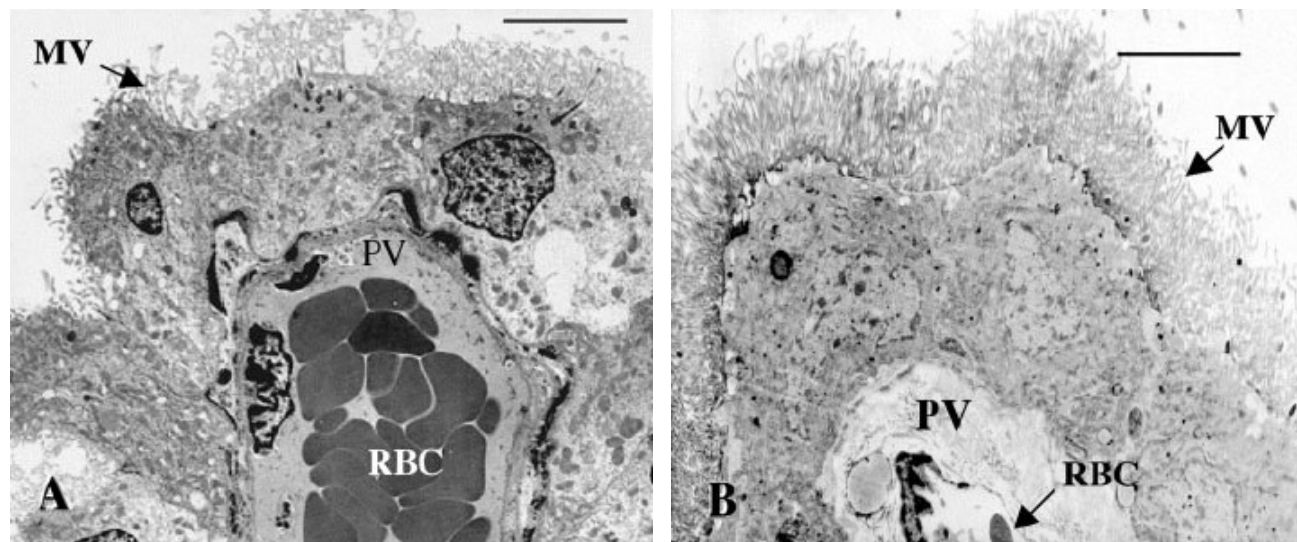
These findings confirm the localization we detected for Mrp4, because extent of radioactivity in the whole tissue was not affected after inhibition of Mrp4.

#### 4.2.3.3 Texas Red Transport in Rat and Dogfish Shark Choroid Plexus

Morphology and ultrastructure of shark IV and rat lateral ventricles were studied by Villalobos et al (2002). A remarkable similarity was found. In both species a monolayer of epithelial cells contains numerous mitochondria and faces the CSF in the ventricles of the brain. Tight junctions (zonula occludens) connect the epithelial cells. Blood capillaries are fenestrated and blood bathes the basolateral membrane of CP epithelial cells. The apical membrane is defined by a dense microvillus border. In Figure 66 electron micrographs of rat lateral (A) and shark IV (B) CPs are shown.

Consistent to the similar morphology and ultrastructure of rat and shark CPs, similar transport mechanisms for the organic anions FL and FL-MTX were found (Baehr et al., in press; Breen et al., 2002; Breen et al., 2004; Miller, 2004; Villalobos et al., 2002).

**Figure 66:** Electron micrographs of adult rat lateral CP (A) and shark IV CP (B). In both species CP tissues look very similar. The blood vessels are surrounded by a monolayer of epithelial cells. At the apical, CSF facing, membrane microvilli are recognizable in rat and shark. MV: microvilli; PV: perivascular space, RBC: red blood cells. The images are modified from Villalobos et al., 2002.



To analyze differences and similarities of transport processes in rat and shark CPs, one more organic anion, the medium sized TR, was used.

**Figure 67:** Confocal image of TR (1  $\mu$ M) transport in shark CP. TR accumulation was highest in vascular/perivascular spaces and the interior of blood vessels followed by epithelial cells. Lowest fluorescence levels were detected in the bath.

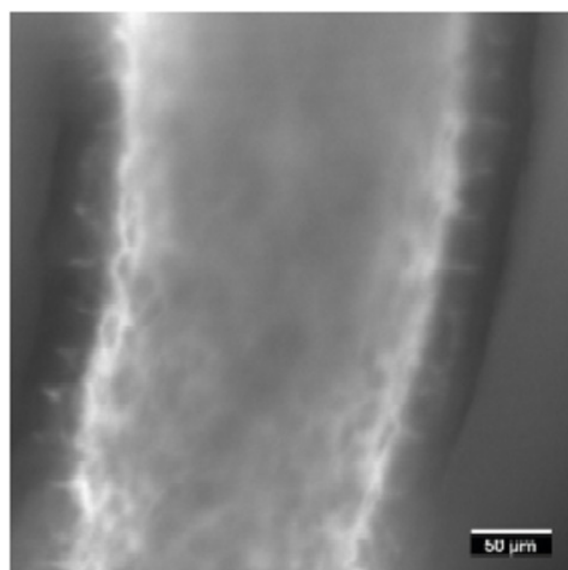
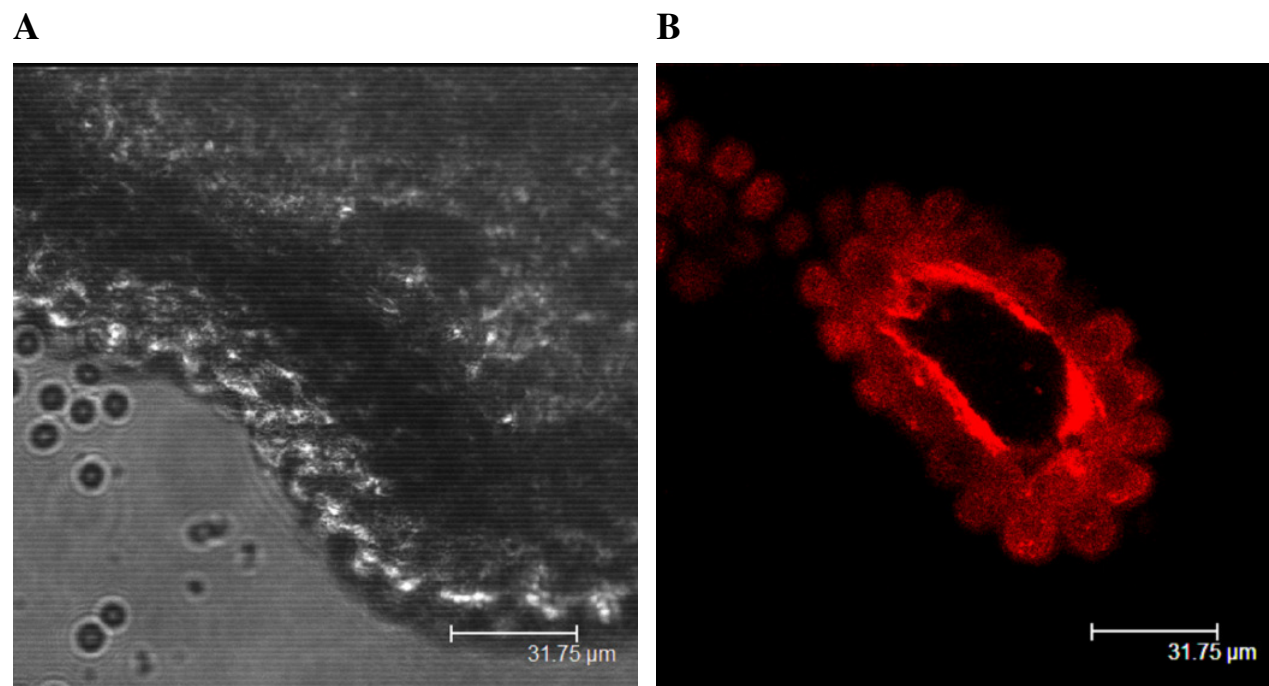


Figure 67 shows a confocal image of dogfish shark CP after incubation with TR 1  $\mu$ M for 60 minutes. BBM and BLM can be recognized as refractile elements between cells and medium or blood. Beneath CP epithelium is a subepithelial space and blood vessels. Blood vessels

contain erythrocytes, which can be seen as areas with low fluorescence intensity in confocal images. In Figure 68 transmitted light (A) and confocal images (B) of rat CP are shown.

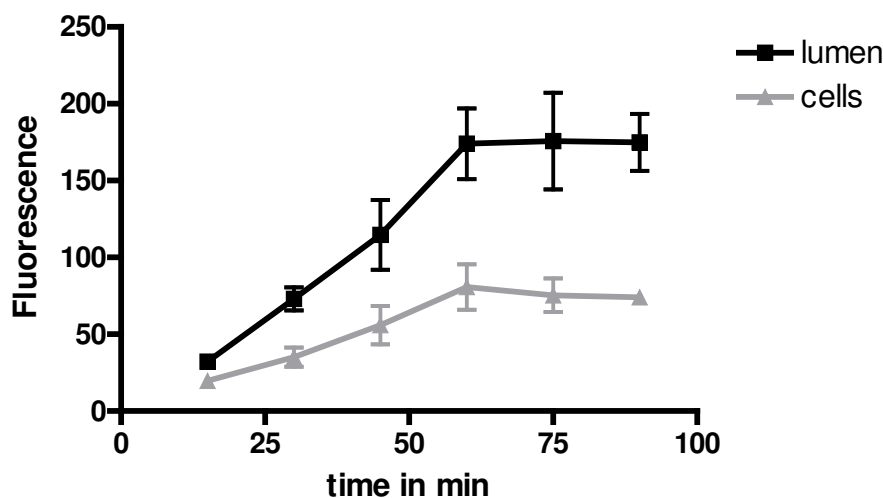
**Figure 68:** Transmitted light (A) and confocal (B) images of TR (2  $\mu\text{M}$ ) transport in rat CP. As in shark CP TR accumulation was highest in vascular/subepithelial spaces and the interior of blood vessels. Cellular fluorescence was lower, bath fluorescence was almost not detectable.



TR accumulated in epithelial cells and in vascular/subepithelial spaces and the interior of blood vessels. Fluorescence intensity was high in vascular/subepithelial spaces and the interior of blood vessels (except areas where erythrocytes are located) and lower in epithelial cells. Medium fluorescence was lower than cellular fluorescence.

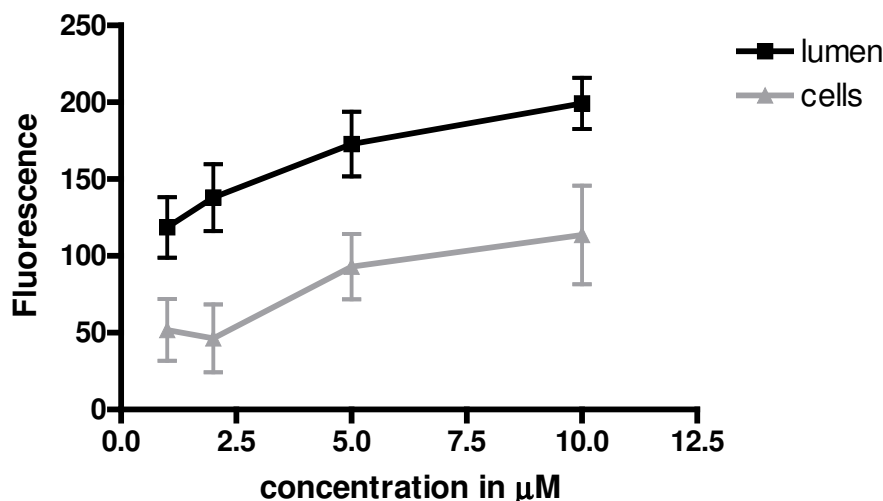
In Figure 69 the time course of TR accumulation in vascular/subepithelial spaces, the interior of blood vessels and epithelial cells in rat CP is shown. TR accumulation (2  $\mu\text{M}$ ) reached steady state within 60 minutes. Further experiments were carried out with incubation times of 90 min. Cellular fluorescence was  $\sim 42\%$  of fluorescence intensity in vascular/subepithelial spaces and the interior of blood vessels at steady state, these findings indicate an effective basolateral efflux. Background fluorescence was, different to the findings obtained from incubation with fluo-cAMP in rat CP, almost not detectable. This distribution: low fluorescence in medium, higher fluorescence in epithelial cells and highest fluorescence in vascular/perivascular spaces and the interior of blood vessels, indicates an active two-step mechanism for TR transport in rat CP.

**Figure 69:** Time course of TR accumulation in rat CP. TR accumulation reached steady state after 60 minutes. Cellular fluorescence was ~42% of fluorescence intensity in vascular/subepithelial spaces and the interior of blood vessels. Data are expressed as mean  $\pm$  SE of 10 CP blood vessels from one representative isolation.



Steady state accumulation in vascular/subepithelial spaces, the interior of blood vessels and epithelial cells was saturated using increasing TR concentrations in the incubation solution. Rat CPs were incubated with TR at concentrations between 1 and 10  $\mu$ M. At concentrations over 5  $\mu$ M TR transport started to reach a plateau as well in vascular/subepithelial spaces and the interior of blood vessels as in epithelial cells in rat CP (Figure 70). For further experiments we used TR at a concentration of 2  $\mu$ M.

**Figure 70:** Concentration dependency of TR transport in rat CP. At concentrations > 5  $\mu$ M transport started to reach a plateau. Data are expressed as mean  $\pm$  SE of 10 CP blood vessels of one representative isolation.



Accumulation of TR was studied in absence and presence of various inhibitors of organic anion transport. Figure 71 shows TR 2  $\mu$ M accumulation in a rat CP (A) and TR distribution after incubation with medium containing TR and Na<sup>+</sup>-taurocholate 25  $\mu$ M (B). Fluorescence

intensity was significantly lower in vascular/subepithelial spaces, the interior of blood vessels and epithelial cells after treatment with Na<sup>+</sup>-taurocholate.

**Figure 71:** Overlay of transmitted light and confocal images of rat CP. TR transport is shown in a control CP (A) and concomitant incubation with TR and Na<sup>+</sup>-taurocholate. In comparison to control CP, fluorescence in vascular/subepithelial spaces, the interior of blood vessels and epithelial cells was reduced after Na<sup>+</sup>-taurocholate treatment.

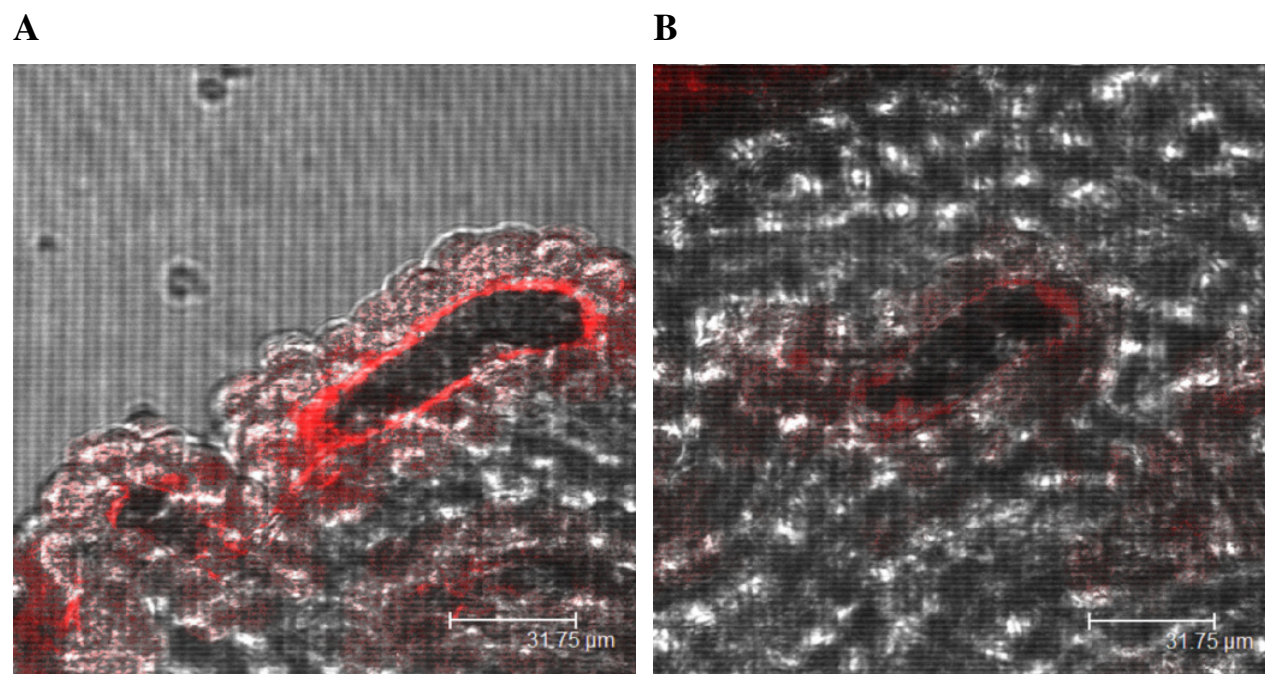
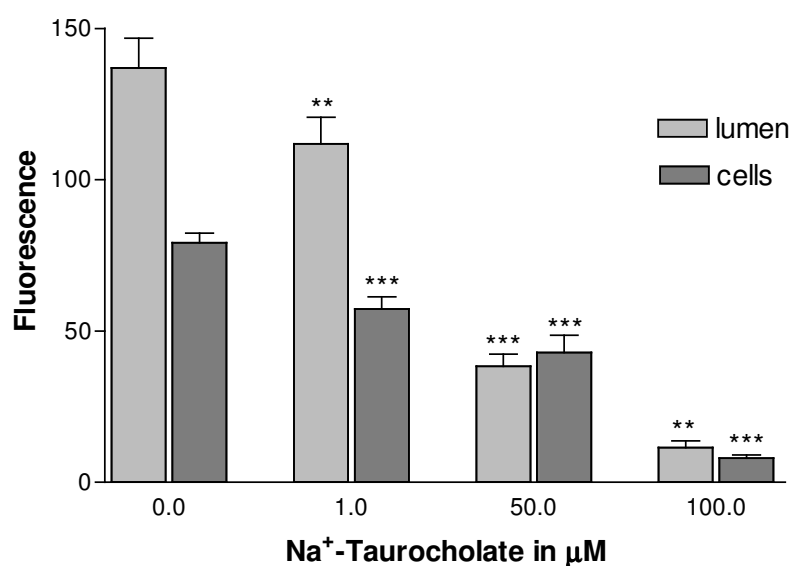


**Figure 72:** Effects of Na<sup>+</sup>-taurocholate on TR transport in rat CP. Na<sup>+</sup>-taurocholate led to a dose-dependent reduction of TR accumulation in vascular/perivascular spaces, the interior of blood vessels and epithelial cells. Data are expressed as mean ± SE of 10 CP blood vessels from one representative isolation. (Significantly different from control values: \* for P<0.05, \*\* for P<0.01 and \*\*\* for P<0.001).



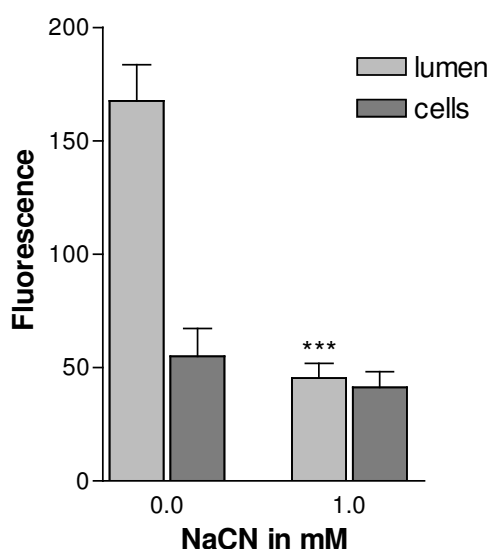
In Figure 72 Na<sup>+</sup>-taurocholate treatment at different concentrations between 1 and 100 μM is diagrammed. A dose dependent inhibition of TR transport across rat CP epithelium could be

recognized, vascular/subepithelial spaces, the interior of blood vessels and epithelial cells are concerned. These results indicate involvement of an Oat or Oatp in TR transport across rat CP epithelium.

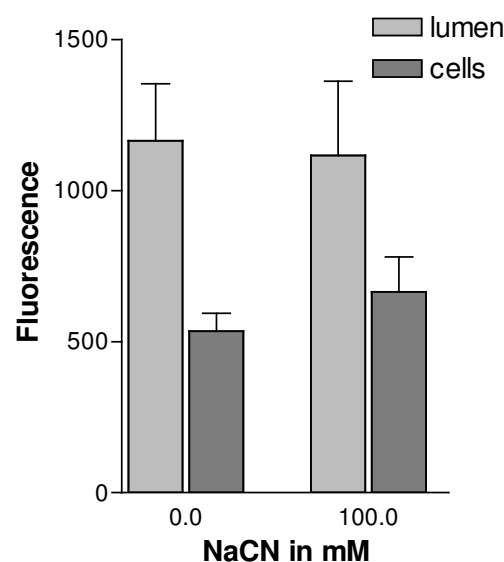
TR transport from aCSF to vascular/subepithelial spaces and the interior of blood vessels in rat CP is dependent on metabolism. Incubation with NaCN caused a strong decrease in vascular/subepithelial and luminal fluorescence. Cellular fluorescence was not affected. Only efflux at the basolateral membrane seems to be affected by NaCN (Figure 73 A). NaCN had no effect on TR transport in shark CP even at 100 mM (Figure 73 B). This is the first difference between TR transport in rat and shark CP.

**Figure 73:** Effects of NaCN on TR transport in rat (A) and shark (B) CP. In rat CP NaCN inhibited basolateral efflux of TR, in shark no effect was obtained. Data are expressed as mean  $\pm$  SE of 10 CP blood vessels from one representative isolation. (Significantly different from control values: \* for  $P < 0.05$ , \*\* for  $P < 0.01$  and \*\*\* for  $P < 0.001$ ).

A



B



Increasing medium  $K^+$  10 fold (isoionic  $Na^+$  replacement) and subsequent depolarisation of epithelial cells had no effect on TR distribution in rat and shark CP (Figure 74 shows the effect of increased  $K^+$  levels on rat CP, the results obtained from incubation with high  $K^+$  ER in shark CP are not shown). The depolarisation of epithelial cells did not affect TR accumulation in rat or shark CP, TR transport is independent from PD differences.

Transport proteins mediating TR transport in rat CP seem to be  $Na^+$ -dependent. Incubation with low- $Na^+$  aCSF had no effect on TR accumulation in rat CP, but removing  $Na^+$  led to much lower fluorescence levels in vascular/subepithelial spaces and the interior of blood vessels. Cellular fluorescence was affected as well (Figure 75 A). These results indicate

involvement of Oats on TR transport in rat CP, especially on apical uptake. Na<sup>+</sup> replacement in shark CP had no effect (Figure 75 B). In shark CP Oatps seem to be concerned with TR uptake at the apical membrane of CP epithelium. With these findings we show the second important difference between TR transport in rat and shark CP.

**Figure 74:** Effects of increasing K<sup>+</sup> by an order of magnitude on TR transport in rat CP. High K<sup>+</sup> levels and therefore depolarisation of epithelial cells did not affect TR transport. Data are expressed as mean ± SE of 10 CP blood vessels from one representative isolation.

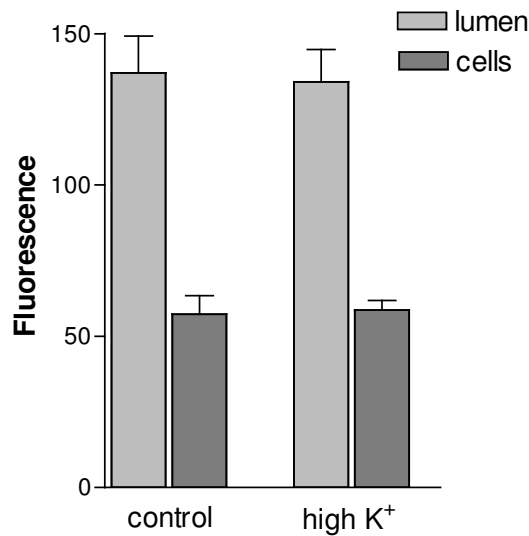
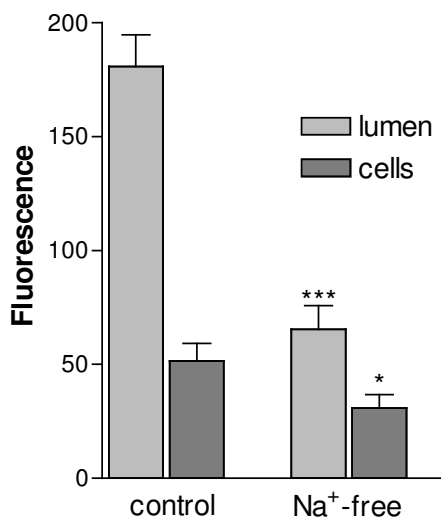
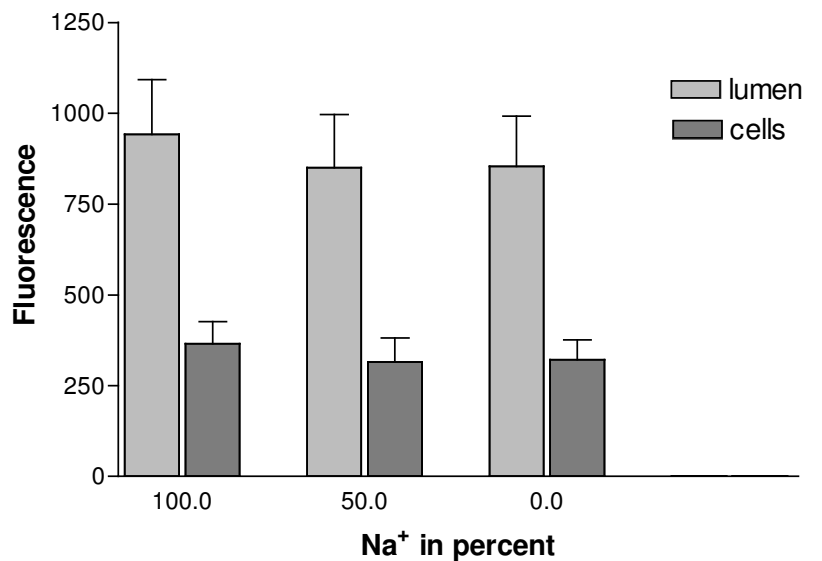


**Figure 75:** Effects of Na<sup>+</sup> replacement on TR transport in rat (A) and shark (B) CP. Incubation with Na<sup>+</sup>-free buffer clearly affected distribution of TR in rat CP, in shark CP Na<sup>+</sup> replacement had no effects. Data are expressed as mean ± SE of 10 CP blood vessels from one representative isolation. (Significantly different from control values: \* for P<0.05, \*\* for P<0.01 and \*\*\* for P<0.001).

**A**



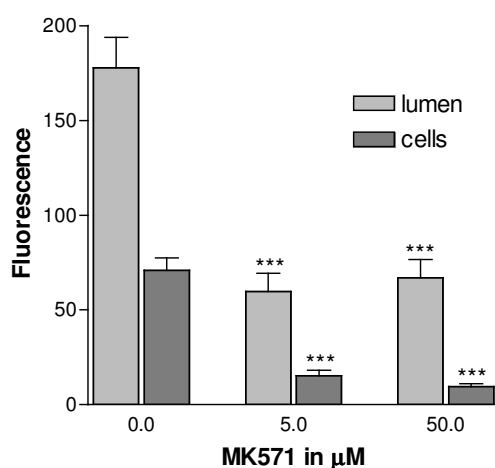
**B**



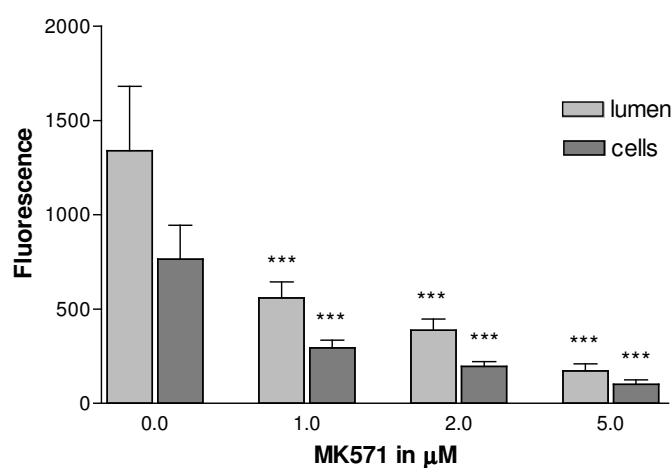
To analyze transport proteins mediating basolateral efflux of TR in rat and shark CP we tested MK571. The Mrp inhibitor MK571 had a strong inhibitory effect on TR accumulation in vascular/subepithelial spaces, the interior of blood vessels and epithelial cells in both, rat (Figure 76 A) and shark (Figure 76 B) CP at micromolar concentrations. The effect in shark CP was initiated by lower MK571 concentrations than in rat CP. These findings are a sign of Mrp involvement in TR transport in rat and shark CP, respectively.

**Figure 76:** Effects of MK571 on TR transport in rat (A) and shark (B) CP. MK571 treatment led to reduced fluorescence in vascular/perivascular spaces, the interior of blood vessels and epithelial cells in both species. Data are expressed as mean  $\pm$  SE of 10 CP blood vessels from one representative isolation. (Significantly different from control values: \* for  $P < 0.05$ , \*\* for  $P < 0.01$  and \*\*\* for  $P < 0.001$ ).

A



B



Methotrexate which is a substrate for different Mrps, had an inhibitory effect on TR transport in rat CP. Only accumulation in vascular/subepithelial spaces and the interior of blood vessels was affected (Figure 77). This result is one more evidence for Mrp participation in TR transport in rat CP, especially for one or more Mrps involved in basolateral efflux, because only accumulation in vascular/subepithelial spaces and the interior of blood vessels was affected.

$\text{LTC}_4$ , which is known to inhibit transport processes mediated by Mrp1, Mrp2, Mrp3 and Oatps, at a concentration of  $0.3 \mu\text{M}$  had no effect on TR distribution in rat CP tissue (Figure 78 A). Therefore Mrp1,2,3 and Oatps seem not to be involved in TR transport in rat CP.

TR transport was examined in Mrp2 deficient  $\text{TR}^-$  rats which are deficient of Mrp2. Compared to wistar wildtype rats no differences were obtained for TR transport in rat CP. Therefore Mrp2 seems not to play a role in TR transport in rat CP (Figure 78B).

**Figure 77:** Effects of methotrexate on TR transport in rat CP. Incubation with methotrexate led to decreased TR accumulation in vascular/subepithelial spaces and the interior of blood vessels, it had no effect on cellular accumulation. Data are expressed as mean  $\pm$  SE of 10 CP blood vessels from one representative isolation. (Significantly different from control values: \* for  $P < 0.05$ , \*\* for  $P < 0.01$  and \*\*\* for  $P < 0.001$ ).

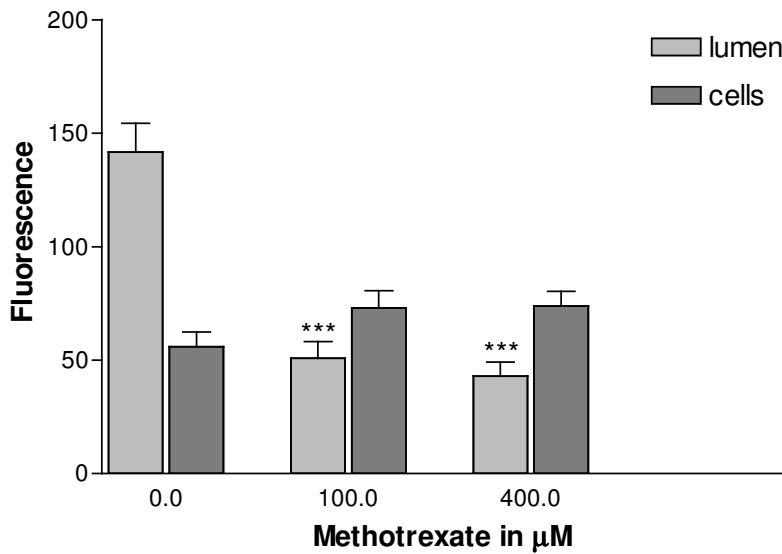
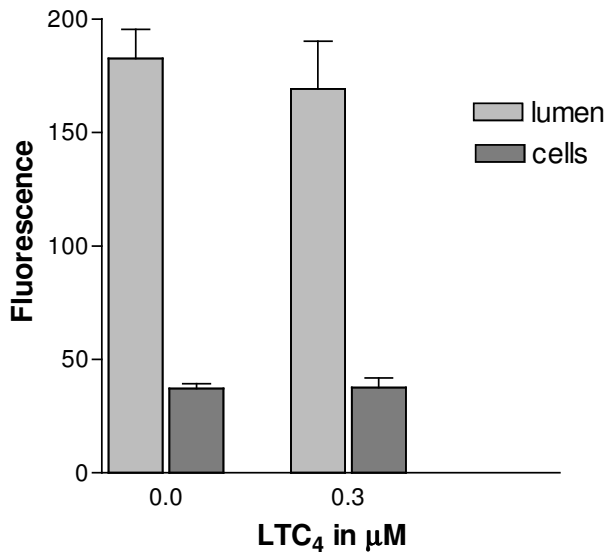
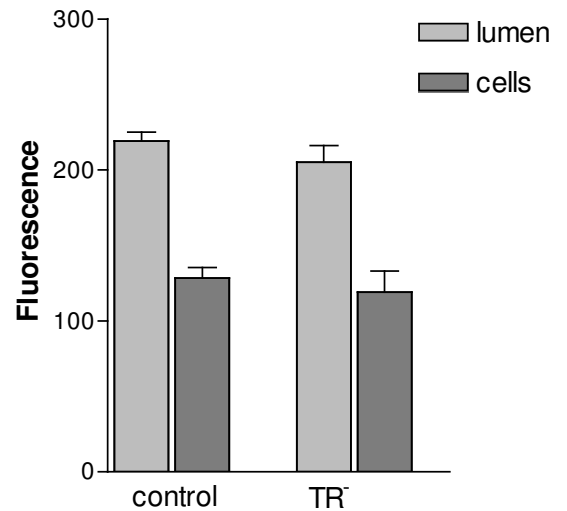


**Figure 78:** Effects of  $\text{LTC}_4$  (A) and  $\text{TR}^-$  rats (B) on TR transport in rat CP.  $\text{LTC}_4$  treatment had no effect on TR distribution and TR transport was not different in  $\text{TR}^-$  rats compared to wildtype rats. Data are expressed as mean  $\pm$  SE of 10 CP blood vessels of one representative isolation. (Significantly different from control values: \* for  $P < 0.05$ , \*\* for  $P < 0.01$  and \*\*\* for  $P < 0.001$ ).

**A**



**B**



The MRP4 substrate AZT was added at concentrations up to 50  $\mu\text{M}$ . It did neither affect accumulation of TR in vascular/perivascular spaces and the interior of blood vessels nor in epithelial cells (Figure 79). It is likely that MRP4 is not involved in TR efflux at the basolateral membrane of rat CP epithelial cells.

## Results

**Figure 79:** Effects of AZT on TR transport in rat CP. AZT at concentrations between 1 and 50  $\mu\text{M}$  had no effect on TR accumulation. Data are expressed as mean  $\pm$  SE of 10 CP blood vessels from one representative isolation. (Significantly different from control values: \* for  $P < 0.05$ , \*\* for  $P < 0.01$  and \*\*\* for  $P < 0.001$ ).

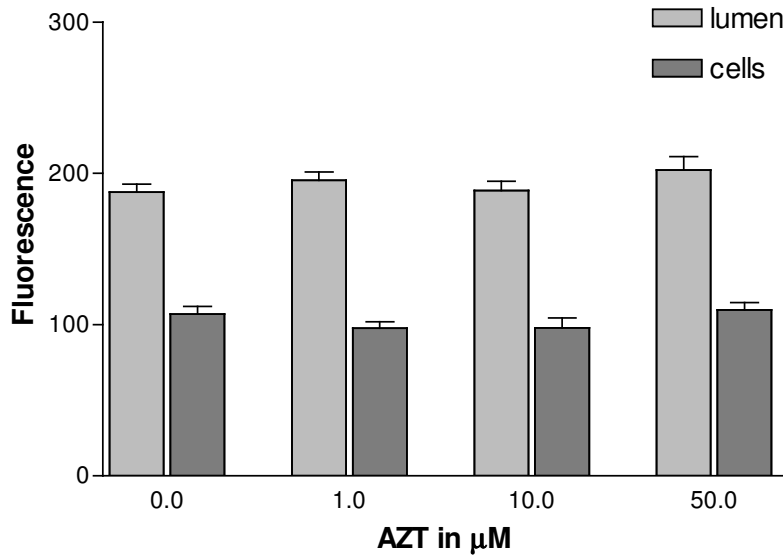
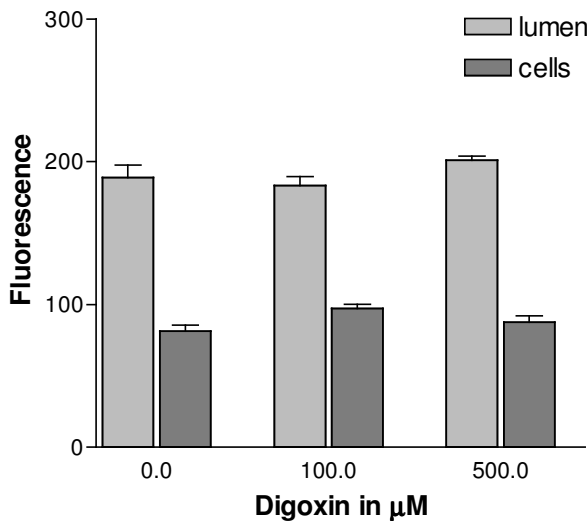
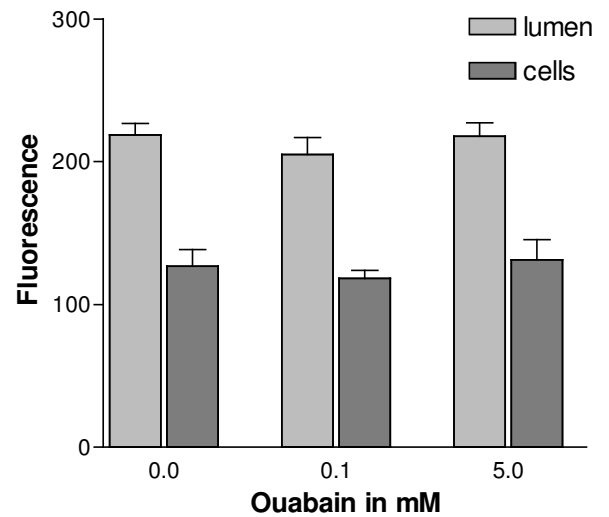


**Figure 80:** Effects of digoxin (A) and ouabain (B) on TR transport in rat CP. Neither digoxin nor ouabain had any effect on TR distribution in vascular/perivascular spaces, the interior of blood vessels and epithelial cells. Data are expressed as mean  $\pm$  SE of 10 CP blood vessels from one representative isolation.

**A**



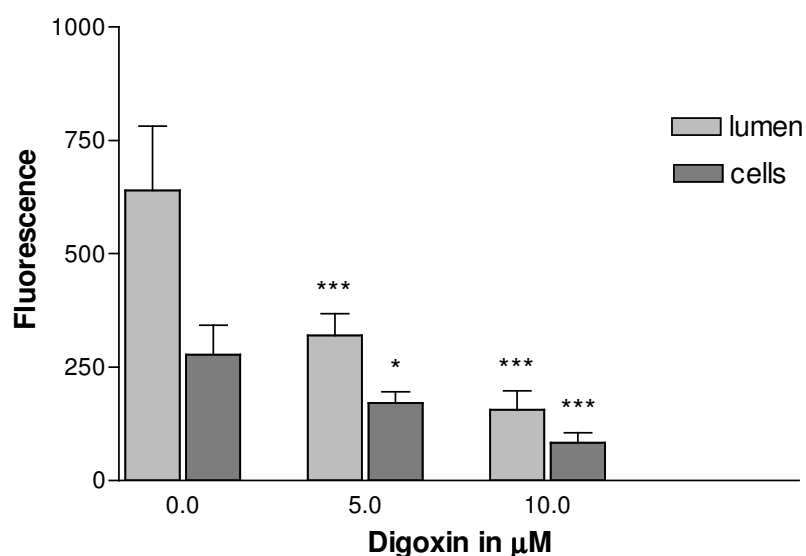
**B**



To examine the role of Oatp2 in TR efflux from epithelial cells into blood at the basolateral membrane, digoxin, an Oatp2 blocker, was tested. Digoxin had no effect on TR distribution in rat CP even at high concentrations (up to 500  $\mu\text{M}$ ) (Figure 80 A). The Oatp2 substrate ouabain had no effect on TR transport in rat CP as well. Ouabain was used at concentrations up to 5 mM (Figure 80 B).

Contrary to the findings in rat, digoxin led to reduced fluorescence in vascular/subepithelial spaces, the interior of blood vessels and epithelial cells in shark CP. The digoxin effect on TR transport in shark CP was dose dependent at concentrations between 5 and 10  $\mu\text{M}$  (Figure 81). These results show another interesting difference between TR transport in rat and shark CP. In rat CP TR seems to be transported out of the cell by one or more Mrps, in shark CP Oatp2 and a Mrp seem to be involved in TR efflux at the basolateral membrane.

**Figure 81:** Effects of digoxin on TR transport in shark CP. Digoxin had an inhibitory effect on TR transport, vascular/perivascular spaces, the interior of blood vessels and epithelial cells were concerned. Data are expressed as mean  $\pm$  SE of 10 CP blood vessels from one representative isolation. (Significantly different from control values: \* for  $P < 0.05$ , \*\* for  $P < 0.01$  and \*\*\* for  $P < 0.001$ ).



Estrone sulfate (ES) is a substrate for Mrps, Oats and Oatps. It had a dose dependent inhibitory effect on TR transport in rat (Figure 82 A) and in shark (Figure 82 B) CP. Fluorescence in vascular/subepithelial spaces and the interior of blood vessels was decreased, cellular fluorescence was reduced as well at ES concentrations between 5 and 100  $\mu\text{M}$ . These results give additional evidence for Mrps, Oats or Oatps involved in mediation of TR transport in rat and shark CP.

Treatment with probenecid led to reduced fluorescence levels in perivascular/subepithelial spaces, the interior of blood vessels and epithelial cells in rat (Figure 83 A) as well as in shark CP (Figure 83 B). Involvement of Mrps, Oats or Oatps in transport of TR in rat and shark CP is likely.

**Figure 82:** Effects of ES on TR transport in rat (A) and shark (B) CP. ES led to reduced fluorescence in vascular/perivascular spaces, the interior of blood vessels and epithelial cells. In rat CP cellular fluorescence was only affected by ES at a concentration of 50  $\mu\text{M}$ . Data are expressed as mean  $\pm$  SE of 10 CP blood vessels from one representative isolation. (Significantly different from control values: \* for  $P < 0.05$ , \*\* for  $P < 0.01$  and \*\*\* for  $P < 0.001$ ).

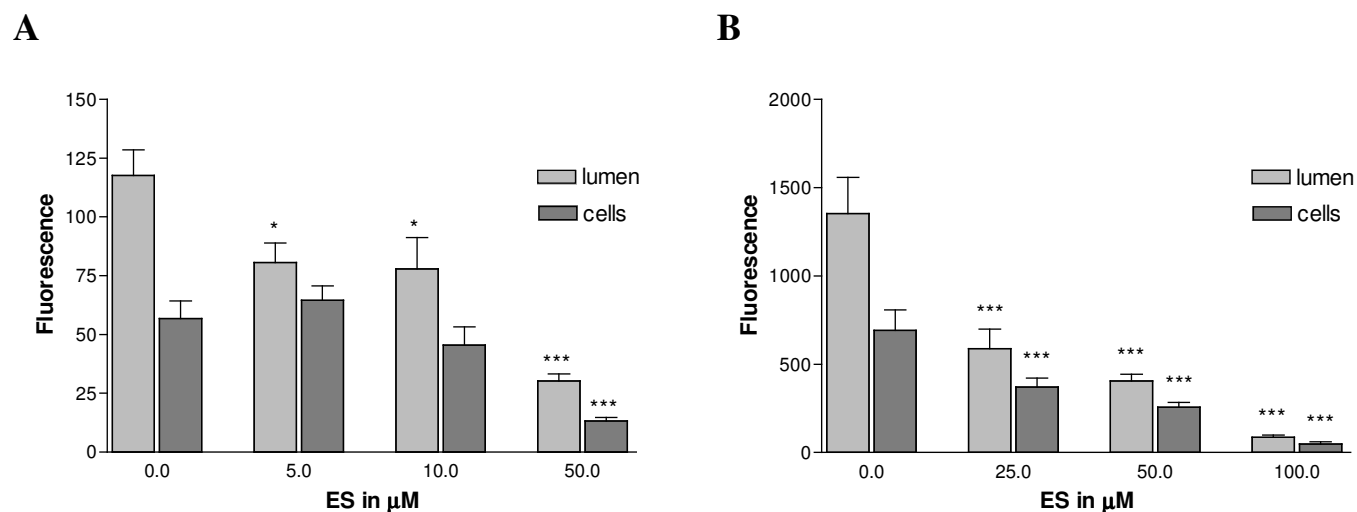
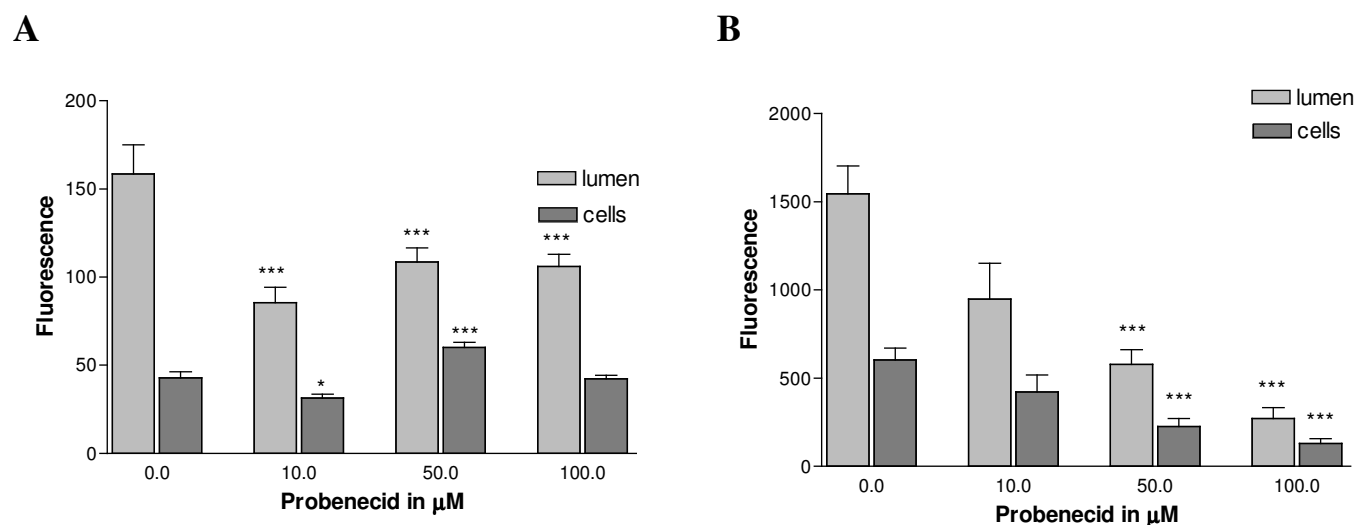


**Figure 83:** Effects of probenecid on TR transport in rat (A) and shark (B) CP. Probenecid reduced TR accumulation in vascular/subepithelial spaces, the interior of blood vessels and in epithelial cells. Data are expressed as mean  $\pm$  SE of 10 CP blood vessels from one representative isolation. (Significantly different from control values: \* for  $P < 0.05$ , \*\* for  $P < 0.01$  and \*\*\* for  $P < 0.001$ ).



Bromosulphophthalein (BSP) is a substance that affects transport processes mediated by Mrps, Oats and Oatps. In the present study we used BSP in micromolar concentrations that led to decreased TR accumulation in vascular/subepithelial spaces, the interior of blood vessels and epithelial cells in rat CP (Figure 84). Therefore we can assume that Mrps, Oats or Oatps are involved in TR transport in rat CP. Due to the results shown previously, we can exclude Mrp1, Mrp2, Mrp4 and Oatps from being involved in TR transport in rat CP tissue.

## Results

**Figure 84:** Effects of BSP on TR transport in rat CP. BSP had an inhibitory effect on TR transport. Data are expressed as mean  $\pm$  SE of 10 CP blood vessels from one representative isolation. (Significantly different from control values: \* for  $P < 0.05$ , \*\* for  $P < 0.01$  and \*\*\* for  $P < 0.001$ ).

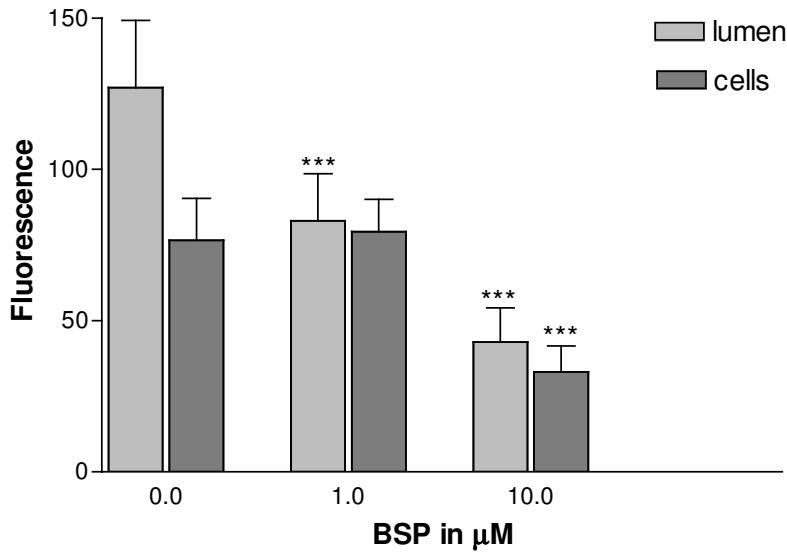
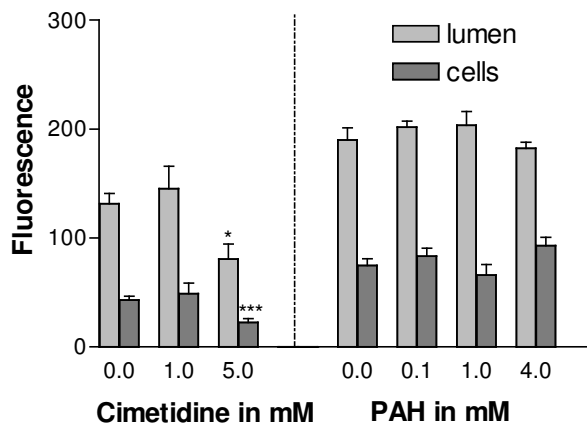
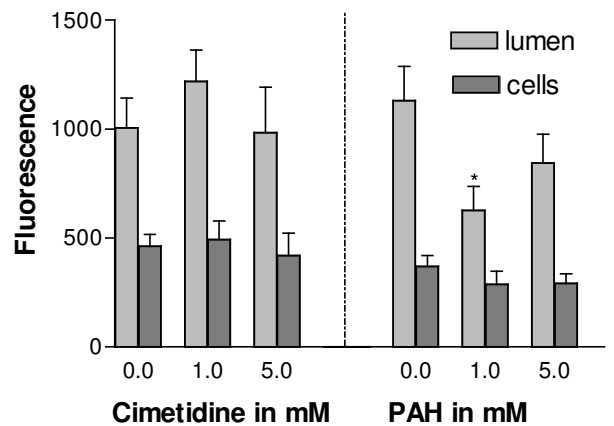


**Figure 85:** Effects of PAH and cimetidine on TR transport in rat (A) and shark (B) CP. Cimetidine had a weak effect on TR transport in rat CP at 5mM, cellular fluorescence was decreased as well as fluorescence in vascular/perivascular spaces and the interior of blood vessels. PAH had no effect on TR transport in rat CP. In shark CP cimetidine did not affect TR transport, but PAH had a weak effect on luminal fluorescence at 1 mM. Data are expressed as mean  $\pm$  SE of 10 CP blood vessels from one representative isolation. (Significantly different from control values: \* for  $P < 0.05$ , \*\* for  $P < 0.01$  and \*\*\* for  $P < 0.001$ ).

**A**



**B**

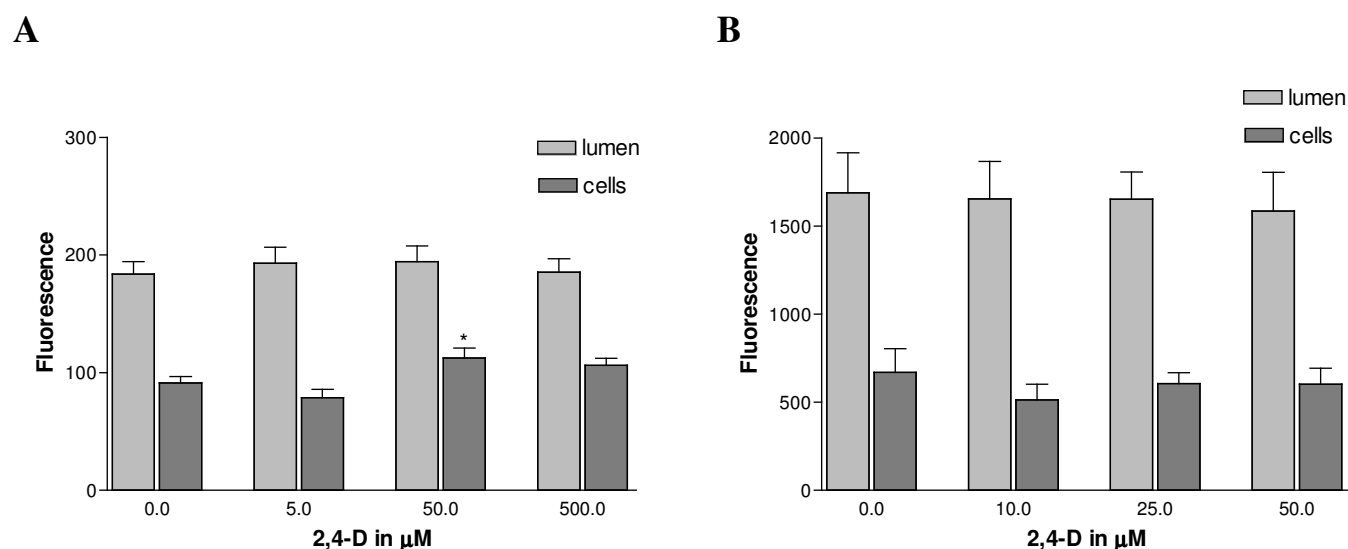


To characterize TR uptake from aCSF/ER into epithelial cells at the apical membrane, we investigated the effects of cimetidine and PAH, both substrates of Oat1 and Oat3. TR transport in rat CP was only affected by cimetidine at a high concentration (5mM), this effect was only weak (Figure 85 A). Cimetidine had no effect on TR transport in shark CP (Figure 85 B) at millimolar concentrations. In rat CP PAH treatment had no effect on TR accumulation (Figure 85 A). In shark CP a weak effect on TR distribution could be

recognized (Figure 85 B), only luminal accumulation of TR was affected. These results favour an involvement of one or more Na<sup>+</sup>-dependent transport proteins, most likely Oats, but not Oat1 or Oat3, in TR transport in rat CP. In shark CP no Na<sup>+</sup>-dependent constituent is involved in TR transport.

2,4-D had a decreasing effect on FL accumulation in vascular/perivascular spaces, the interior of blood vessels and epithelial cells in rat and shark CP (Breen et al., 2002), but had no effect on TR distribution in rat (Figure 86 A) or shark (Figure 86 B) CP. Transport proteins involved in transport of the medium sized organic anion TR seem to be different from those transporting the smaller sized FL in rat and shark CP, respectively.

**Figure 86:** Effects of 2,4-D on TR transport in rat (A) and shark (B) CP. 2,4-D did not affect TR transport in rat and shark CP respectively. Data are expressed as mean ± SE of 10 CP blood vessels from one representative isolation. (Significantly different from control values: \* for P<0.05, \*\* for P<0.01 and \*\*\* for P<0.001).



To investigate into regulatory processes mediating transport of TR in shark CP, we analyzed the effects of PKC and PKA activation. As described above activation of protein kinase C (PKC) downregulates Oat3 action. In contrast activation of protein kinase A (PKA) leads to upregulation of Oat3 mediated transport.

PKC can be activated by phorbol ester, but incubation with PMA at concentrations from 1 nM to 100 nM did not affect TR accumulation in vascular/subepithelial spaces, the interior of blood vessels and epithelial cells in shark CP (Figure 87). PKC seems not to be involved in regulation of TR transport in shark CP.

To examine if PKA activation increased TR excretion in shark CP we used the indirect PKA activator forskolin. At the used concentration 10  $\mu\text{M}$  forskolin had an inhibitory effect on TR distribution in the tissue, fluorescence was decreased in vascular/subepithelial spaces and the

interior of blood vessels, epithelial cell fluorescence was not concerned (Figure 88). The same was found for TR transport in shark rectal salt gland tubules, but there was no evidence for mediation of this effect by PKA (Miller et al., 2002). Different from this result, an activation of FL-MTX transport in shark CP was found using forskolin at a concentration of 10  $\mu$ M. Due to the abolishment of the forskolin effect by the PKA inhibitor H-89, PKA involvement was ascertained (Baehr et al., in press).

**Figure 87:** Effects of PMA on TR transport in shark CP. PMA, at concentrations between 1 and 100 nM, had no effect on TR distribution in vascular/subepithelial spaces, the interior of blood vessels and epithelial cells. Data are expressed as mean  $\pm$  SE of 10 CP blood vessels from one representative isolation.

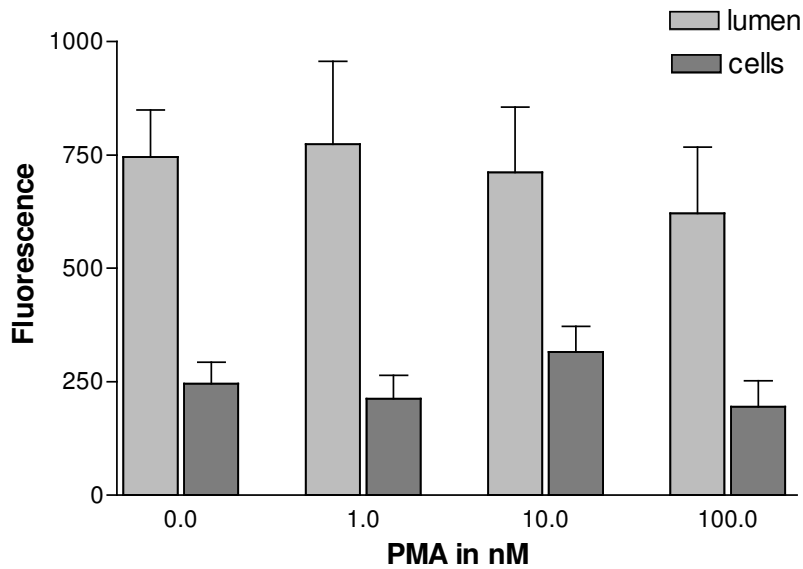
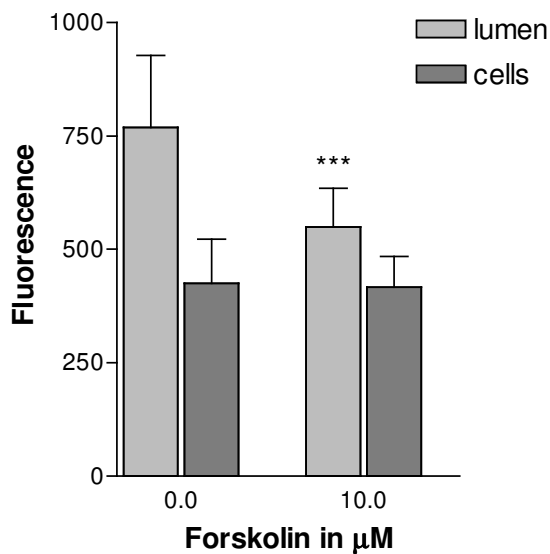


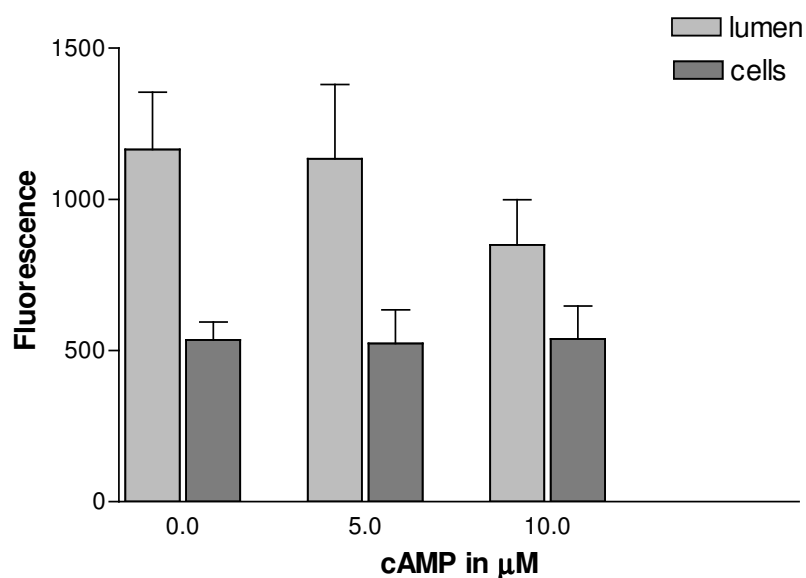
**Figure 88:** Effects of forskolin on TR transport in shark CP. Forskolin treatment led to reduced TR accumulation in vascular/perivascular spaces and the interior of blood vessels, TR accumulation in epithelial cells was not affected. Data are expressed as mean  $\pm$  SE of 10 CP blood vessels from one representative isolation. (Significantly different from control values: \* for  $P < 0.05$ , \*\* for  $P < 0.01$  and \*\*\* for  $P < 0.001$ ).



To test whether the forskolin effect is caused by PKA activation we used the direct PKA

activator cAMP. cAMP did not affect TR transport in shark CP at concentrations of 1 and 10  $\mu\text{M}$  (Figure 89). Thus the forskolin effect seems to be provoked by forskolin itself and not by high intracellular cAMP levels caused by forskolin. PKA seems not to be involved in the forskolin effect. Taken together these results, PKC and PKA activation are not involved in regulation of TR transport in shark CP.

**Figure 89:** Effects of cAMP on TR transport in shark CP. cAMP did not affect distribution of TR within CP tissue. Data are expressed as mean  $\pm$  SE of 10 CP blood vessels from one representative isolation.



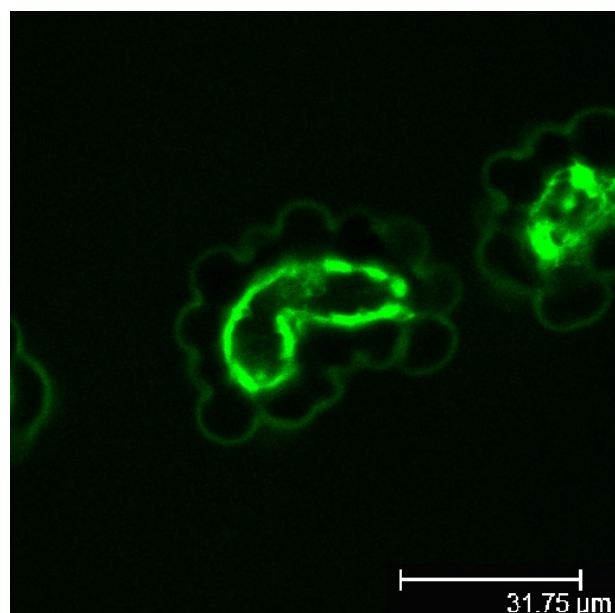
#### 4.2.3.4 Regulation of Fluorescein-Methotrexate Transport in Rat Choroid Plexus

Regulation of FL-MTX transport was investigated by Baehr et al. (in press) in dogfish shark CP. Here we demonstrate the results found for regulatory processes concerning FL-MTX transport in rat CP.

From previous studies we know that transport proteins involved in FL-MTX transport in rat and dogfish shark CP epithelium are the same, but regulation of FL-MTX transport in rat and shark CP was not compared by now.

In Figure 90 major characteristics of FL-MTX transport in rat CP are shown. FL-MTX accumulates in vascular/perivascular spaces and the interior of blood vessels, cellular fluorescence intensities are low, as bath fluorescence is. At the apical membrane an area of higher fluorescence is located. This indicates a strong apical efflux.

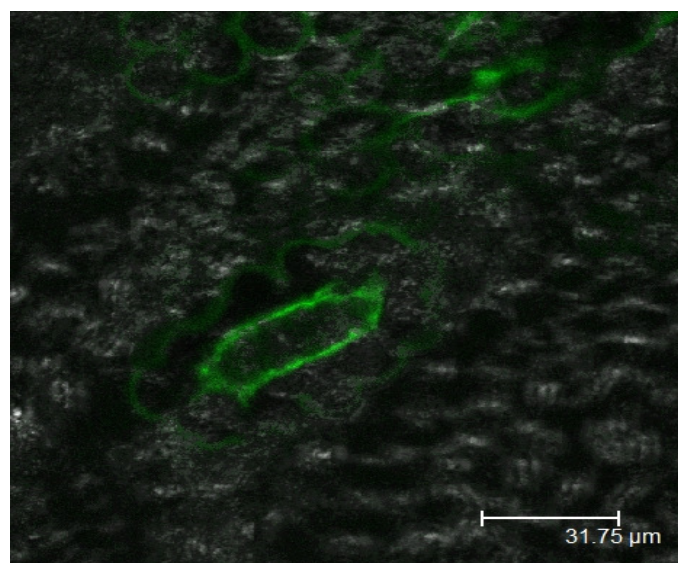
**Figure 90:** Major characteristics of FL-MTX transport in rat CP. FL-MTX accumulation is highest in vascular/subepithelial spaces and the interior of blood vessels. Cellular fluorescence barely exceeded bath fluorescence. At the apical membrane an area of high fluorescence is recognizable.



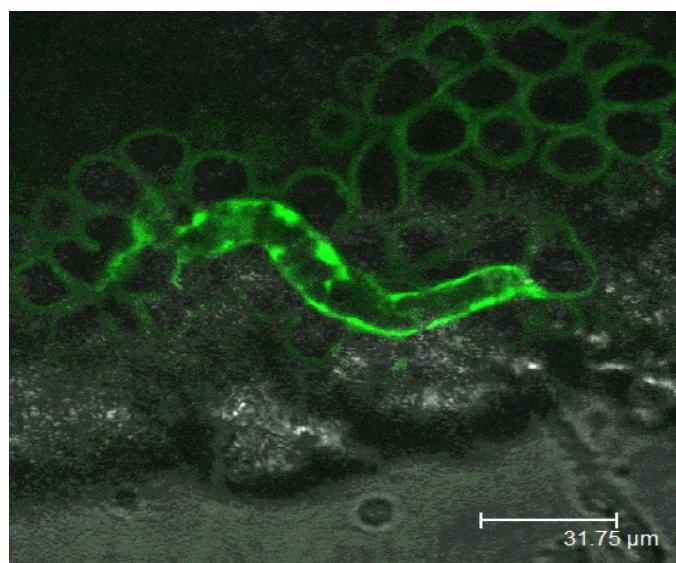
In Figure 91 A a control CP and in Figure 91 B a CP after concomitant incubation with forskolin and FL-MTX are shown. Forskolin affected FL-MTX accumulation in vascular/perivascular spaces and the interior of blood vessels, epithelial cells were not concerned. Fluorescence intensities in vascular/perivascular spaces and the interior of blood vessels were higher than in control CPs using different concentrations (5-50  $\mu\text{M}$ ) of forskolin (Figure 92). These results indicate activation of efflux transporters for FL-MTX caused by PKA activation.

**Figure 91:** Forskolin effect on FL-MTX transport in rat CP. Forskolin, at a concentration of 10  $\mu\text{M}$  (B), led to increased fluorescence in vascular/subepithelial spaces and the interior of blood vessels compared to control (A). Cellular fluorescence was not affected.

**A**



**B**



To examine whether this activation is actually caused by PKA activation, we incubated with forskolin and H-89 as described above. The PKA inhibitor H-89 had no effect on FL-MTX transport in rat CP on its own, but could alter the forskolin effect (Figure 93). PKA seems to be involved in regulation of FL-MTX transport in rat CP.

**Figure 92:** Effects of forskolin on FL-MTX transport in rat CP. Forskolin led to increased FL-MTX accumulation in vascular/subepithelial spaces and the interior of blood vessels. Cellular accumulation was not affected. Data are expressed as mean  $\pm$  SE of 10 CP blood vessels of one representative isolation. (Significantly different from control values: \* for  $P < 0.05$ , \*\* for  $P < 0.01$  and \*\*\* for  $P < 0.001$ ).

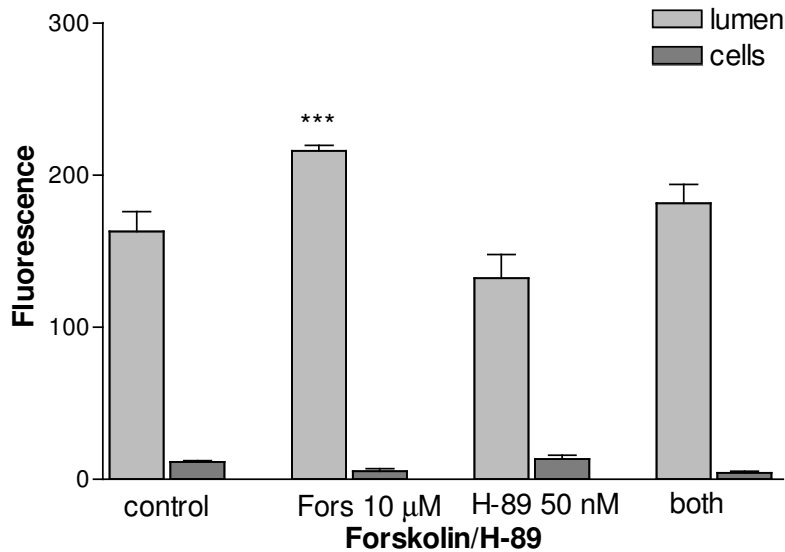
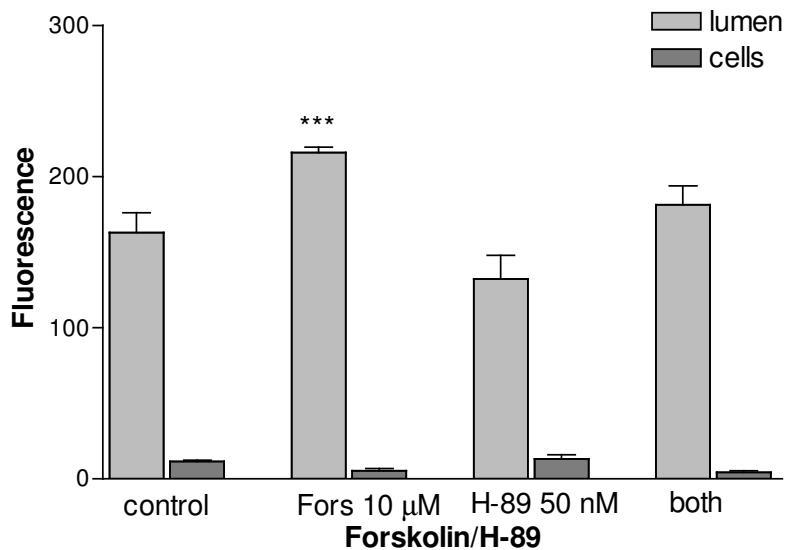


**Figure 93:** Effects of forskolin and H-89 on FL-MTX transport in rat CP. As described above forskolin led to higher fluorescence levels in vascular/perivascular spaces and the interior of blood vessels. H-89 had no effect but could alter the forskolin effect. Data are expressed as mean  $\pm$  SE of 10 CP blood vessels from one representative isolation. (Significantly different from control values: \* for  $P < 0.05$ , \*\* for  $P < 0.01$  and \*\*\* for  $P < 0.001$ ).



To analyze the effect of PKC on FL-MTX transport in rat CP, PMA was used at

concentrations up to 1  $\mu\text{M}$ . PMA had no effect on FL-MTX transport suggesting no involvement of PKC. Incubation with the PKC inhibitor bisindolylmaleimide (BIM) did not affect FL-MTX transport in rat CP as well (Figure 94). Taken together, these results exclude PKC involvement in regulation of FL-MTX transport in rat CP.

**Figure 94:** Effects of PMA and BIM on FL-MTX transport in rat CP. Both substances had no effect on FL-MTX transport. Data are expressed as mean  $\pm$  SE of 10 CP blood vessels from one representative isolation.

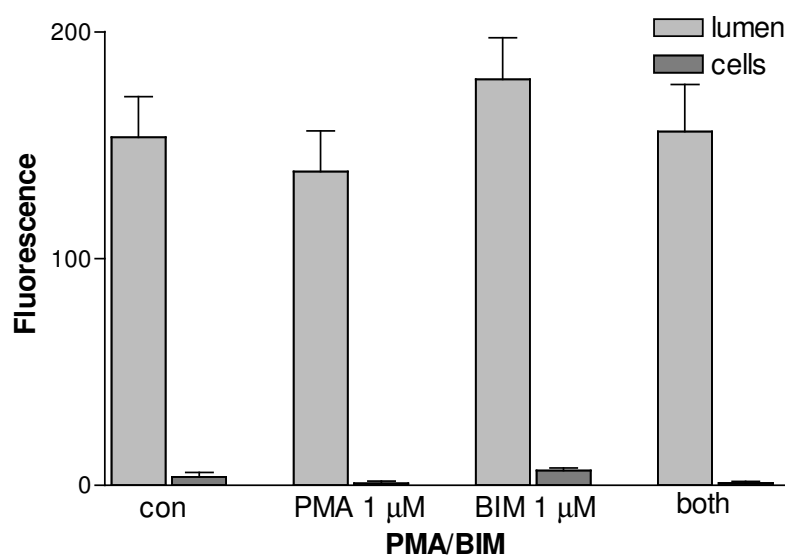
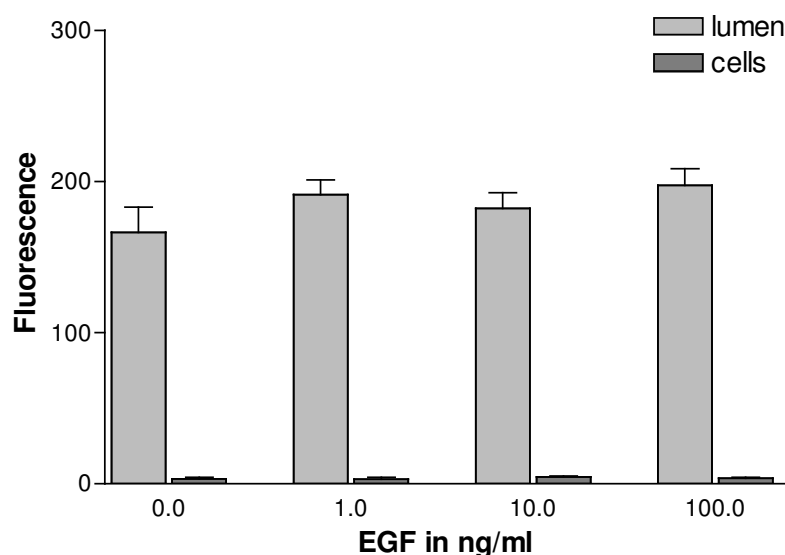


**Figure 95:** Effects of EGF on FL-MTX transport in rat CP. At concentrations up to 100 ng/ml EGF did not affect FL-MTX accumulation in vascular/subepithelial spaces, the interior of blood vessels and epithelial cells. Data are expressed as mean  $\pm$  SE of 10 CP blood vessels from one representative isolation.



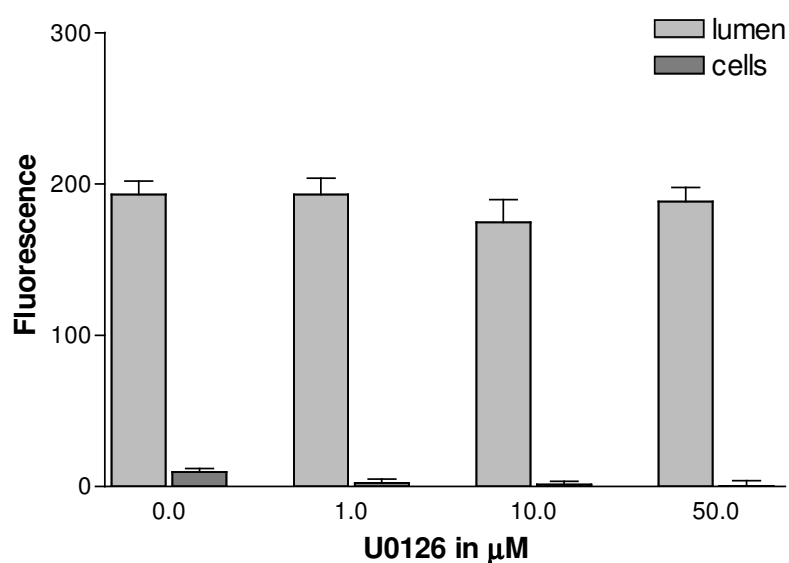
To examine contribution of the MAPK pathway, EGF was used at concentrations between 1 and 100 ng/ml. EGF leads to phosphorylation of mitogen-activated/extracellular signal-regulated kinase (MEK), extracellular signal-regulated kinase 1 and 2 (ERK1/2) and

phospholipase A<sub>2</sub> (PLA<sub>2</sub>), this cascade ends in PKA activation via adenylate cyclase activation (Soodvilai et al., 2004).

EGF had no effect on FL-MTX accumulation in rat CP epithelium, luminal and cellular fluorescence did not differ compared to fluorescence in control CPs (Figure 95).

The MEK inhibitor U0126 did not affect FL-MTX transport at concentrations of 1 to 50  $\mu$ M (Figure 96). Taken together with the results obtained from experiments using EGF, the MAPK pathway seems not to play a role in regulation of FL-MTX transport in rat CP.

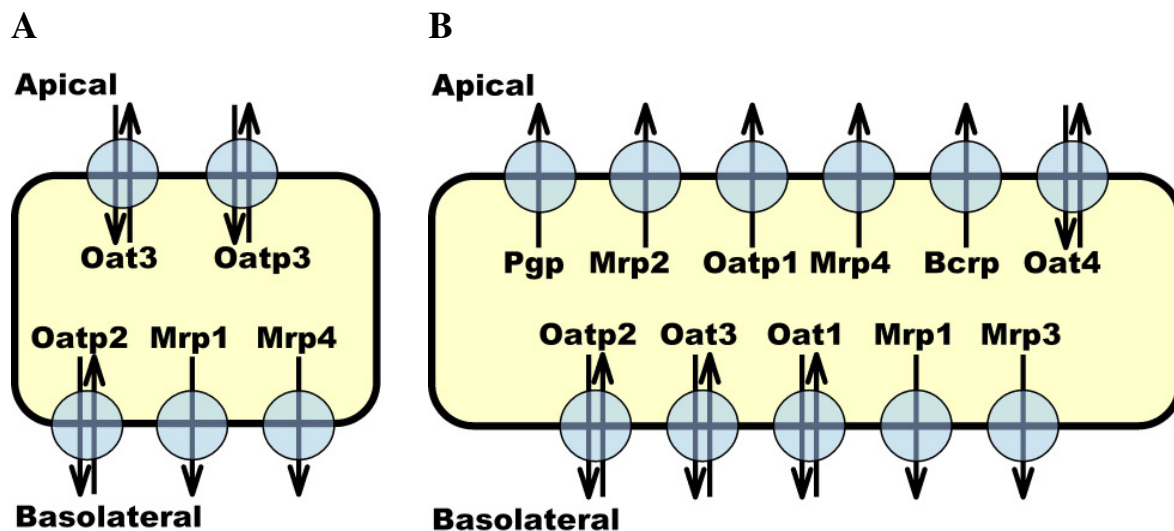
**Figure 96:** Effects of U0126 on FL-MTX transport in rat CP. U0126 had no effects on FL-MTX accumulation in vascular/perivascular spaces, the interior of blood vessels and epithelial cells. Data are expressed as mean  $\pm$  SE of 10 CP blood vessels from one representative isolation.



## 5 Discussion

In the presented project we analyzed transport mechanisms for organic anions in different models including killifish proximal tubules, rat and dogfish shark choroid plexus (CP) and MDCKII-MRP2 and Sf9-MRP4 cell membrane vesicles. We analyzed molecular and functional aspects of transport of the fluorescent dyes fluo-cAMP, texas red (TR) and fluorescein-methotrexate (FL-MTX) using RT-PCR, indirect immunohistochemistry and confocal laserscanning microscopy. Functional analyses were carried out using different inhibitors and activators of organic anion transport. To give an overview of transport proteins for organic anions expressed in kidney and CP. Figure 97 shows schematic diagrams of CP and proximal tubules epithelial cells and transport proteins expressed in both tissues.

**Figure 97:** Schematic diagrams of CP (A) and proximal tubules (B) epithelial cells. Transport proteins are expressed to both membranes of the polarized epitheliums. In CP (A) the apical membrane is the cerebrospinal fluid site, the basolateral membrane faces the blood. In kidney proximal tubules (B) the apical membrane faces the urine, the basolateral membrane faces the blood. Only transporters are shown that are clearly localized to one membrane by immunostaining. Bcrp: breast cancer resistance protein; Mrp: multidrug resistance-associated protein; Oat: organic anion transporter; Oatp: organic anion transporting polypeptide; Pgp: P-glycoprotein.



As described above we performed functional analyses with fluorescent dyes with inhibitors or activators of organic anion transport added. Summarizing the results from different inhibitor/activator studies we could draw conclusions about transport proteins involved in transport of the particular fluorescent dye. In Table 6 the used inhibitors or activators of organic anion transport and their inhibitory mechanisms are shown. Most of the shown substances affect transport processes mediated by several transport proteins, some substances have higher affinities to one transporter family or to one transport proteins.

**Table 6:** Inhibitors and activators of organic anion transport and mechanisms driving their effects. Only substances are shown, that were used in the presented study.

| <b>Modulators</b>                                | <b>Mechanisms</b>  |
|--|--|
| Adefovir (PMEA)                                  | Mrp4   |
| Azidothymidine (AZT)                             | Mrp4   |
| Bisindolylmaleimide (BIM)                        | Proteinkinase C (PKC) inhibitor                              |
| 8-Bromo-cGMP                                     | Mrp4,  |
| Bromosulfophthalein (BSP)                        | Mrps, Oats, Oatps  |
| cAMP   | Mrp4, PKA activator  |
| Cimetidine                                       | Oat1, Oat3   |
| cGMP   | Mrp4   |
| Dibutryl cAMP (db-cAMP)                          | Proteinkinase A (PKA) activator                              |
| 2,4-dichlorophenoxyacetic acid (2,4-D)           | Inhibits fluorescein transport                               |
| Digoxin  | Oatp2  |
| Dipyridamole                                     | Mrps   |
| Epidermal growth factor (EGF)                    | Activation mitogen activated proteinkinase pathway (MAPK)    |
| Estrone Sulfate (ES)                             | Mrps, Oats, Oatps  |
| Endothelin 1 (ET1)                               | PKC activator  |
| Forskolin  | PKA activator  |
| H-89   | PKA inhibitor  |
| High Potassium (high K <sup>+</sup> )            | Inhibits potential differences sensitive transport processes |
| Leukotriene C <sub>4</sub> (LTC <sub>4</sub> )   | Mrp1, 2, 3; Oatps  |
| Methotrexate                                     | Mrps   |
| MK571  | Mrps   |
| NaCN   | Metabolic poison: inhibits active transport processes        |
| Nitroprusside-Na <sup>+</sup>                    | NO-donor, activation PKC                                     |
| Ouabain  | Oatp2, Na <sup>+</sup> -dependent transport processes        |
| <i>p</i> -Aminohippurate (PAH)                   | Oat1, Oat3, Mrp2, Mrp4                                       |
| Phorbol-12-myristate-13-acetate (PMA)            | PKC activation   |
| Probenecid                                       | Mrps, Oats, Oatps  |
| Prostaglandin E <sub>2</sub> (PGE <sub>2</sub> ) | Mrp4   |
| Sodium free (Na <sup>+</sup> -free)              | Oats   |
| Taurocholate-Na <sup>+</sup>                     | Oats, Oat  |
| U0126  | MEK1/2, inhibition MAPK                                      |

Involvement of specific transport proteins in transport of one substance can only be evidenced by combining results from multiple inhibitor studies.

## **5.1 Fluo-cAMP Transport in Killifish Proximal Tubules**

One aim of our research project was the investigation of organic anion transport in choroid plexus (CP) tissue. Since CP function is similar to function of the kidney and similar transport proteins are expressed in CP and kidney epithelium (Kusuhara et al., 2004; Miller, 2004; Breen et al., 2004), we used renal proximal tubules as a comparative model. As the kidney is responsible for homeostasis in blood, the CP is an important organ for homeostasis in the CSF (Spector/Johanson, 1991). Renal tubules of the teleost killifish represent a renal clearance system similar to the one of mammals with transport proteins being at the same morphological position (Pritchard and Miller, 1991). Mrp2 is located to the apical membrane of killifish proximal tubules (Masereeuw et al., 2000) and here we demonstrate the same localization for Mrp4.

We used this physiological similarities to study the excretory mechanisms of the fluorescent cAMP analog fluo-cAMP, which seems to be transported by the same transporters as nucleoside and nucleotide analogs being used in clinical practice for HIV treatment. Participation of these transporters is of particular interest for the assessment of the disposition of these drugs since they determine the rate and extent of access to HIV sanctuaries like the central nervous system (Bachmayer et al., 2005; Miller et al., 2000; Park and Sinko, 2005) as well as the extent of excretion by renal cells (Schaub et al., 1997, Van Aubel et al., 2002).

Tubular secretion of fluo-cAMP is a concentrative two-step mechanism composed of basolateral uptake from blood into epithelial cells at the basolateral membrane and apical efflux into urine. We found evidences that both transport proteins Mrp2 and Mrp4 are involved in fluo-cAMP cell to lumen transport at the apical membrane in killifish proximal tubules. The teleost analogs of Mrp4 and Mrp2 are located to the apical membrane of proximal tubules epithelial cells in killifish kidney.

The inhibitory effect of LTC<sub>4</sub> on fluo-cAMP transport as well as the inhibition by ES, probenecid, PAH and MK571 is similar to the inhibition pattern previously seen for FL-MTX transport (Masereeuw et al., 1996; Breen et al., 2004; Miller et al., 2002a) and suggest participation of Mrp2. The strong inhibitory effect of LTC<sub>4</sub>, especially on cellular

fluorescence, leads also to the assumption that an Oatp is involved in fluo-cAMP uptake into proximal tubulus epithelial cells.

On the other hand, the Mrp4 substrates PMEA and AZT had inhibitory effects on fluo-cAMP accumulation in tubular lumen, whereas the same concentrations did not affect transport of the Mrp2 substrate FL-MTX, suggesting differences in the affinity of fluo-cAMP and FL-MTX. cAMP itself reduced fluo-cAMP accumulation in an assumably competitive manner. The phosphodiesterase inhibitor 8-Br-cGMP, which increases cellular cAMP levels, reduced fluorescence levels in proximal tubular lumens as well. Taken together, these results indicate involvement of Mrp4 in fluo-cAMP transport in killifish proximal tubules.

## 5.2 Fluo-cAMP Transport in Membrane Vesicles

To confirm the role of MRP2 and MRP4 in fluo-cAMP transport, we tested transport processes in Sf9-MRP4 and MDCKII-MRP2 membrane vesicles. We found that MRP2 and MRP4 mediate fluo-cAMP transport with the same affinity (Km values were 4.8 and 5.3  $\mu$ M, respectively). Compared with the Km value for FL-MTX transport in MDCKII-MRP2, which is around 10  $\mu$ M (J.J.M.W. van den Heuvel, personal communication), fluo-cAMP seems to have a higher affinity for MRP2 than FL-MTX. Interestingly fluo-cAMP is a high affinity substrate for MRP4 as well. Contrary to these findings the high affinity Mrp2 substrate FL-MTX is transported selectively by MRP2. FL-MTX is not transported by MRP4 in Sf9-MRP4 vesicles (R. Masereeuw, personal communication). As fluo-cAMP, the organic anion PAH is a substrate for both, MRP2 expressed in MDCKII cells and MRP4 expressed in Sf9 cells. In opposition to transporter affinities for fluo-cAMP, MRP2 (Km value  $2.1 \pm 0.6$  mM) and MRP4 (Km  $160 \pm 50$   $\mu$ M) show only low affinities to PAH (Smeets et al., 2004). Summarizing these results, fluo-cAMP seems to have a high affinity to MRP2 and MRP4, even higher than the affinity of FL-MTX to MRP2 and much higher than affinities of the low affinity substrate PAH to both transporters. These results are very interesting, because normally high affinity substrates show high affinity to one of the transporters, as described for FL-MTX. With fluo-cAMP we found a high affinity substrate for both, MRP2 and MRP4.

### **5.3 Regulation of Fluo-cAMP Transport in Killifish Kidney**

For further comparison of transport processes mediated by Mrp2 and Mrp4 in killifish proximal tubules, we investigated into regulatory mechanisms for fluo-cAMP transport. The ET pathway signaling through PKC starts with the binding of ET1 to the ET<sub>B</sub> receptor and a subsequent cascade via NO-synthase and PKC. ET signaling involves activation of an ET receptor-coupled G protein which in turn activates phospholipase C and PKC (Notenboom et al., 2002). In contrast to FL-MTX transport mediated by Mrp2, transport of fluo-cAMP in killifish proximal tubules seems to be independent from ET pathway. Neither ET1 nor the PKC activator PMA or NO donor nitroprusside-Na<sup>+</sup> had an effect on fluo-cAMP transport in killifish kidney proximal tubules. Summarizing these results, ET pathway and activation of PKC are not involved in regulation of fluo-cAMP transport in killifish proximal tubules.

We know that transport of ES mediated by Oat1 and Oat3 in rabbit proximal tubules is up-regulated by activation of PKA (Sauvant et al., 2004; Soodvilai et al., 2004). Contrary to these findings, db-cAMP, a direct activator of PKA, had no effect on fluo-cAMP accumulation. To clarify this effect we used the indirect PKA activator forskolin which inhibits phosphodiesterase and causes increasing intracellular cAMP levels. Forskolin had an inhibitory effect on fluo-cAMP transport, presumably caused by increased cAMP levels, because the direct PKA activator db-cAMP did not effect fluo-cAMP transport. H-89, a PKA inhibitor, could not alter the forskolin effect, suggesting inhibition by forskolin is independent from PKA activation.

Taking together these results, regulation of fluo-cAMP transport in killifish proximal tubules is apparently not mediated via PKC and PKA. This is different to results found for FL-MTX transport mediated by Mrp2 in killifish proximal tubules, which is sensitive to nanomolar concentrations of ET1 or PMA (Masereeuw et al., 2000). Thus, the regulatory mechanisms underlying the excretion of fluo-cAMP in killifish proximal tubules remain to be identified.

### **5.4 Fluo-cAMP Transport in Rat Choroid Plexus**

Since the brain is an important sanctuary for HIV (Miller et al., 2000; Bachmayer et al., 2005; Park and Sinko, 2005) it is crucial to know more about barrier functions in the brain and transport proteins involved in active transport processes overcoming those barriers. CP epithelium which forms the blood-cerebrospinal fluid (CSF)-barrier is significantly involved in excretion of xenobiotic compounds and metabolites from CSF into blood (Nishino et al.,

1999). To analyze transport processes across the blood-CSF barrier, we researched into transport of different substrates across CP epithelium. Transport processes were regarded in direction from aCSF into blood, comparable to excretion processes in CP epithelium.

In rat CP the findings for fluo-cAMP transport are different to those obtained for transport in killifish proximal tubules. Transport proteins mediating transport of the fluorescent cAMP analog fluo-cAMP are others in rat CP than in killifish proximal tubules. Fluo-cAMP accumulation in rat CP is an active two-step mechanism that is metabolism driven, NaCN treatment caused a decrease in luminal accumulation. Fluo-cAMP distribution was highest in vascular/perivascular spaces and the interior of blood vessels followed by epithelial cells and bath. Fluorescence in epithelial cells was only quite higher compared with bath fluorescence. Fluo-cAMP transport is composed of two steps, Na<sup>+</sup>-dependent uptake at the apical membrane and potential differences (PD) insensitive efflux at the basolateral membrane of CP epithelium. The inhibitory effects of ES and probenecid indicate involvement of Mrps, Oatps or Oats in fluo-cAMP transport in rat CP.

By immunocytological staining we showed, that Mrp4 is located to the basolateral membrane of CP epithelium, as well as Mrp1 and Oatp2 (Kusuhara et al., 2004; Miller, 2004, Breen et al., 2004), in rat. This localization was evidenced by functional analyses using the Mrp4 substrate [<sup>3</sup>H]-cGMP as well. On basis of the results obtained from functional analyses in killifish proximal tubules, we assumed involvement of Mrp4 in transport of fluo-cAMP in rat CP. To prove this speculation, we tested various substrates for Mrp4, including adefovir, AZT, cAMP, cGMP and PGE<sub>2</sub>. Non of these compounds had any effect on fluo-cAMP transport across rat CP epithelium, suggesting that Mrp4 is not involved in fluo-cAMP transport, especially basolateral efflux. But the results obtained from different inhibition studies led to the presumption that one or more transport proteins belonging to the Mrp family are involved in mediation of fluo-cAMP transport in rat CP: the Mrp inhibitor MK571 reduced fluo-cAMP accumulation, the effect was strong. LTC<sub>4</sub> had an inhibitory effect as well, but only fluorescence in vascular/perivascular spaces and the interior of blood vessels was reduced, suggesting an inhibition of basolateral efflux. The LTC<sub>4</sub> effect only on luminal accumulation of fluo-cAMP in rat CP, in addition to the effect of MK571, leads to the assumption that Mrp1 is involved in basolateral efflux from epithelial cells into blood in rat CP. From experiments with Mrp2 deficient TR<sup>-</sup> rats we know, that Mrp2 plays no role in fluo-cAMP transport in rat CP. Another transport protein localized to the basolateral membrane of rat CP is Oatp2 (Kusuhara et al., 2004; Miller, 2004, Breen et al., 2004), but this protein is not

involved in fluo-cAMP transport in rat CP, as the Oatp2 inhibitor digoxin had no effect, even at high concentrations.

Apical efflux into CP epithelial cells is Na<sup>+</sup>-dependent, as shown by removing Na<sup>+</sup> from incubation medium, indicating an Oat involved in uptake from aCSF into CP epithelial cells. The inhibitory effects of Na<sup>+</sup>-taurocholate treatment are evidence for participation of an Oat or Oatp as well, but Oatps mediate transport of their substrates in a Na<sup>+</sup>-independent manner. rOat3 is the most abundant Oat isoform expressed in CP epithelium and located to the apical membrane (Miller, 2004), but is not involved in fluo-cAMP uptake at the apical membrane of CP epithelial cells. rOat1 is only expressed at low levels in rat CP, it was detected only at RNA level (Choudhuri et al., 2003), but protein expression could not be verified (Kusuhara et al., 2004). From the PAH effect it can be concluded that neither Oat1 or Oat3 nor Mrp2 or Mrp4 are involved in mediating transport of fluo-cAMP in rat CP. As found for ES and taurocholate transport in mice CP (Sykes et al., 2004) and FL-MTX transport in rat CP (Breen et al., 2004), one or more Na<sup>+</sup>-dependent transporters different from Oat3 are involved in fluo-cAMP uptake at the apical membrane of rat CP epithelium. mRNA expression of one more member of the Oat family, Oat2, was described by Choudhuri et al., 2003. But localization of this protein is not evidenced by now.

Taking together these results, fluo-cAMP transport in rat CP is an active two-step mechanism composed of apical uptake mediated by one or more Na<sup>+</sup>-dependent transport proteins and basolateral efflux mediated by a Mrp, most probably Mrp1.

## **5.5 Comparison of Fluo-cAMP and Fluorescein Transport**

As described above, fluo-cAMP is a cAMP analog with FL coupled to C8 via a six-atom spacer. We compared fluo-cAMP transport with transport of its substituent, the small-sized Fluorescein (FL).

FL transport across CP epithelium is a concentrative two-step mechanism consisting of Na<sup>+</sup>-dependent uptake from aCSF into epithelial cells at the apical membrane and PD-driven efflux into blood at the basolateral membrane (Breen et al., 2002). The first differences between transport of FL and fluo-cAMP can be recognized from those findings, basolateral efflux of fluo-cAMP was PD-insensitive. A second difference is, that transport of FL is affected by treatment with the herbicide 2,4-D (Breen et al., 2002) which had no effects on fluo-cAMP transport. As proved by Sykes et al (2004) in mice CP, apical uptake of FL is

mediated by Oat3. Different to the effect on fluo-cAMP transport, LTC<sub>4</sub> had no effect on transport of FL in rat CP. Mrp1, Mrp2, Mrp3 and Oatps seem not to be involved in basolateral efflux of FL in rat CP. Transport proteins involved in PD-driven FL efflux at the basolateral membrane of CP epithelium are not evidenced by now (Breen et al., 2002). Combining these results, fluo-cAMP transport is mediated by different proteins than transport of its substituent FL in rat CP. This is an evidence for fluo-cAMP being stable and transported as a whole in rat CP.

## **5.6 Comparison of Fluo-cAMP and FL-MTX Transport**

Due to the similarity of molecular weights for both substances (fluo-cAMP: 815.7, Da FL-MTX: 979.1 Da) a further interesting comparison is the one between transport of fluo-cAMP and fluorescein-methotrexate (FL-MTX) in rat CP. Transport of FL-MTX in rat CP is a concentrative, metabolism-driven two-step mechanism as well as transport of fluo-cAMP. Apical uptake of FL-MTX is Na<sup>+</sup>-dependent, basolateral efflux is insensitive to PD. FL-MTX accumulation is in vascular/subepithelial spaces and the interior of blood vessels > medium > epithelial cells (Breen et al., 2004). This distribution is different to distribution of fluo-cAMP in rat CP which was in vascular/perivascular spaces > epithelial cells > medium. Na<sup>+</sup>-dependent uptake and PD-insensitive efflux were in the same manner for both substances. Mrp1 is involved in basolateral efflux of FL-MTX (Breen et al., 2004) in rat CP epithelium as well as in fluo-cAMP efflux at the basolateral membrane, but different to FL-MTX efflux, Oatp2 plays no role in mediation of fluo-cAMP efflux at the basolateral membrane. Oat3 is not involved in apical uptake of both substances in rat CP. For FL-MTX transport experiments with an Oat3-null mouse brought evidence for Oat3 not being a party of FL-MTX transport. The Na<sup>+</sup>-dependent transporter mediating transport of FL-MTX in rat CP remains to be found (Breen et al., 2004). Summarizing these results, we found similarities between fluo-cAMP and FL-MTX transport in rat CP. Both substances are transported by Mrp1, but FL-MTX efflux is also mediated by Oatp2. For both fluorescent dyes apical uptake is Na<sup>+</sup>-dependent and the transporter (s) involved remain (s) to be identified.

## **5.7 Regulation of Fluo-cAMP and FL-MTX Transport**

To characterize further differences or similarities concerning transport mechanisms driving transport of fluo-cAMP and FL-MTX in rat CP, we investigated into regulatory processes

behind those mechanisms. We found differences in regulatory pathways for transport of fluo-cAMP and FL-MTX in rat CP. The indirect PKA activator forskolin had an inhibitory effect on fluo-cAMP transport, that could not be altered by the PKA inhibitor H-89. That result leads to the presumption, that PKA is not involved in regulation of fluo-cAMP transport in rat CP. Different to those findings, forskolin led to increased FL-MTX accumulation in vascular/perivascular spaces and the interior of blood vessels in rat CP, this effect could be altered by H-89. Therefore, PKA activation seems to cause an activation of FL-MTX efflux at the basolateral membrane of CP epithelium in rat. This is one more important difference between transport mechanisms for fluo-cAMP and FL-MTX in rat CP. The endothelin pathway, including ET1 binding on ET<sub>B</sub> receptor and a subsequent cascade via NO-synthase and activation of PKC, is not a part of regulation for neither fluo-cAMP nor FL-MTX transport in rat CP. Concerning the MAPK pathway (described in results), we found differences between both substances. The MEK1/2 inhibitor U0126 had a strong inhibitory effect on fluo-cAMP transport, but FL-MTX transport was not affected by U0126 at the same concentrations. EGF had no effects on both, transport of fluo-cAMP and FL-MTX. We assume that the MAPK pathway is not involved in regulation of fluo-cAMP transport in rat CP, because EGF could not alter the U0126 effect. The U0126 effect seems to be independent from MAPK pathway activation. With regard to regulatory mechanisms driving transport of fluo-cAMP and FL-MTX in rat CP, respectively, we found more differences. PKA is involved in regulation of FL-MTX transport but not of fluo-cAMP transport, but fluo-cAMP transport is affected by the MEK1/2 inhibitor, this effect seems to be independent from the MAPK pathway. Although FL-MTX and fluo-cAMP have a similar molecular weight, transport mechanisms for both are different in total, even though we found some similarities.

## **5.8 FL and FL-MTX Transport in Shark Choroid Plexus**

For the small-sized molecule FL and the larger FL-MTX, respectively, similarities in transport mechanisms across CP epithelium in different species, rat and dogfish shark, were found. We investigated regulation of FL-MTX in rat CP and compared it with regulatory processes driving transport of FL-MTX in dogfish shark CP. FL-MTX transport is composed of Na<sup>+</sup>-dependent uptake at the apical membrane and basolateral efflux mediated by Mrp1 and Oatp2 in both, rat and dogfish shark CP (Breen et al., 2004; Baehr et al., in press). PKA is involved in regulation of FL-MTX in dogfish shark CP, we found the same for FL-MTX transport in rat CP. But different to the findings in rat CP, activation of PKC using PMA, led

to reduced FL-MTX accumulation in vascular/perivascular spaces, the interior of blood vessels and epithelial cells in shark CP. The PMA effect could be altered by the PKC inhibitor BIM (Baehr et al., in press). In dogfish shark CP, but not in rat CP, PKC activation leads to downregulation of FL-MTX transport. Here we showed differences concerning regulatory processes in rat and dogfish shark CP for the first time.

## **5.9 Texas Red Transport in Rat and Shark CP**

As described above, similar transport mechanisms for FL and FL-MTX were found in rat and dogfish shark CP. In the present study we examined transport of the medium-sized organic anion texas red (TR) in rat and dogfish shark CP and compared it with transport of FL and FL-MTX. Different to FL and FL-MTX transport, TR transport is different in both species. This is important due to the use of dogfish shark CP as a model for transport processes in mammalian CP.

Dogfish shark CP was used by reason of its larger size, better accessibility, less fragility and longer viability in *ex vivo* experiments compared with rat CP. The ultrastructure of rat and shark CP are similar to each other as described in results (Villalobos et al., 2002), but only little molecular and immunohistochemical information on shark CP is available. Interpretation of results obtained in shark CP depends on data from mammals.

In the study we found specific and concentrative transport mechanisms for TR in both species, rat and dogfish shark. But transport proteins involved in TR transport in CP seem to be different for both species. By confocal microscopy we could visualize TR transport from aCSF (ER) into blood across CP epithelium, TR accumulation was in vascular/perivascular spaces and the interior of blood vessels > epithelial cells > medium. By the use of different modulators of organic anion transport, we could draw conclusions about transport proteins involved in TR transport.

In rat CP the results indicate an active two-step mechanism for transepithelial TR transport, transport processes seem to be Na<sup>+</sup>-dependent, not PD-driven, but dependent on metabolism. TR transport in rat CP was affected by ES, BSP and probenecid, these results give evidence for transport mechanisms mediated by Oats, Oatps or Mrps. Na<sup>+</sup>-dependent uptake is typical for transport processes mediated by Oats. In rat CP the most abundant Oat isoform is Oat3, Oat1 is only expressed at low levels (Kusuhara et al., 2004). Transport processes mediated by

Oat1 or Oat3 should have been inhibited by PAH or cimetidine treatment. But PAH had no effect and cimetidine only a weak effect on TR transport in rat CP. Therefore, one or more Na<sup>+</sup>-dependent transport proteins different from Oat1 and Oat3 seem to be involved in TR transport, but these proteins remain to be analyzed. The inhibitory effect of the Mrp inhibitor MK571 indicates a Mrp involved in TR transport in rat CP, but LTC<sub>4</sub>, that is an inhibitor of i.a. Mrp1 mediated transport, had no effect on TR transport: Mrp1 seems not to be involved in the transport process of TR in rat CP. Methotrexate had an inhibitory effect on basolateral efflux into blood in rat CP epithelium, that result give us one more evidence for a Mrp involved in TR transport in rat CP. mRNA of Mrps different from Mrp1 was detected in CP (Choudhuri et al., 2003), but localization is not analyzed by now. We also tested the Oatp2 selective inhibitor digoxin, but it had no effect on TR transport in rat CP, Oatp2 seems not to be involved in basolateral TR efflux into blood in rat CP.

Interestingly, transport processes in shark CP seem to be Na<sup>+</sup>-independent and not metabolism driven. Like TR transport in rat CP, transport in shark CP is not PD-driven. Na<sup>+</sup>-independent uptake at the apical membrane indicates involvement of an Oatp. Because Oatp3 is the most abundant isoform in CP and located to the apical membrane (Kusuhara et al., 2004), it is likely that Oatp3 is involved in apical TR uptake in dogfish shark CP. Furthermore TR transport in shark CP was affected by ES and probenecid, these results can be more evidences for an Oatp involved in TR transport. The Oat1 and 3 inhibitors cimetidine and PAH had no or only a weak effect on TR accumulation at millimolar concentrations. These results are against an involvement of Oat1 and Oat3 in transport of TR in dogfish shark CP. Regarding the basolateral efflux step, different results were found for TR transport in rat and shark CP as well. MK571 had an inhibitory effect on TR transport in shark as well as in rat CP. This leads to the suggestion that a Mrp is involved in transport, most likely Mrp1. The second transporter involved in TR efflux at the basolateral membrane in shark CP seems to be Oatp2, because treatment with digoxin led to decreased fluorescence levels.

Summarizing the results, TR transport in rat CP is an active two-step mechanism which is metabolism driven, Na<sup>+</sup>-dependent and PD-insensitive. The transport protein(s) involved in apical uptake are Na<sup>+</sup>-dependent, but remain(s) to be identified. It is likely, that a Mrp different from Mrp1, Mrp2 and Mrp4 is involved in basolateral efflux, but we don't know by now, which one (or more) is concerned.

In shark CP TR transport is an active two-step mechanism as well. It is not metabolism driven, but Na<sup>+</sup>-independent and not PD-driven. Na<sup>+</sup>-independent uptake at the apical membrane is most likely mediated by Oatp3. Probably transport proteins involved in basolateral efflux are Mrp1 and Oatp2.

## 5.10 Comparison of TR, FL and FL-MTX Transport

With these results we demonstrate the main differences between TR, FL and FL-MTX transport in CP: FL and FL-MTX transport mechanisms are equal in rat and shark CP, TR is transported by different transport proteins in rat and shark CP. Further differences between FL, FL-MTX and TR transport concern the proteins involved.

As described above, FL-MTX is a concentrative, metabolism-driven two-step mechanism as well. Apical uptake was Na<sup>+</sup>-dependent and mediated most likely by Oat like protein (s), basolateral efflux was insensitive to PD and mediated by Mrp1 and Oatp2 in both rat and dogfish shark CP (Breen et al., 2004; Baehr et al., in press).

TR efflux in dogfish shark CP is mediated by Mrp1 and Oatp2 as well, but apical uptake is Na<sup>+</sup>-independent and most probably mediated by Oatp3. In rat CP transport proteins involved in TR transport remain to be identified. A Mrp seems to be involved in basolateral efflux, uptake at the apical membrane of rat CP epithelium is mediated by Oat like, Na<sup>+</sup>-dependent protein(s). Outlining the results, FL-MTX and TR transport share some similarities, but in total they differ in rat as well as in shark CP.

FL transport across CP epithelium is a concentrative two-step mechanism consisting of Na<sup>+</sup>-dependent uptake at the apical membrane and PD-driven efflux at the basolateral membrane into blood. The herbicide 2,4-D had an inhibitory effect on FL transport across CP epithelium (Breen et al., 2002; Villalobos et al., 2002). As described above, FL uptake is mediated by Oat3. Different to FL efflux, TR efflux at the basolateral membrane was not PD driven in both rat and shark CP. Totally different transport proteins seem to be involved in FL and TR efflux. Like in rat CP, FL uptake at the apical membrane is Na<sup>+</sup>-dependent, but FL uptake is mediated by Oat3 and the proteins involved in TR uptake in rat CP are not identified by now. Different to FL uptake and TR uptake in rat CP, TR uptake in dogfish shark CP is Na<sup>+</sup>-independent and mediated by Oatp3. Summarizing these findings, FL and TR transport are mediated by different transport proteins.

## 6 Summary

Together with the blood-brain-barrier (BBB), the blood-cerebrospinal fluid (CSF)-barrier (BCSFB) formed by CP epithelium, plays an important role in protection of the brain and elimination of eventually toxic xenobiotics or metabolic waste out of the CNS. Due to the accretion of CNS diseases including brain cancer, HIV, schizophrenia, meningitis, depression and epilepsy, CP tissue gets more relevance as target for pharmacotherapy (Bachmayer et al., 2005; Ghersi-Egea/Strazielle, 2001; Löscher/Potschka, 2005; Miller, 2004). To come to know more about CP function and elimination mechanisms we investigated into transport processes at the CP using different fluorescent compounds as model substances.

Due to the tissue localization, small size and sensitivity of CP tissue in mammals, we used different models to study mechanisms of organic anion transport before studies in rat CP were accomplished. Killifish proximal tubules are an excellent model for studying transport processes, because killifish can be obtained and held easily and proximal tubules isolation is facile. Killifish proximal tubules are stable at room temperature for a long period of time and fish analogs to the transport proteins expressed in mammalian kidneys are expressed in killifish proximal tubules. To a large extent transport proteins in kidney and CP are the same, as CP is also called the kidney of the brain (Spector/Johanson, 1991).

We showed localization of the fish analog to Mrp4 to the luminal site of killifish proximal tubules and demonstrated transport of the fluorescent cAMP analog fluo-cAMP by Mrp2 and Mrp4 in killifish proximal tubules using confocal microscopy. Luminal efflux of fluo-cAMP in killifish proximal tubules was mediated by Mrp2 and Mrp4, transporters involved in basolateral uptake remain to be identified. Fluo-cAMP transport in killifish proximal tubules is, different to transport of FL-MTX transport mediated by Mrp2 (Notenboom et al., 2002), not regulated by the ET pathway or PKA. Further analyses are needed to assess regulation of fluo-cAMP transport in killifish proximal tubules.

As shown for killifish proximal tubules, we demonstrated MRP2 and MRP4 mediated fluo-cAMP transport in MDCKII-MRP2 and Sf9-MRP4 membrane vesicles. Membrane vesicles of transfected cells are used as model for transport processes due to the possibility to regard specific transport processes mediated by one protein. By the use of membrane vesicle studies we got evidences for specific, ATP-dependent fluo-cAMP transport by MRP2 and MRP4 with fluo-cAMP as high affinity substrate for both proteins.

To examine these findings in rat CP we used the fluorescent molecule fluo-cAMP and confocal microscopy. Fluo-cAMP was transported from aCSF through CP epithelial cells in a dose-dependent and saturable manner. High accumulation in vascular/perivascular spaces and the interior of blood vessels are signs for an active, concentrative two-step mechanism of fluo-cAMP transport. Fluo-cAMP uptake at the apical membrane of CP epithelial cells is mediated by one or more Na<sup>+</sup>-dependent, most probably Oat like, proteins. Basolateral efflux is mediated by a Mrp, presumably Mrp1. Different to the findings we got from experiments in killifish proximal tubules and membrane vesicles of MDCKII-MRP2 and Sf9-MRP4 cells, fluo-cAMP transport in rat CP was not mediated by Mrp4, even though we demonstrated Mrp4 localization parallel to Mrp1 to the basolateral membrane of CP epithelium. Regulatory cascades were researched in rat CP and led to the result, that fluo-cAMP transport is insensitive to activation of PKC or PKA by ET or MAPK pathway.

Another model used for investigation of transport processes in mammalian CP, is the CP of dogfish sharks by reason of its larger size, better accessibility and longer stability at room temperature. Morphology and ultrastructure of rat and dogfish shark CP showed several similarities (Villalobos et al., 2002). FL-MTX and FL transport were analyzed in rat and shark CP and the results were similar transport proteins involved in transport of FL and FL-MTX, respectively, in rat and shark CP. Transport proteins mediating transport of FL and FL-MTX were different, but similar for each organic anion in both species (Baehr et al., in press; Breen et al., 2002; Breen et al., 2004; Villalobos et al., 2002). To investigate into TR transport in CP, we used rat and dogfish shark CP and obtained interesting results. Transport proteins involved in TR transport in rat and shark CP were different. In rat CP TR transport was composed of Na<sup>+</sup>-dependent uptake at the apical membrane and basolateral efflux mediated by a Mrp, but not Mrp1, Mrp2 or Mrp4. In dogfish shark CP the findings were different: apical uptake of TR was Na<sup>+</sup>-independent and mediated by Oatp3. Efflux at the basolateral membrane of dogfish shark CP was mediated by Mrp1 and Oatp2.

Further differences between both species were found investigating regulation of FL-MTX transport. FL-MTX transport was activated by PKA activation and inhibited by PKC activation in dogfish shark CP. Different to these findings PKA activation led to increased efflux of FL-MTX in rat CP, but PKC activation did not effect transport of FL-MTX in rat CP.

Summarizing, we could demonstrate different transport mechanisms for transport of organic anions in different models. The small sized molecule FL, the medium sized dye TR and the

larger sized substances fluo-cAMP and FL-MTX seem to be transported by different transport proteins, but molecular weight seems not to be the crucial factor for the different mediations.

Fluo-cAMP transport is different to transport of the nonfluorescent compound cAMP which is transported by Mrp4 (Van Aobel et al., 2002), and different to transport of its substituent FL. Despite the homology of CP and kidney proximal tubules, transport of fluo-cAMP is mediated by different transport proteins in rat CP and killifish proximal tubules, suggesting that killifish proximal tubules cannot be used as a model for transport processes in rat CP.

Different from transport proteins involved in FL and FL-MTX transport, respectively, transport proteins mediating transport of TR seem to be different in rat and dogfish shark CP. The same was found for regulation of FL-MTX transport in rat and shark CP, even though transport proteins involved in transport of FL-MTX are the same in rat and shark CP, regulatory processes behind those proteins are different. We sum up, that defiant of the similar morphology and ultrastructure to rat CP, dogfish shark CP allows only limited predictions with respect to transport proteins in mammalian CP.

Confocal microscopy is a distinguished tool for functional analyses because uptake step, transport through the cells and efflux can be visualized. Due to the use of different models we could draw conclusion about characteristics of organic anion transport and transport proteins involved. In CP tissue several proteins are detected on RNA level, but protein localization remains to be studied to get a clearer view of transport processes at the BCSFB. First insights into regulatory processes involved in transport processes could be taken, but further experiments are needed to be done to understand regulation of transport processes for organic anions.

## 7 Outlook

The blood-CSF-barrier is an important barrier which protects the brain and actively regulates homeostasis of the liquor. Most water soluble substances can only be transported actively through the epithelium. For the therapy of brain diseases, especially HIV, it is very important to get a better knowledge about transport proteins involved in transport across CP epithelium. In the presented study we used fluorescent molecules and confocal laserscanning microscopy to visualize transport processes across CP epithelium. The advantage of this technique is the facility of watching both steps of transport across the epithelium: uptake at the apical membrane and efflux into blood at the basolateral site. We demonstrated transport processes for the fluorescent molecules fluo-cAMP and TR and compared it with results previously found for FL and FL-MTX (Baehr et al., in press; Breen et al., 2002; Breen et al., 2004; Villalobos et al., 2002). We could interpret the transport mechanisms and found transport proteins involved either in apical uptake or in basolateral efflux. Some transporters involved in transport of the fluorescent dyes are not identified by now. Choudhuri et al. (2003) described expression of other Mrps, Oats and Oatps on RNA level in rat CP epithelium, but protein expression is not revealed by now.

In further studies we will prove expression of transport proteins on protein level and localization in CP epithelium. We will analyze expression of breast cancer resistance protein using RT-PCR and indirect immunostaining and start transport studies using the Bcrp substrate mitoxantrone.

Furthermore, we want to accomplish more specific transport studies in membrane vesicles from transfected cells to verify fluo-cAMP transport mediated by MRP1. We produce MDCKII-MRP1 cell membrane vesicles and carry out western blot studies to reveal protein expression in those vesicles. Uptake studies using fluo-cAMP as substrate will be performed next.

Another interesting field is the regulation of transport processes in CP. Not much is known about regulatory processes in CP epithelium. We found that PKA is involved in regulation of FL-MTX transport in rat CP and PKA as well as PKC are involved in regulation of FL-MTX transport in dogfish shark CP. The other tested pathways were not involved in regulatory processes involved in transport of fluo-cAMP, TR or FL-MTX. Further studies will investigate regulation of fluo-cAMP transport in rat CP and killifish proximal tubules and the hormones and cascades involved. Xiang et al. (2005) analyzed expression and localization of

P2X receptors in rat CP and assume involvement of P2X receptors in secretion of CSF. These receptors may play a role in regulation of transport processes in rat CP as well.

All in all, not much is known about transport processes in CP, proteins involved and regulation. Protein localization of several transport proteins as well as their involvement in transport processes at the BCSFB and regulation of these transport processes remain to be analyzed.

## 8 References

### A

Abe T., Kakyo M., Sakagami H., Tokui T., Nishio T., Tanemoto M., Nomura H., Hebert S.C., Matsuno S., Kondo H., Yawo H.; Molecular characterization and tissue distribution of a new organic anion transporter subtype (oatp3) that transports thyroid hormones and taurocholate and comparison with oatp2. J. Biol. Chem. 273 (1998) 22395-22401

Alebouyeh M., Takeda M., Onozato M.L., Tojo A., Noshiro R., Hasannejad H., Inatuniconi J., Narikawa S., Huang X.-L., Khamdang S., Anzai N., Endou H.; Expression of Human Anion Transporters in the Choroid Plexus and their Interactions with Neurotransmitter Metabolites. Journal of Pharmacological Sciences 93 (2003) 430-436

Algara-Suárez P., Espinosa-Tanguma R.; 8-Br-cGMP mediates relaxation of tracheal smooth muscle through PKA. Biochemical and Biophysical Communications 314 (2004) 597-601

Ambudkar S.V., Dey S., Hrycyna C.A., Ramachandra M., Pastan I., Gottesmann M.M.; Biochemical, Cellular, and Pharmacological Aspects of the Multidrug Resistance Transporter. Annu. Rev. Pharmacol. Toxicol. 39 (1999) 361-98

### B

Baehr C.H., DiPasquale K.D., Fricker G., Miller D.S: Regulation and Transport of FL-MTX at the Blood-Liquor Barrier of *Squalus Acanthias*. American Journal of Physiology: Comparative Physiology in press

Bai J., Lai L., Yeo H.C., Goh B.C., Tan T.M.C.; Multidrug resistance protein 4 (MRP4/ABCC4) mediates efflux of bimane-glutathione. The International Journal of Biochemistry & Cell Biology 36 (2004)

Bakos É., Evers R., Sinkó E., Varádi A., Borst P., Sarkadi B.; Interactions of the Human Multidrug Resistance Proteins MRP1 and MRP2 with Organic Anions. Molecular Pharmacology 57 (2000) 760-768

Borst P., Elferink R.O.; Mammalian ABC Transporters in Health and Disease. Annu. Rev. Biochem. 71 (2002) 537-92

Borst P., Evers R., Kool M., Wijnholds J.; A Family of Drug Transporters: The Multidrug Resistance-Associated Proteins. Journal of the National Cancer Institute 92 (16) (2000) 1295-1302

Borst P., Evers R., Kool M., Wijnholds J.; The multidrug resistance protein family: Biochimica et Biophysica Acta 1461 (1999) 347-357

Breen C.M., Sykes D.B., Baehr C., Fricker G., Miller D.S.; Fluorescein-Methotrexate Transport in rat Choroid Plexus using confocal microscopy. Am J Physiol Renal Physiol. 287 (2004) F562-F569

Breen C.M., Sykes D.B., Fricker G., Miller D.S.; Confocal imaging of organic anion transport in intact rat choroid plexus. Am J Physiol Renal Physiol 282 (2002) F877-F885

Buist S.C.N., Cherrington N.J., Klaassen C.D.; Endocrine Regulation of Rat Organic Anion Transporters: Drug Metabolism and Distribution 31 (2003) 559-564

## C

Cattori V., van Montfoort J.E., Stieger B., Landmann L., Meijer D.K.F., Winterhalter K.H., Meier P.J., Hagenbuch B.; Localization of organic anion transporting polypeptide 4 (Oatp4) in rat liver and comparison of its substrate specificity with Oatp1, Oatp2 and Oatp3. Pflügers Arch-Eur J Physiol 443 (2001) 188-195

Chen C., Klaassen C.D.; Rat multidrug resistance protein 4 (Mrp4, Abcc4): molecular cloning, organ distribution, postnatal renal expression, and chemical inducibility. Biochemical and Biophysical Research Communications 317 (2004) 46-53

Chen Z.S., Lee K., Kruh G.D.; Transport of cyclic nucleotides and estradiol-17-beta-D-glucuronide by multidrug resistance protein 4. Resistance to 6-mercaptopurine and 6-thioguanine: J Biol Chem. 276(36) (2001) 33747-54

Chen Z.-S., Lee K., Walther S., Raftogianis R.B., Kuwano M., Zeng H., Kruh G.D.; Analysis of Methotrexate and Folate Transport by Multidrug Resistance Protein 4 (ABCC4): MRP4 is a component of the Methotrexate Efflux System. Cancer Research 62 (2002) 3144-3150

Chodobski A., Szmydynger-Chodobska J.; Choroid Plexus: Target for Polypeptides and Site of their Synthesis. Microscopy Research and Technique 52 (2001) 65-82

Choudhuri S., Cherrington N.J., Li N., Klaassen C.D.; Constitutive Expression of various xenobiotic and endobiotic Transporter mRNAs in the Choroid Plexus of Rats: Drug Metabolism and Disposition 31 (2003) 1337-1345

Cole S.P., Bhardwaj G., Gerlach J.H., Mackie J.E., Grant C.E., Almquist K.C., Stewart A.J., Kurz E.U., Duncan A.M., Deeley R.G.; Overexpression of a transporter gene in a multidrug-resistant human lung cancer cell line. Science 258 (1992) 1650-1654

Cserr H.F.; Physiology of the Choroid Plexus. Physiological Reviews 51 (2) (1971) 273-311

## D

Dallas S., Schlichter L.; MRP4- and MRP5-mediated Efflux of 9-(2-phosphonylmethoxyethyl)adenine (PMEA) by Microglia: J Pharmacol Exp Ther. 309 (3) (2004) 1221-9

Dantzig A.H., de Alwis D.P., Burgess M.; Considerations in the design and development of transport inhibitors as adjuncts to drug therapy: Advanced Drug Delivery Reviews 55 (2003) 133-150

D'Aquila, R.T., Bechtel, L.J., Videler, J.A., Eron, J.J., Gorzycy, P., Kaplan, J.C. (1991). Maximizing sensitivity and specificity of PCR by preamplification heating: Nucleic Acids Res. 19 (1991) 3749

Dean M., Allikmets R.; Complete Characterization of the Human ABC Gene Family: J Bioenerg Biomembr. 33(6) (2001) 475-9

De Boer A.G.; The Blood-Brain Barrier (BBB): Fundamentals, Strategies and Models. (1997)

Denk G.U., Soroka C.J., Takeyama Y., Chen W.-S., Schuetz J.D., Boyer J.L.; Multidrug resistance-associated protein 4 is up-regulated in liver but down-regulated in kidney in obstructive cholestasis in the rat. Journal of Hepatology 40 (2004) 585-591

Dreuw A., Hermanns H.M., Heise R., Joussem S., Rodríguez F., Marquardt Y., Jugert F., Merk H.F., Heinrich P.C., Baron J.M.; Interleukin-6-Type Cytokines Upregulate Expression of Multidrug Resistance-Associated Proteins in NHEK and Dermal Fibroblasts: J Invest Dermatol 124 (2005) 28-37

## E

Ekarantanawong S., Anzai N., Jutabha P., Miyazaki H., Noshiro R., Takeda M., Kanai Y., Sophasan S., Endou H.; Human Organic Anion Transporter 4 Is a Renal Apical Organic Anion/Dicarboxylate Exchanger in the Proximal Tubules: J Pharmacol Sci 94 (2004) 297-304

Evans, D.H.; Physiology of Fishes: Boca Raton, New York: CRC-Press

## F

Faber K.N., Müller M., Jansen P.L.M.; Drug transport proteins in the liver: Advanced Drug Delivery Reviews 55 (2003) 107-124

Fishman R.A.; Cerebrospinal Fluid in Diseases of the Nervous System. 2.Ed., Philadelphia Saunders W.B., 1992

Forestier C., Frangne N., Eggmann T., Klein M.; Differential sensitivity of plant and yeast MRP (ABCC)-mediated organic anion transport processes towards sulfonylureas. Federation of European Biochemical Societies Letters 554(2003) 23-29

## G

Gao B., Hagenbuch B., Kullak-Ublick G.A., Benke D., Aguzzi A., Meier P.J.; Organic Anion-Transporting Polypeptides Mediate Transport of Opioid Peptides across Blood-Brain Barrier. The Journal of Pharmacology and Experimental Therapeutics 294 (2000) 73-79

Gao B., Meier P.J.; Organic Anion Transport Across the Choroid Plexus. Microscopy Research and Technique 52 (2001) 60-64

Gherzi-Egea J.-F., Strazielle N.; Brain Drug Delivery, Drug Metabolism, and Multidrug Resistance at the Choroid Plexus. Microscopy Research and Technique 52 (2001) 83-88

Gloor S.M., Wachtel M., Bolliger M.F., Ishihara H., Landmann R., Frei K.; Molecular and cellular permeability control at the blood-brain barrier. Brain Research Reviews 36 (2001) 258-264

Grundemann D., Gorboulev V., Gambaryan S., Vehyl M., Koepsell H.; Drug excretion mediated by a new prototype of polyspecific transporter. Nature 372 (1994) 549-552

Gutmann H., Miller D.S., Droulle A., Drewe J., Fahr A., Fricker G.; P-glycoprotein- and mrp2-mediated octreotide transport in proximal tubule. British Journal of Pharmacology 129 (2000) 251-256

Gutmann H., Török M., Fricker G., Huwyler J., Beglinger C., Drewe J.; Modulation of Multidrug Resistance Protein Expression in Porcine Brain Capillary Endothelial Cells in vitro. Drug Metabolism and Disposition 27 (8) (1999) 937-941

Gygi S.P., Rochon Y., Franza B.R., Aebersold R.; Correlation between Protein and mRNA Abundance in Yeast. Molecular and Cellular Biology 19 (3) (1999) 1720-1730

## H

Habu Y., Yano I., Takeuchi A., Saito H., Okuda M., Fukatsu A., Inui K.-I.; Decreased activity of basolateral organic ion transporters in hyperuricemic rat kidney: roles of organic ion transporters rOAT1, rOAT3 and rOCT2. Biochemical Pharmacology 66 (2003) 1107-1114

Hagenbuch B., Meier P.J.; The superfamily of organic anion transporting polypeptides. Biochem. Biophys. Acta 1609 (2003) 397-421

Haselbach M., Wegener J., Decker S., Engelbertz C., Galla H.-J.; Porcine Choroid Plexus Epithelial Cells in Culture: Regulation of Barrier Properties and Transport Processes. Microscopy Research and Technique 52 (2001) 137-152

Hediger M.A., Romero M.F., Peng J.-B., Rolfs A., Takanaga H., Bruford E.A.; The ABC of solute carriers: physiological, pathological and therapeutic implications of human membrane transport proteins. Pflügers Arch-Eur J Physiol 447 (2004) 465-468

Hirrlinger J., König J., Dringen R.; Expression of mRNAs of multidrug resistance proteins (Mrps) in cultured rat astrocytes, oligodendrocytes, microglial cells and neurons: Journal of Neurochemistry 82 (2002) 716-719

## I

Imaoka T., Kusuhara H., Adachi-Akahane S., Hasegawa M., Morita M., Endou H., Sugiyama Y.; The Renal-Specific Transporter Mediates Facilitative Transport of Organic Anions at the Brush Border Membrane of Mouse Renal Tubules. J Am Soc Nephrol 15 (2004) 2012-2022

Ito K., Suzuki H., Horie T., Sugiyama Y.; Apical/Basolateral Surface Expression of Drug Transporters and its Role in Vectorial Drug Transport: Pharm Res. 22 (10) (2005) 1559-77

## J

Jedlitschky G., Burchell B., Keppler D.; The Multidrug Resistance Protein 5 Functions as an ATP-dependent Export Pump for Cyclic Nucleotides. The Journal of Biological Chemistry 275 (39) (2000) 30069-30074

Johanson C.E.; Arachnoid membrane, subarachnoid CSF and pia-glia. Introduction to the Blood-Brain Barrier Methodology, biology and pathology (1998) 259-269

Johanson C.E.; Ventricles and Cerebrospinal Fluid. Neuroscience in Medicine (1995) 171-196

Johanson C.E., Preston J.E., Chodobski A., Stopa E.G., Szmydynger-Chodobska J., McMillan P.N.; AVP V1 receptor-mediated decrease in Cl. Am J Physiol. 276 (1) (1999) C82-90

Jonker J.W., Schinkel A.H.; Pharmacological and physiological functions of the polyspecific organic cation transporters OCT1, 2 and 3 (SLC22A1-3). J. Pharmacol. Exp. Ther. 308 (2004) 2-9

Jonker J.W., Wagenaar E., Mol C.A., Buitelaar M., Koepsell H., Smit J.W., Schinkel A.H.; Reduced hepatic uptake and intestinal excretion of organic cations in mice with a targeted disruption of the organic cation transporter 1 (Oct1 [Slc22a1]) gene. Mol. Cell. Biol. 21 (2001) 5471-5477

Jonker J.W., Wagenaar E., Van Eijl S., Schinkel A.H.; Deficiency in the organic cation transporters 1 and 2 (Oct1/Oct2 [Slc22a1/Slc22a2]) in mice abolishes renal secretion of organic cations. Mol. Cell. Biol. 23 (2003) 7902-7908

Jorajuria S., Dereuddre-Bosquet N., Naissant-Storck K., Dormont D., Clayette P.; Differential Expression Levels of MRP1, MRP4, and MRP5 in Response to Human Immunodeficiency Virus Infection in Human Macrophages. Antimicrobial Agents and Chemotherapy 48 (5) (2004) 1889-1891

## K

Kabanov A.V., Batrakova E.V., Miller D.W.; Pluronic block copolymers as modulators of drug efflux transporter activity in the blood-brain-barrier: Advanced Drug Delivery Reviews 55 (2003) 151-164

Keppler D., König J.; Hepatic canalicular membrane 5: Expression and localization of the conjugate export pump encoded by the MRP2 (cMRP/cMOAT) gene in liver. FASEB J. 11 (1997) 509-516

Klein I., Sarkadi B., Váradi A.; An inventory of the human ABC proteins. Biochimica et Biophysica Acta 1461 (1999) 237-262

Kobayashi D., Nozawa T., Imai K., Nezu J., Tsuji A., Tamai I.; Involvement of human organic anion transporting polypeptide OATP-B (SLC21A9) in pH-dependent transport across intestinal apical membrane. J. Pharmacol. Exp. Ther. 306 (2003) 703-708

Kool M., de Haas M., Scheffer G.L., Scheper R.J., van Eijk M.J.T., Juijin J.A., Baas F., Borst P.; Analysis of Expression of cMOAT (MRP2), MRP3, MRP4 and MRP5, Homologues of the Multidrug Resistance-associated Protein Gene (MRP1), in Human Cancer Cell Lines: Cancer Research 57 (1997) 3537-3547

Koepsell H., Endou H.; The SLC22 drug transporter family. Plügers Arch. 447 (2004) 666-676

Kusuhara H., He Z., Nagata Y., Nozaki Y., Ito T., Masuda H., Meier P.J., Abe T., Sugiyama Y.; Expression and functional involvement of organic anion transporting polypeptide subtype 3 (Slc21a7) in rat choroid plexus. Pharm. Res. 20 (2003) 720-727

Kushura H., Sugiyama Y.; Efflux transport systems for drugs at the blood-brain barrier and blood-cerebrospinal fluid barrier (Part1). Drug Discovery Today 6 (3) (2001)150-156

Kushura H., Sugiyama Y.; Efflux transport systems for drugs at the blood-brain barrier and blood-cerebrospinal fluid barrier (Part2). Drug Discovery Today 6 (4) (2001) 206-212

Kusuhara H., Sugiyama Y.; Efflux transport systems for organic anions and cations at the blood-CSF barrier. Advanced Drug Delivery Reviews 56 (2004) 1741-1763

## L

Lee G., Dallas S., Hong M., Bendayan R.; Drug Transporters in the Central Nervous System: Brain Barriers and Brain Parenchyma Considerations. Pharmacological Reviews 53 (4) (2001) 569-596

## References

---

Lee K., Klein-Szanto A.J.P., Kruh G.D.; Analysis of the MRP4 Drug Resistance Profile in Transfected NIH3T3 Cells. Journal of the National Cancer Institute 92 (23) (2000) 1934-1940

Lee Y.J, Kushuhara H., Sugiyama Y.; Do Multidrug Resistance-associated Protein-1 and -2 Play Any Role in the Elimination of Estradiol-17 $\beta$ -glucuronide and 2,4-Dinitrophenyl-S-glutathione across the Blood-Cerebrospinal Fluid Barrier? Journal of Pharmaceutical Sciences 93 (1) (2003) 99-107

Leggas M, Adachi M, Scheffer GL, Sun D, Wielinga P, Du G, Mercer KE, Zhuang Y, Panetta JC, Johnston B, Scheper RJ, Stewart CF, Schuetz JD; Mrp4 confers resistance to topotecan and protects the brain from chemotherapy. Mol Cell Biol 24 (17) (2004) 7612-21

Leier I., Jedlitschky G., Buchholz U., Cole S.P.C., Deeley R.G., Keppler D.; The MRP Gene Encodes an ATP-dependent Export Pump for Leucotriene C<sub>4</sub> and Structurally Related Conjugates. The Journal of Biological Chemistry 269 (45) (1994) 27807-27810

Li L., Lee T.K., Meier P.J., Ballatori N.; Identification of Glutathione as a Driving Force and Leukotriene C<sub>4</sub> as a Substrate for oatp1, the Hepatic Sinusoidal Organic Solute Transporter. The Journal of Biological Chemistry 273 (26)

Li L., Meier P.J., Ballatori N.; Oatp2 mediates bidirectional organic solute transport: a role for intracellular glutathione: Mol Pharmacol (58) (2000) 335-340

Li N., Hartley D.P., Cherrington N.J., Klaassen C.D.; Tissue expression, ontogeny, and inducibility of rat organic anion transporting polypeptide 4. J. Pharmacol. Exp. Ther. 301 (2002) 551-560

Li J.Y., Boado R.J., Pardrige W.M.; Blood-brain barrier genomics. J. Cereb. Blood Flow Metab. 21 (2001) 61-68

Lin J.H.; Drug-drug interaction mediated by inhibition and induction of P-glycoprotein: Advanced Drug Delivery Reviews 55 (2003) 53-81

Löscher W., Potschka H.; Drug Resistance in Brain Diseases and the Role of Drug Efflux Transporters: Neuroscience 6 (2005) 591-602

Lowes S., Sykes D., Breen C.M., Ragone L.J., Miller D.S.; Multiple Components of 2,4-Dichlorophenoxyacetic Acid Uptake by Rat Choroid Plexus: The Journal of Pharmacology and Experimental Therapeutics 315 (1) (2005) 136-143

Lu R., Chan B.S., Schuster V.L.; Cloning of the human kidney PAH transporter: narrow substrate specificity and regulation by protein kinase C: The American Physiological Society (1999)

Lu H., Klaassen C. Tissue distribution and thyroid hormone regulation of Pept1 and Pept2 in rodents. Peptides (2005, in print)

## M

Masereeuw R., Moons M.M., Toomey B.H., Russel F.G.M., Miller D.S.; Active Lucifer Yellow Secretion in Renal Proximal Tubule: Evidence for Organic Anion Transport System Crossover. The Journal of Pharmacology and Experimental Therapeutics 289 (2) 1999 1104-1111

Masereeuw R., Notenboom S., Smeets P.H.E., Wouterse A.C., Russel F.G.M.; Impaired Renal Secretion of Substrates for the Multidrug Resistance Protein 2 in Mutant Transport-Deficient (TR<sup>-</sup>) Rats. Journal of the American Society of Nephrology 14 (2003) 2741-2749

Masereeuw R., Russel F.G., Miller D.S.: Multiple pathways of organic anion secretion in renal proximal tubulus revealed by confocal microscopy. Am J Physiol 271(6 pt 2) (1996) F1173-82

Masereeuw R., Terlouw S.A., Van Aubel R.A.M.H., Russel F.G.M., Miller D.S.; Endothelin B Receptor-Mediated Regulation of ATP-Driven Drug Secretion in Renal Proximal Tubule. Molecular Pharmacology 57 (2000) 59-67

Matsuzaki M., Nakano A., Jiang Q.-J., Pulkkinen L., Uitto J.; Tissue-Specific Expression of the ABCC6 Gene. J Invest Dermatol 125 (2005) 900-905

Miller D.S.; Confocal imaging of xenobiotic transport across the choroid plexus. Advanced Drug Delivery Reviews 56 (2004) 1811-1824

Miller D.S., Masereeuw R., Karnaky K.J.; Regulation of MRP2-mediated transport in shark rectal salt gland tubules. Am J Physiol Regulatory Integrative Comp Physiol 282 (2002) R774-R781

Miller D.S., Pritchard J.B.; Dual Pathways for Organic Anion Secretion in Renal Proximal Tubule. The Journal of Experimental Zoology 279 (1997) 462-470

Mitani A., Nakahara T., Sakamoto K., Ishii K.; Expression of multidrug resistance protein 4 and 5 in the porcine coronary and pulmonary arteries. European Journal of Pharmacology 466 (2003) 223-224

Mühlhardt C.; Molekularbiologie/Genomics. Spektrum Akademischer Verlag (2002)

## N

Nagata Y., Kusuhara H., Endou H., Sugiyama Y.; Expression and functional characterization of rat organic anion transporter 3 (rOat3) in the choroid plexus. Mol. Pharmacol. 61 (2002) 430-436

Nies A.T., Jedlitschky G., König J., Herold-Mende C., Steiner H.H., Schmitt H.P., Keppler D.; Expression and Immunolocalization of the Multidrug Resistance Proteins, MRP1-6 (ABCC1-6), in Human Brain. Neuroscience 129 (2004) 349-360

Nilsson C., Lindvall-Axelsson M., Owman C.; Neuroendocrine regulatory mechanisms in the choroid plexus-cerebrospinal fluid system. Brain Research Reviews 17 (1992) 109-138

Nishino J.I., Suzuki H., Sugiyama D., Kitazawa T., Ito K., Hanano M., Sugiyama Y.; Transepithelial Transport of Organic Anions across the Choroid Plexus: Possible Involvement of Organic Anion Transporter and Multidrug Resistance-Associated Protein. JPET 290 (1999) 289-294

Nishio T., Adachi H., Nakagomi R., Tokui T., Sato E., Tanemoto M., Fujiwara K., Okabe M., Onogawa T., Suzuki T., Nakai D., Shiiba K., Suzuki M., Ohtani H., Kondo Y., Unno M., Ito S., Inuma K., Nunoki K., Matsuno S., Abe T.; Molecular identification of a rat novel organic anion transporter moat1, which transports prostaglandin D(2), leukotriene C(4), and taurocholate. Biochim. Biophys. Res. Commun. 275 (2000) 831-838

Notenboom S., Miller D.S., Smits P., Russel F.G.M., Masereeuw R.; Role of NO in endothelin-regulated drug transport in the renal proximal tubulus. AJP-Renal 282 (2002) 458-464

## O

Ocheltree S.M., Shen H., Hu Y., Xiang J., Keep R.F., Smith D.E.; Role of PEPT2 in the Choroid Plexus Uptake of Glycylsarcosine and 5-Aminolevulinic Acid: Studies in Wild-type and Null mice. Pharmaceutical Research 21 (9) (2004) 1680-1685

Ohtsuki S., Takizawa T., Takanaga H., Terasaki N., Kitazawa T., Sasaki M., Abe T., Hosoya H.I., Terasaki T.; In Vitro Study of the Functional Expression of Organic Anion Transporting Polypeptide 3 at Rat Choroid Plexus Epithelial Cells and Its Involvement in the Cerebrospinal Fluid-to-Blood Transport of Estrone-3-Sulfate. Molecular Pharmacology 63 (3) (2003) 532-537

## P

Pardridge W.M., Triguero D., Yang J., Cancilla P.A.; Comparison of in Vitro and in Vivo Models of Drug Transcytosis through the Blood-Brain Barrier. The Journal of Pharmacology and Experimental Therapeutics 253 (2) (1990) 884-891

Petito C.K.; Human Immunodeficiency virus type 1 compartmentalization in the central nervous system. Journal of NeuroVirology 10 (2004) 21-24

Pritchard J.B., Miller D.S.; Comparative insights into the mechanisms of renal organic anion and cation secretion: Am J Physiol 261 (6 Pt 2) (1991) R1329-40

Pritchard J.B., Sweet D.H., Miller D.S., Walden R.; Mechanism of Organic Anion Transport across the Apical Membrane of Choroid Plexus. The Journal of Biological Chemistry 274 (47) (1999) 33382-33387

Reichel C., Gao B., Van Montfoort J., Cattori V., Rahner C., Hagenbuch B., Stieger B., Kamisako T., Meier P.J.; Localization and function of the organic anion transporting polypeptide Oatp2 in rat liver. Gastroenterology 117 (1999) 688-695

Reid G., Wielinga P., Zelcer N., de Haas M., van Deemter L., Wijnholds J., Balzarini J., Borst P.; Characterization of the Transport of Nucleoside Analog Drugs by the Human Multidrug Resistance Proteins MRP4 and MRP5: Molecular Pharmacology 63 (2003) 1094-1103

Reid G., Wielinga P., Zelcer N., van der Heijden I., Kuil A., de Haas M., Wijnholds J., Borst P.; The human multidrug resistance protein MRP4 functions as a prostaglandin efflux transporter and is inhibited by nonsteroidal antiinflammatory drugs: PNAS 100 no.16 (2003) 9244-9249

Rost D., Herrmann T., Sauer P., Schmidts H.L., Stieger B., Meier P.J., Stremmel W., Stiehl A.; Regulation of Rat Organic Anion Transporters in Bile Salt-Induced Cholestatic Hepatitis: Effect of Ursodeoxycholate. Hepatology 38 (1) (2003) 187-195

Russel F., Masereeuw R., Van Aubel R.A.M.H.; Molecular Aspects of Renal Anionic Drug Transport: Annu. Rev. Physiol. 64 (2002) 563-594

## S

Sager G.; Cyclic GMP transporters: Neurochemistry International 45 (2004) 865-873

Sampath J., Adachi M., Hatse S., Naesens L., Balzarini J., Flatley R., Matherly L., Schuetz J.; Role of MRP4 and MRP5 in Biology and Chemotherapy. AAPS PharmSci 4 (3) (2002) article 14

Sato K., Sugawara J., Sato T., Mizutamari H., Suzuki T., Ito A., Mikkaichi T., Onogawa T., Tanemoto M., Unno M., Abe T., Okamura K.; Expression of organic anion transporting polypeptide E (OATP-E) in human placenta. Placenta 24 (2003) 144-148

Sauvant C., Hesse D., Holzinger H., Evans K.K., Dantzer W.H., Gekle H.; Action of EGF and PGE<sub>2</sub> on basolateral organic anion uptake in rabbit proximal tubulus and hOAT1 expressed in human kidney epithelial cells: Am J Physiol Renal Physiol 286 (2004) F774-F783

Schaub T.P., Kartenbeck J., Konig J., Voge O., Witzgall R, Kritz W., Keppler D.; Expression of the conjugate export pump encoded by the *mrp2* gene in the apical membrane of kidney proximal tubulus: J Am Soc Nephrol. 8 (8) (1997) 1213-21

Schinkel A.H., Jonker J.W.; Mammalian drug efflux transporters of the ATP binding cassette (ABC) family: an overview: Advanced Drug Delivery Reviews 55 (2003) 3-29

Schinkel A.H., Smit J.J., van Tellingen O., Beijnen J.H., Wagenaar E., van Deemter L., Mol C.A., van der Valk M.A., Robanus-Maandag E.C., te Riele H.P., et al.; Disruption of the mouse *mdr1a* P-glycoprotein gene leads to a deficiency in the blood-brain barrier and to increased sensitivity to drugs. Cell 77 (1994) 357-365

Schreiber G., Richardson S.J., Prapunpoj P.; Structure and Expression of the Transthyretin Gene in the Choroid Plexus: A Model for the Study of the Mechanism of Evolution. Microscopy Research and Technique 52 (2001) 21-30

Schuetz J.D., Connelly M.C., Sun D., Paibir S.G., Flynn P.M., Srinivas R.V., Kumar A., Fridland A.; MRP4: A previously unidentified factor in resistance to nucleoside-based antiviral drugs. Nature Medicine 5 (9) (1999) 1048-1051

Schwede F., Christensen A., Liauw S., Hippe T., Kopperud R., Jastorff B., Doskeland S.O.; 8-Substituted cAMP Analogues Reveal Marked Differences in Adaptability, Hydrogen Bonding, and Charge Accomodation between Homologues Binding Sites (AI/AII and BI/BII) in cAMP Kinase I and II. Biochemistry 39 (2000), 8803-8812

Sekine T., Cha S.H., Tsuda M., Apiwattanakul N., Nakajima N., Kanai Y., Endou H.; Identification of multispecific organic anion transporter 2 expressed predominantly in the liver. FEBS Lett. 429 (1998) 179-182

Sekine T., Kusuhara H., Utsunomiya-Tate N., Tsuda Y., Sugiyama Y., Kanai Y., Endou H.; Molecular cloning and characterization of high-affinity carnitine transporter from rat intestine. Biochem. Biophys. Res. Commun. 251 (1998) 586-591

Simonson G.G., Vincent A.C., Roberg K.J., Huang Y., Imanij V.; Molecular cloning and characterization of a novel liver-specific transport protein. J. Cell. Sci. 107 (1994) 1065-1072

Smeets P.H.E., Van Aubel R.A.M.H., Wouterse A.C., Van den Heuvel J.J.M.W., Russel F.G.M.; Contribution of Multidrug Resistance Protein 2 (MRP2/ABCC2) to the Renal Excretion of p-aminohippurate (PAH) and Identification of MRP4 (ABCC4) as a Novel PAH Transporter. J Am Soc Nephrol 15 (2004) 2828-2835

Soodvilai S., Chatsudthipong V., Evans K.K., Wright S.H., Dantzer W.H.; Acute Regulation of OAT3-Mediated Estrone Sulfate Transport in Isolated Rabbit Renal Proximal Tubules. American Journal of Physiology Renal Physiology 287 (5)(2004) F1021-9

Spector R.; Johanson C.E.; Plexus chorioidei: Adergeflechte des Säugerhirns. Spektrum der Wissenschaft (1991)

Strazielle N., Belin M.-F., Gherzi-Egea J.-F.; Choroid plexus controls brain availability of anti-HIV nucleoside analogs via pharmacologically inhibitable organic anion transporters. AIDS 17 (2003) 1473-1485

Strazielle N., Gherzi-Egea J.-F.; Demonstration of a Coupled Metabolism-Efflux Process at the Choroid Plexus as a Mechanism of Brain Protection toward Xenobiotics. The Journal of Neuroscience 19 (15) (1999) 6275-6289

Sugiyama D., Kusuhara H., Taniguchi H., Ishikawa S., Nozaki Y., Aburatani H., Sugiyama Y.; Functional Characterization of Rat Brain-specific Organic Anion Transporter (Oatp14) at the Blood-Brain Barrier. The Journal of Biological Chemistry 278 (44) (2003) 43489-43495

## References

---

Sun H., Dai H., Shaik N., Elmquist W.F.; Drug efflux transporters in the CNS: Advanced Drug Delivery Reviews 55 (2003) 83-105

Sun H., Johnson D.R., Finch R.A., Sartorelli A.C., Miller D.W., Elmquist W.F.; Transport of Fluorescein in MDCKII-MRP1 Transfected Cells and mrp1-Knockout Mice. Biochemical and Biophysical Research Communications 284 (2001) 863-869

Sweet D.H.; Organic anion transporter (Slc22a) family members as mediators of toxicity. Toxicol Appl Pharmacol 204 (3) (2005) 198-215

Sweet D.H., Miller D.S., Pritchard J.B.; Ventricular choline transport: a role for organic cation transporter 2 expressed in choroid plexus. J. Biol. Chem. 276 (2001) 41611-41619

Sweet D.H., Miller D.S., Pritchard J.B., Fujiwara Y., Beier D.R., Nigam S.K.; Impaired Organic Anion Transport in Kidney and Choroid Plexus of Organic Anion Transporter 3 (Oat3 (Slc22a8)) Knockout Mice. The Journal of Biological Chemistry 277 (30) (2002) 26934-26943

Sweet D.H., Wolff N.A., Pritchard J.B.; Expression, cloning and characterization of rOat1. The basolateral organic anion transporter in rat kidney. J. Biol. Chem. 272 (1997) 30088-30095

Sykes D., Sweet D.H., Lowes S., Nigam S.K., Pritchard J.B., Miller D.S.; Organic anion transport in choroid plexus from wild-type and organic anion transporter 3 (Slc22a8)-null mice: Am J Physiol Renal Physiol 286 (2004) F972-F978

Tamai I., Ohashi R., Nezu J.I., Sai Y., Kobayashi D., Oku A., Shimane M., Tsuij A.; Molecular and functional characterization of organic cation/carnitine transporter family in mice. J. Biol. Chem. 275 (2000) 40064-40072

Tan B., Piwnicka-Worms D., Ratner L.; Multidrug resistance transporters and modulation. Current Opinion in Oncology 12 (5) (2000) 450-458

Taylor E.M.; The Impact of Efflux Transporters in the Brain on the Development of Drugs for CNS Disorders. Clin. Pharmacokinet. 41 (2) (2002) 81-92

Terlouw S.A., Masereeuw R., van der Broeck P.H.H., Notenboom S., Russel F.G.M.; Role of multidrug resistance protein 2 (MRP2) in glutathione-bimane efflux from Caco-2 and rat renal proximal tubule cells. British Journal of Pharmacology 134 (2001) 931-938

Török M., Huwyler J., Gutmann H., Fricker G., Drewe J.; Modulation of transendothelial permeability and expression of ATP-binding cassette transporters in cultured brain capillary endothelial cells by astrocytic factors and cell-culture conditions: Exp Brain Res 221 (2003) 356-365

## V

Van Aubel R.A.M.H., van Kuijck M.A., Koenderink J.B., Deen P.M.T., van Os C.H., Russel F.G.M.; Adenosine Triphosphate-Dependent Transport of Anionic Conjugates by the Rabbit Multidrug Resistance-Associated Protein Mrp2 Expressed in Insect Cells. Molecular Pharmacology 53 (1998) 1062-1067

Van Aubel R.A.M.H., Masereeuw R., Russel F.G.M.; Molecular pharmacology of renal organic anion transporters: American Journal of Physiology Renal Physiology 279 (2000) F216-F232

Van Aubel R.A.M.H., Peters J.G.P., Masereeuw R., van Os C.H., Russel F.G.M.; Multidrug Resistance Protein Mrp2 mediates ATP-dependent transport of classic renal organic anion *p*-aminohippurate. Am J Physiol Renal Physiol 279 (2000) F713-F717

Van Aubel R.A.M.H., Smeets P.H.E., Peters J.G.P., Bindels R.J.M., Russel F.G.M.; The MRP4/ABCC4 Gene Encodes a Novel Apical Organic Anion Transporter in Human Kidney Proximal Tubulus: Putative Efflux Pump for Urinary cAMP and cGMP: Journal of the American Society of Nephrology 13 (2002) 595-603

Van Aubel R.A.M.H., Smeets P.H.E., Van den Heuvel J.J.M.W., Russel F.G.M.; Human organic anion transporter MRP4 (ABCC4) is an efflux pump for the purine and metabolite urate with multiple allosteric substrate binding sites. Am J Physiol Renal Physiol 288 (2005) 327-333

Van de Water F.M., Masereeuw R., Russel F.G., Function and regulation of multidrug resistance proteins (Mrps) in the renal elimination of organic anions. Drug Metab. Rev. 37 (3) (2005) 443-471

Van Montfoort J.E., Hagenbuch B., Groothuis G.M., Koepsell H., Meier P.J., Meijer D.K.; Drug uptake systems in liver and kidney. Curr. Drug Metab. 4 (2003) 185-211

Villalobos A.R.A., Miller D.S., Renfro J.L.; Transepithelial organic anion transport by shark choroid plexus. Am J Physiol Regulatory Integrative Comp Physiol 282 (2002) R1308-R1316

Villalobos A.R.A., Parmelee J.T., Pritchard J.B.; Choline uptake across the ventricular membrane of neonate rat choroid plexus. Am J Physiol 282 (2) (1999) C1288-96

## W

Walters H.C., Craddock A.L., Fusegawa H., Willingham M.C., Dawson P.A.; Expression, transport properties, and chromosomal location of organic anion transporter subtype 3. Am. J. Physiol. Gastrointest. Liver Physiol. 279 (2000) G1188-G1200

Wielinga P.R., van der Heijden I., Reid G., Beijnen J.H., Wijnholds J., Borst P.; Characterization of the MRP4- and MRP5-mediated Transport of Cyclic Nucleotides from Intact Cells . The Journal of Biological Chemistry 278 (20) (2003) 17664-17671

Wijnholds J., Mol C.A.A.M., van Deemter L., de Haas M., Scheffer G.L., Baas F., Beijnen J.H., Scheper R.J., Hatse S., de Clercq E., Balzarini J., Borst P.; Multidrug-resistance protein 5 is a multispecific organic anion transporter able to transport nucleotide analogs. PNAS 97 (13) (2000) 7476-7481

Wolbold R., Klein K., Burk O., Nüssler A.K., Neuhaus P., Eichelbaum M., Schwab M., Zanger U.M.; Sex is a Major Determinant of CYP3A4 Expression in Human Liver: Hepatology (2003) 978-988

Wolff N.A., Thies K., Kuhnke N., Reid G., Friedrich B., Lang F., Burckhardt G.; Protein Kinase C Activation Downregulates Human Organic Anion Transporter 1-Mediated Transport through Carrier Internalization. J Am Soc Nephrol 14 (2003) 1959-1968

## X

Xiang Z., Burnstock G.; Expression of P2X receptors in rat choroid plexus. Neuroreport 16 (9) (2005) 903-908

## Y

Yabuuchi Y., Tamai I., Nezu J., Sakamoto K., Oku A., Shimane Y., Sai Y., Tsujii A.; Novel membrane transporter OCTN1 mediates multispecific, bidirectional, and pH-dependent transport of organic cations. J. Pharmacol. Exp. Ther. 289 (1999) 768-773

## Z

Zelcer M., Reid G., Wielinga P., Kuil A., van der Heijden I., Schuetz J.D., Borst P.; Steroid and bile acid conjugates are substrates of human multidrug-resistance protein (MRP) 4 (ATP-binding cassette C4). Biochemical Journal 371 (2003) 361-367

Zhang Y., Bachmeier C., Miller D.W.; In vitro and in vivo models for assessing drug efflux transporter activity. Advanced Drug Delivery Reviews 55 (2003) 31-51

Zhang Y., Zhang D., Li W., Chen J., Peng Y., Cao W.; A novel real-time quantitative PCR method using attached universal template probe. Nucleic Acids Research 31 (2003) e123

Zhe-Sheng C., Lee K., Kruh G.D.; Transport of Cyclic Nucleotides and Estradiol 17- $\beta$ -D-Glucuronide by Multidrug Resistance Protein 4. The Journal of Biological Chemistry 276 (36) (2001) 33747-33754

Zwart R., Verhaagh S., Buitelaar M., Popp-Snijders P., Barlow P.D.; Impaired activity of the extraneuronal monoamine transporter system known as uptake-2 in rOct3/Slc22a3-deficient mice. Mol. Cell. Biol. 21 (2001) 4188-4196

## Websites

About the blood- brain barrier: Anatomy and physiology of blood-csf barrier.  
<http://users.ahsc.arizona.edu/davis/csfanatomy.htm>

Competitive RT-PCR: The Society for Endocrinology-Molecular Endocrinology Workshop 11/99: [http://www.endocrinology.org/SFE/training/mew/mew2\\_sug.htm](http://www.endocrinology.org/SFE/training/mew/mew2_sug.htm)

Nervous System Form and Function.  
<http://www.colorado.edu/epob/epob3730rlynch/05cns.html>

Quantitative RT-PCR: PCR Protocols:  
<http://www.cas.psu.edu/docs/CASDEPT/VET/jackvh/jvhpcr.htm>